NASA Contractor Report 172238

Final Report:

Conceptual Design of a Noncontacting Power Transfer Device for the ASPS Vernier System

J. Kroeger, J. Drilling, and
T. Gunderman

Sperry Corporation
Phoenix, Az 85036

Contract NAS1-16909,
Task Number 3
April 1984

National Aeronautics and
Space Administration

Langley Research Center
Hampton, Virginia 23665

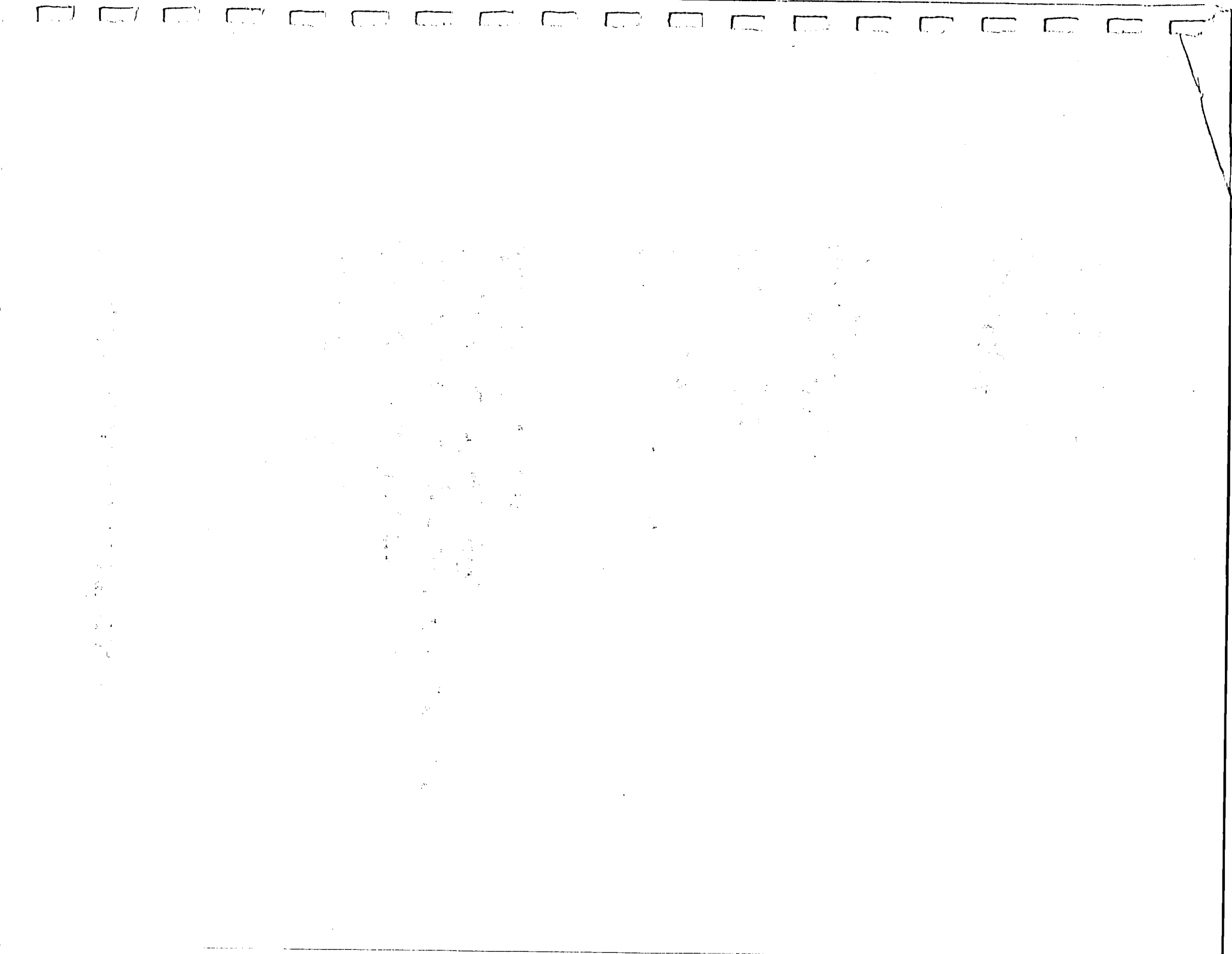

NASA Contractor Report 172238

Final Report:

Conceptual Design of a Noncontacting Power Transfer Device for the ASPS Vernier System

J. Kroeger, J. Drilling, and
T. Gunderman

Sperry Corporation
Phoenix, Az 85036

Contract NAS1-16909,
Task Number 3
April 1984

National Aeronautics and
Space Administration

Langley Research Center
Hampton, Virginia 23665

SUMMARY

The concept of electrical power transfer across a magnetically controlled gap has been discussed for several years. The design which is presented in this document represents the culmination of the first serious attempt to design a very low force, noncontacting power transfer mechanism.

The electromagnetic device advanced herein is an Ironless, Translatable Secondary Transformer in which one of the two coils is fixed to the entire magnetic core. The second coil is free to move within the core over the full range of motions required by the application under study.

The specific application considered for this design was the vernier subsystem of the Annular Suspension and Pointing System (ASPS).

The development of and rationale for the Electromagnetics Design is presented in Part 1 of this report. Part 2 provides similar documentation for the Electronics Design. The Appendices detail the results of small scale model tests, disturbance force calculations, the baseline transformer fabrication drawings, the AVS Converter Parts List, and model schematic diagrams.

A third design was originally planned, a variable load device. However, for the converter design chosen ($\overline{\text{Cuk}}$), the worst case load is resistive. As a result, a variable resistor will suffice as the worst case load.

TABLE OF CONTENTS

PART ONE - ELECTROMAGNETICS DESIGN

1.1	Introduction	2
1.2	Requirements	5
1.3	Configuration	6
1.4	Preliminary Test Phase	9
1.5	Ironless, Translatable Secondary Transformer Design	10
1.5.1	General Design	10
1.5.2	Transformer Core Design	12
1.5.3	Transformer Coil Design	14
1.5.4	Transformer Disturbance Force Calculations	15
1.5.5	Transformer Equivalent Circuit	22
1.5.6	Transformer Performance and Weight Summaries	24
1.5.7	Frequency Selection	25

PART TWO - ELECTRONICS DESIGN

2.1	Introduction	27
2.2	Topology Considerations	27
2.3	Basic Operation of the Cuk Converter	30
2.3.1	Modification of Simple Circuit for AVS	33
2.4	Computer Design Programs	36
2.4.1	Design Program "CUK.DES"	36
2.4.1.1	EMI Filter Component Values	37
2.4.1.2	Cuk Inductor Value Selection	41
2.4.1.3	Cuk Capacitor Value Selection	42
2.4.1.4	Output Capacitor Value Selection	43
2.4.1.5	Program Operation	43
2.4.1.6	Air-Gapped Inductor Design Subroutine	49
2.4.1.6.1	Standard Geometry	50
2.4.1.6.2	Determinating "x" from Weight	52
2.4.1.6.3	Number of Turns	52
2.4.1.6.4	Number of Wires to Parallel	54
2.4.1.6.5	Power Losses	55
2.4.1.7	Transformer Design Subroutine	57
2.4.2	Summary Program "CUK Sum"	61
2.5	Operating Frequency Selection	68
2.5.1	Efficiency vs. Weight	68
2.5.2	Analaysis of CUK.SUM Data	70
2.5.3	Rotary Transformer Consideration	71
2.5.4	Frequency Selection	71
2.6	Component Selection	72
2.6.1	Power Transistor	72

TABLE OF CONTENTS (Cont.)

2.6.1.1	Transistor Requirements	72
2.6.1.2	Technology Selection - MOSFET vs Bipolar	72
2.6.1.3	Transistor Selection	76
2.6.2	Power Diode	77
2.6.2.1	Diode Requirements	77
2.6.2.2	Analysis of Diode Power Loss	77
2.6.2.3	Diode Selection	78
2.6.3	Capacitor	78
2.6.3.1	Capacitor Requirements	78
2.6.3.2	Selection	79
2.7	Drive Circuitry	79
2.7.2.1	Clock Generator	81
2.7.2.1.1	Functional Description	81
2.7.2.1.2	Circuit Description	81
2.7.2.2	Duty Cycle Control	83
2.7.2.2.1	Functional Description	83
2.7.2.2.2	Circuit Description	83
2.7.2.3	Power Drive	86
2.7.2.3.1	Functional	86
2.7.2.3.2	Circuit Description	88
2.7.2.4	Current Balance	93
2.7.2.5	Over Current Protection	94
2.7.2.5.1	Functional	94
2.7.2.5.2	Circuit Description	95
2.8	Transformer/Inductor Specifications	97
2.8.1	Output Isolation Transformer	97
2.8.1.1	Requirements	97
2.8.1.2	Specifications	98
2.8.2	Base Drive Transformer	98
2.8.2.1	Requirements	98
2.8.2.2	Specifications	99
2.8.3	Current Balance Transformer	100
2.8.3.1	Requirements	100
2.8.3.2	Specifications	101
2.8.4	Input Filter Inductor	101
2.8.4.1	Requirements	101
2.8.4.2	Specifications	102
2.8.5	Cuk Inductor	102
2.8.5.2	Specifications	102

TABLE OF CONTENTS (Cont.)

Appendix 1 - SMALL SCALE MODEL TESTS

A1.1	Model Description	A1-1
A1.2	Model #1	A1-1
A1.3	Model #2	A1-2
A1.4	Discussion of Results and Additional Tests	A1-3
A1.4.1	Conductor Skin Effect	A1-3
A1.4.2	Core Loss Measurements and Calculations	A1-7
A1.4.3	Inductance Calculations and Measurement	A1-11
A1.5	Conclusions	A1-14
A1.6	References	A1-15

Appendix 2 - DISTURBANCE FORCE CALCULATIONS

A2.1	Force Calculation Techniques	A2-1
A2.2	Calculation Technique Confirmation	A2-4
A2.3	Force Calculations	A2-9

Appendix 3 - BASELINE TRANSFORMER FABRICATION DRAWINGS

Appendix 4 - AVS CONVERTER PARTS LIST

Appendix 5 - SCHEMATIC DIAGRAM

LIST OF FIGURES

Figure	Title	Page
1	Conventional Rotary Transformer	3
2	Ironless Secondary Rotorless Transformer	4
3	Ironless, Translatable Secondary Transformer	8
4	Baseline Transformer Design	11
5	Flux Leakage Due to Unit Current in Primary	19
6	Flux Leakage Due to Unit Current in Secondary	20
7	Flux Leakage at Full Load	21
8	Transformer Equivalent Circuit	23
9	Transformer Power Loss Versus Frequency	26
10	Cuk Converter Operation	30
11	Waveforms	31
12	Voltage Transfer Ratio	32
13	Cuk Modification	34
14	General Layout	35
15	Calculation of L1, L2	38
16	Program Listing 1	39
17	Calculation of L3, L4	41
18	Calculation of C2, C3	42
19	Calculation of C4	43
20	Program Listing 2	44
21	Program Listing 3	45
22	Normalized Core	50
23	Program Listing 4	51
24	Deriving "x" From Weight	52
25	Number of Turns	53
26	Loss Calculations	55
27	Core Loss of Metglass	56
28	Program Listing 5	58
29	"E" Core Dimensions	59
30	"CUK.SUM" Entry	61
31	Program Listing 6	62
32	Typical Program Output for 15KHz	66
33	Frequency Tradeoffs	69
34	5KHz to 15KHz Tradeoffs	70
35	Device Switching Diagram	74
36	Semiconductor Dissipation	75
37	Drive Circuitry Block Diagram	80
38	Clock Generator Schematic Diagram	81
39	Duty Cycle Control Schematic Diagram	84
40	Power Drive Circuitry Schematic Diagram	87
41	Current Balance Circuitry Schematic Diagram	93
42	Over Current Circuitry Schematic Diagram	95
43	Output Isolation Transformer Schematic Diagram	97
44	Base Drive Transformer Schematic Diagram	99
45	Current Balance Transformer Schematic Diagram	100

LIST OF FIGURES (Cont.)

Figure	Title	Page
A1-1	Transformer Model #1 Equivalent Circuit	A1-1
A1-2	Transformer Model #2 Equivalent Circuit	A1-3
A1-3	RAC/RDC Ratio Versus Frequency, Models #1 and #2	A1-4
A1-4	RAC/RDC Ratio Curves	A1-5
A1-5	RAC/RDC Ratio vs Frequency Litz Wire and Baseline Coils	A1-7
A1-6	Manufacturer's Preliminary Revised Coreloss vs Flux Density Curves for 3C8 Material	A1-9
A1-7	Leakage Path	A1-13
A2-1	Single Conducting Loop Finite Element Grid	A2-6
A2-2	Equipotential Lines Single Conducting Loop	A2-7
A2-3	Equipotential Lines Solenoid	A2-8
A2-4	Hysteresis Loop	A2-9
A2-5	Finite Element Grid	A2-11
A2-6	Baseline Transformer	A2-12
A2-7	Flux Leakage Due to Unit Current in Primary	A2-13
A2-8	FLux Leakage Due to Unit Current in Secondary	A2-14
A2-9	Flux Leakage at Full Load	A2-15
A3-1	Baseline Transformer	A3-2
A3-2	Baseline Transformer Explosion	A3-3
A3-3	Core Segment (End)	A3-4
A3-4	Core Segment (Outer)	A3-5
A3-5	Core Segment (Inner)	A3-6
A3-6	Support Posts (Coil)	A3-7
A3-7	Coil, Primary	A3-8
A3-8	Coil, Secondary, with Support Posts	A3-9
A5-1	Baseline Transformer Schematic Diagram	A5-1

LIST OF TABLES

Table	Title	Page
I	Performance of Baseline Transformer Design	10
II	Principle Core Parameters	13
III	Design of Primary and Secondary Transformer Coils	14
IV	AC and DC Resistance of Litz Wire Coils and Solid Conductor Coils	15
V	Disturbance Forces for Transformer at Full Load as Predicted by Finite Element Model	22
VI	Transformer Parameters	23
VII	Transformer Electrical Performance Parameters	24
VIII	Transformer Weight Breakdown	24
IX	EMI Requirements	37
X	CUK.SUM Output Lines	67
XI	CUK.SUM Columns	66
XII	Winding Specifics, Output Isolation Transformer	98
XIII	Winding Specifics, Base Drive Transformer	100
XIV	Winding Specifics, Current Balance Transformer	101
A1-I	Model #1 Test Results	A1-2
A1-II	Model #2 Test Results	A1-3
A1-III	Core Loss Test Results	A1-10
A1-IV	Magnetizing Inductance Values	A1-12
A1-V	Leakage Inductance Values	A1-14
A2-I	Self-Inductance Numerical Comparisons	A2-5
A2-II	Flux Density Numerical Comparisons	A2-5
A2-III	Inductance Summary	A2-16
A2-IV	Power Coupling Summary	A2-16
A2-V	Peak Force Summary	A2-16

ABSTRACT

A study was conducted to design a device to transfer power between noncontacting stationary and levitating platforms of the vernier subsystem of the Annular Suspension and Pointing System (ASPS). The power transfer mechanism was to: (1) require no physical contact between the two platforms, and (2) achieve high efficiency, high reliability, low weight, and low EMI susceptibility. Electromagnetic design considerations led to selection of an Ironless, Translatable Secondary Transformer. Electronics design considerations led to selection of a modified Cuk converter operating at a 10 KHz frequency. The design transfers approximately 2500 watts output power with 99.2% efficiency.

PART I - ELECTROMAGNETICS DESIGN

1.1 Introduction[1]

The subject of this activity is to design a power transfer mechanism for the vernier subsystem of the Annular Suspension and Pointing System (ASPS). In order to permit highly accurate and stable pointing of various payloads, this device must have no physical contact between the stationary and levitated portions of the ASPS vernier subsystem. The most viable approach for satisfying the requirement of noncontacting power transfer rests in rotary transformer techniques.

In addition to the noncontacting requirement, the power transfer device must produce a minimum amount of disturbance force between the two vernier portions. The ASPS vernier subsystem, in the course of performing its pointing function, experiences motions of greater than 0.2 inches between the stationary and levitated portions in all six degrees of freedom. The conventional rotary transformer, consisting of primary and secondary coils each wound into sections of the magnetic core and separated by a radial (or axial) gap (Figure 1), produces significant disturbance forces when subjected to a radial offset and is, therefore, not appropriate for this application. The device designed in this activity is an Ironless, Translatable Secondary Transformer in which one of the two coils is fixed to the entire magnetic core. The second coil, located inside but not contacting the core, is free to move within the core over the motions required by application (Figure 2).

[1]The use of trade names or names of manufacturers in this report does not cconstitute endorsement, either expressed or implied, by the National Aironautics and Space Administration.

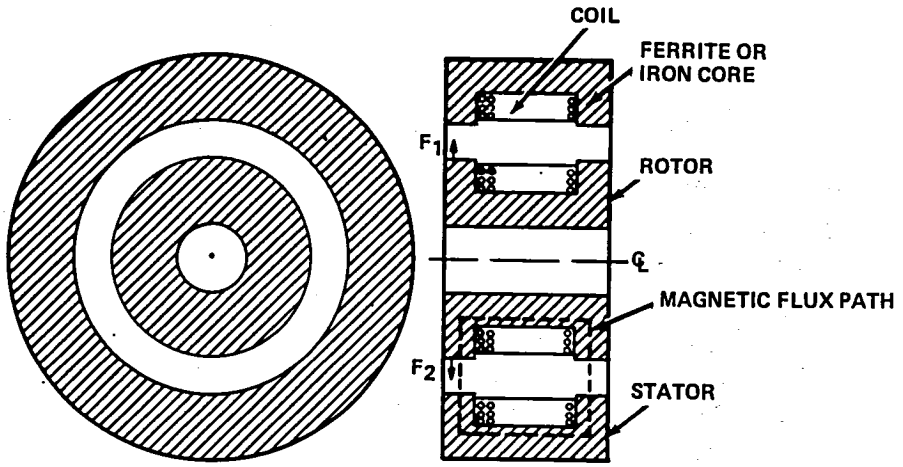

a.) TRANSFORMER CENTERED
FORCES $F_1 = F_2$, NO NET FORCE TRANSMITTED BETWEEN
ROTOR AND STATOR.

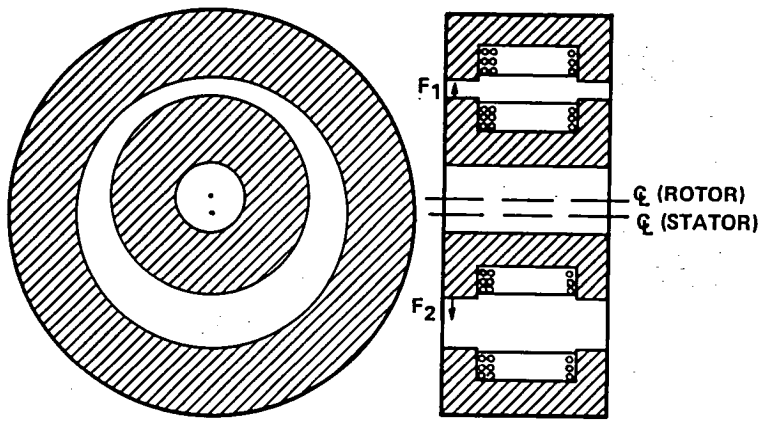

b.) TRANSFORMER ROTOR RADIALLY OFFSET
SINCE FORCE $\approx$ GAP^2, $F_1 >> F_2$, SIGNIFICANT NET
IS TRANSMITTED

S714-104-1

Figure 1
Conventional Rotary Transformer

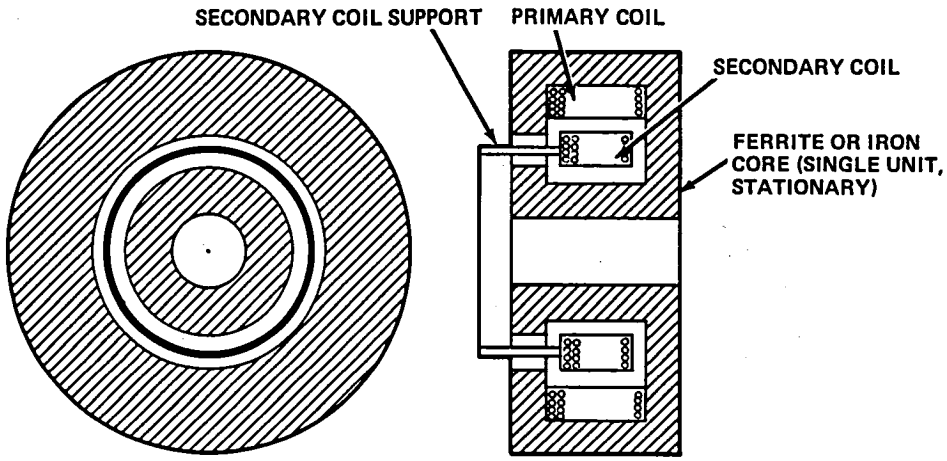

a.) TRANSFORMER CENTERED

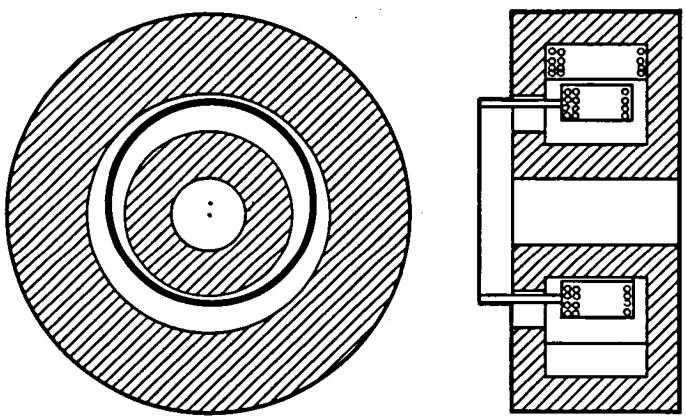

b.) TRANSFORMER SECONDARY COIL RADIALLY OFFSET

S714-104-2

Figure 2
Ironless Secondary Rotary Transformer

1.2 Requirements

1.2.1 The design goals for the rotary transformer were:

a. Power transfer across a variable gap as established by the vernier assembly operation, using noncontacting techniques.

b. Present a minimum load to the control of the thermal environment of the ASPS vernier assembly as well as to minimize demands on the limited supply power bus.

c. Provide a minimum of 2.5Kw of power to the payload(s) mounted atop the ASPS vernier assembly assuming adequate input power is available.

d. Impart minimum disturbance forces to the ASPS vernier assembly magnetic suspension system at any power level. The maximum allowable disturbance force, at any power level, shall not exceed 0.1 percent of the force capability of a single ASPS magnetic bearing.

e. In the course of development, be subjected to weight minimization efforts.

f. Minimum source of EMI to the ASPS, the payload, and equipment mounted onboard, as well as to the shuttle orbiter and its equipment.

1.2.2 Converting these general requirements into more definitive terms, the following working requirements were established.

a. Minimum allowable motions between the transformer primary and secondary elements (derived from ASPS Vernier requirements):

1. Radial Translations: +/-0.20 inches

2. Axial Translations: +/-0.22 inches

3. Tilt (non concurrent with other motions): +/-0.75 degrees

4. Roll (rotation): +/-2.0 degrees

b. Efficiency at 2.5Kw output power: 98% minimum goal

c. Disturbance forces between primary and secondary elements

1. Axial direction: .0077 lbs. force maximum

2. Radial direction: .0032 lbs. force maximum

1.3 Configuration

The initial transformer configuration, similar to that shown in Figure 2, included a gap in the magnetic path and allowed 360 degree rotation

of the secondary coil with respect to the primary coil and magnetic core. This 360 degree rotation capability was consistent with the then current capability of the ASPS vernier. The magnetic path gap, however, introduced several relatively minor disadvantages including dissymetry in the magnetic path, increased transformer losses, and a source of EMI.

Subsequent addition of a roll gimbal to the ASPS system for coarse roll positioning reduced the full rotation requirement to +/-2.0 degrees for the vernier subsystem and for the rotary transformer. As shown in Figure 3, the transformer configuration could now consist of a continuous magnetic path with access holes or slots for output coil lead exit and supports. The access holes could be located through the end surface, as shown in figure 3, or through the inside diameter of the core. At some future point in the ASPS vernier development, it may be desirable to have the transformer I.D. open to locate some other device. For the baseline configuration, it was therefore decided that support for the secondary coil would be through the end surface.

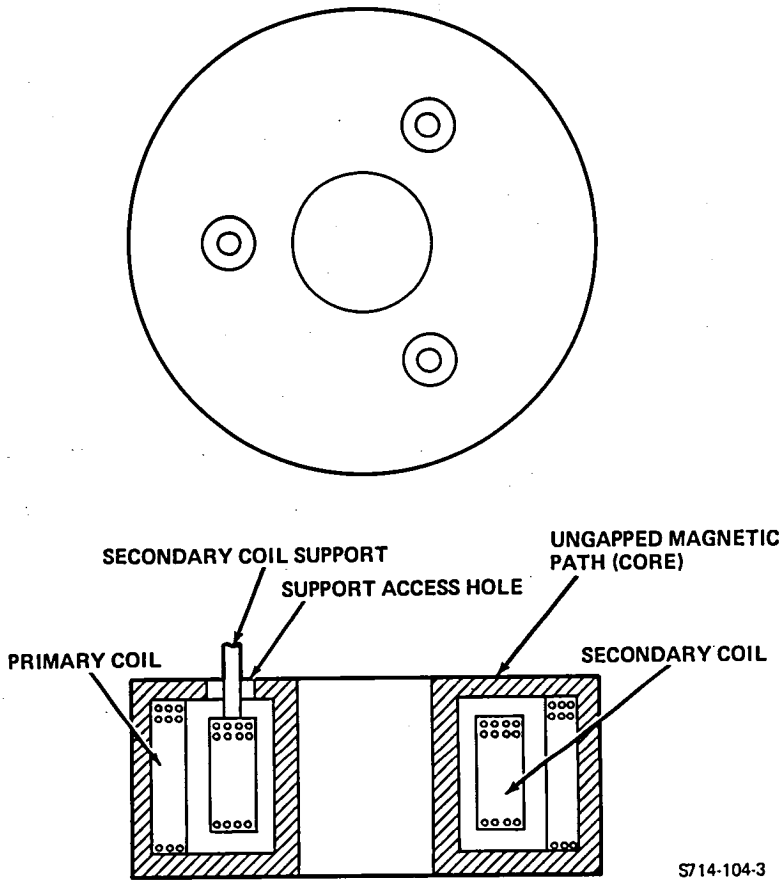

Figure 3
Ironless, Translatable Secondary Transformer

1.4 Preliminary Test Phase

As a preliminary step in the transformer design activity, a test phase was initiated on small scale versions of the anticipated transformer configuration. Tests were performed using existing ferrite pot cores and coil bobbins and were directed toward verifying performance and equivalent circuit calculation procedures. (Model descriptions and test results are detailed in Appendix 1). Principal results of the test phase were:

a. The AC resistance of a transformer coil using solid conductor magnet wire and operating at 10KHz can easily be ten times the DC resistance value with a corresponding I^2R power loss increase. This phenomenon is due to "skin effect" in the conductor and may be partially eliminated by using woven stranded magnet wire, Litz wire.

b. Measured core losses were up to 6.3 times those calculated using the material vendor's published core loss curves and were 3 times those calculated using his revised curves.

c. The calculation procedure to determine magnetizing and leakage inductances to a reasonable accuracy was established.

1.5 Ironless, Translatable Secondary Transformer Design

1.5.1 General Design

The baseline transformer design (Figure 4) consists of the ferrite core and primary coil which comprise the stationary element and a secondary coil and three support posts comprising the movable element. The performance of this design is shown in Table I.

TABLE I - Performance of Baseline Transformer Design

Parameter	Performance	Requirement
Excitation	100Vrms, 26 amps, 10KHz	-
Loaded Output	28Vrms, 89 amps	-
Efficiency @2.5Kw output	99.2%	Maximize
Motion Capability-Axial	+/-0.22 inch	+/-0.22 inch
-Radial	+/-0.20 inch	+/-0.20 inch
-Tilt	+/-0.75 degrees	+/-0.75 degrees
Disturbance Forces		
Axial for +/-.22 inch motion	.00244 lb_f	.0077 lb_f
Radial for +/-.20 inch motion	.00124 lb_f	.0032 lb_f
Weight	12 pounds	Minimize
EMI	Minimized*	Minimize
Outside Diameter	7.50 inches	-
Inside Diameter	2.10 inches	-
Length	3.00 inche	-

*The electro-magnetic interference (EMI) will be very low, since:

1) the coils are completely enclosed by the magnetic core,
2) there is no magnetic gap in the flux path and
3) the magnetic core is operating at a very low flux density, 900 gauss average, compared to its 4500 gauss saturation flux density.

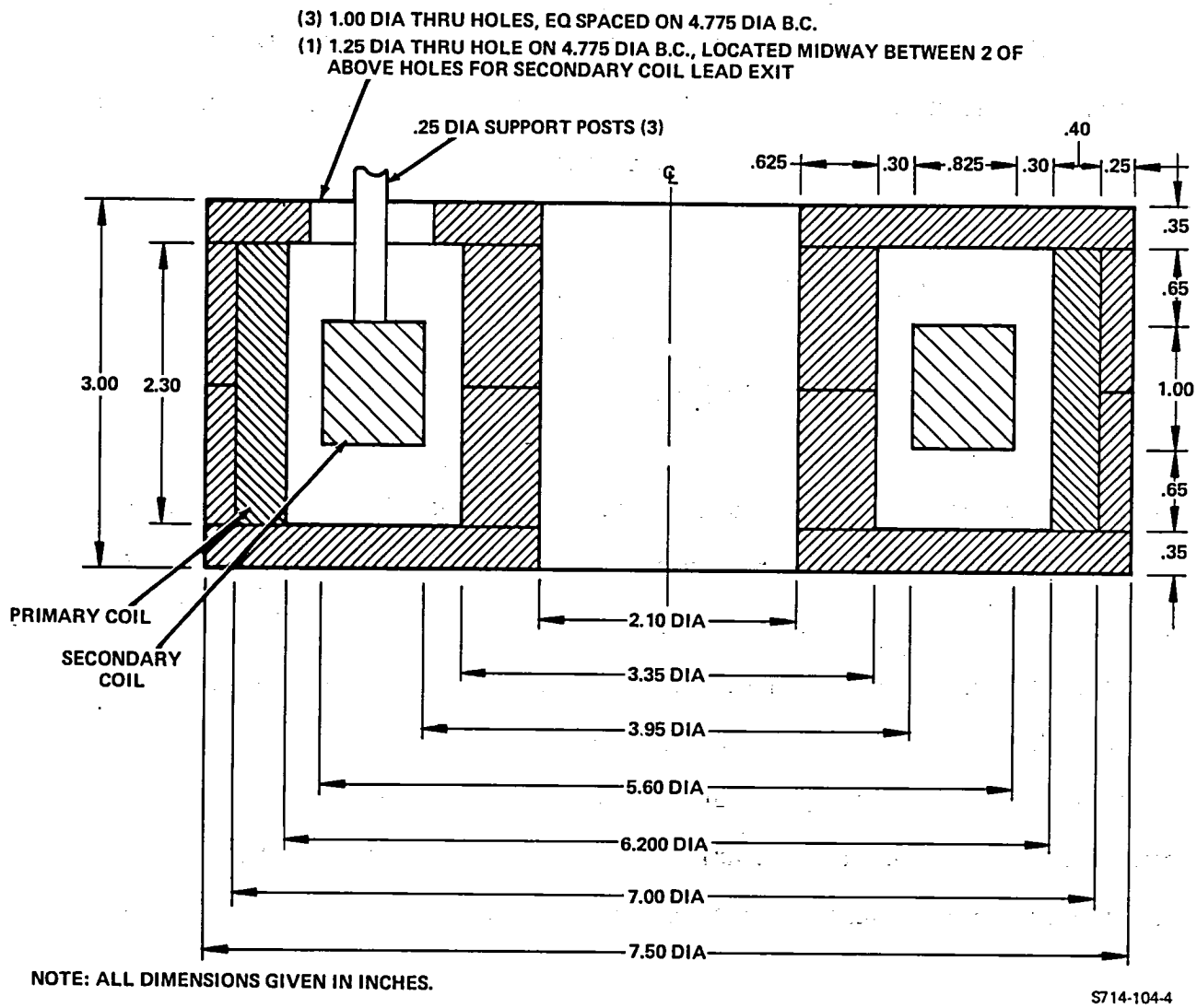

Figure 4
Baseline Transformer Design
(Ironless, Translatable Secondary Transformer)

The principal requirements addressed in settling on the present design were to achieve both low disturbance forces and high efficiency. At this stage in the development, weight was considered a secondary requirement. The ferrite core sections were conservatively sized to insure ease of fabrication. To save weight, core sections could be reduced in size and/or coil areas could also be reduced with a corresponding loss of efficiency.

1.5.2 Transformer Core Design

The core was to be fabricated in several mating sections from a manganese zinc ferrite, Ceramic Magnetics MN60. Ferrite was selected for its Isotropic property and availability in any desired shape. The MN60 material was specifically selected because of its high permeability, low core losses, and successful performance in previous applications. The method of sectioning the core was based on discussions with the material vendor. The first requirement was to ascertain the most economical method of fabricating the desired shapes. The second requirement was to achieve configuration versatility. Specifically, a requirement to be able to assemble the transformer with one-half the axial cavity length of the baseline design was imposed to provide characterization capability for potential design iterations.

The primary determinants for the physical size of the transformer were:

a. The 2.1 inch diameter thru-bore was provided as a possible location for some other device in the ASPS system.

b. The internal cavity was sized to provide space for reasonable coil cross sections, allowance for secondary coil motions, and adequate coil clearance.

c. The .25 inch outer wall thickness was required for mechanical strength and manufacturability.

d. The ferrite end plates and inner wall were conservatively sized such that the cross section areas are approximately equal to the outer wall, thus maintaining relatively uniform flux density and minimizing EMI.

The principal core parameters are listed in Table II.

TABLE II - Principal Core Parameters

Material ..... MN60 Ferrite Flux Path Length ..... 9.83 inches (25 cm.) Effective Area ..... 5.51 sq. in. (35.6 sq. cm) Volume ..... 54.2 cu. in. (888 cc.) Weight ..... 9.40 pounds (4.26 Kgm)		
Cross Section Area, Summary		
Section	Cross Section Area	Flux Density
Outer wall	5.69 sq. in	875 gauss
Inner wall	5.35	931
End Plate, @ 7.0 Dia.	7.70	647
End Plate, @ 5.175 Dia.	5.69	875
End Plate, @ 3.35 Dia.	3.68	1354
End Plate, thru access holes	3.76	1325

1.5.3 Transformer Coil Design

The coil sizes were determined using an iterative process to trade off coil areas, clearance space allocations, and overall transformer size. Earlier iterations maintained the secondary coil clearances at about 1.5 times the required motions in all directions. Force calculations on one of these configurations predicted force levels only slightly below the required goals (The force calculations are discussed in detail in Section 1.5.4). Further design iterations determined that force levels were most sensitive to axial coil clearance. This clearance was increased to about 3 times the required motion thus providing reasonable margin between the required and predicted forces. The coil design is defined in Table III.

TABLE III - Design of Primary and Secondary Transformer Coils

Parameter	Primary Coil	Secondary Coil
Cross Section Area	0.92 sq. in.	0.825 sq. in.
Copper Allocation @ 46% Fill Factor	0.423 sq. in.	0.380 sq. in.
Litz Wire Cu. (Area=2 x solid cond.)	0.212 sq. in.	0.190 sq. in.
Turns	7	2
Number of strands (#33 Litz)	630	1995
DC Resistance (including leads)	.0044 ohm	.00036 ohm

As discussed in Paragraph 1.4 and Appendix 1, the use of Litz wire is expected to reduce significantly the winding I^2R losses in spite of the fact that the actual copper volume is reduced by two with a corresponding DC resistance increase. For comparison purposes, the expected AC and DC resistance values are presented in Table IV for the planned Litz wire coils and equivalent volume solid conductor coils.

TABLE IV - AC and DC Resistance of Litz Wire Coils and Solid Conductor Coils

Parameter	Primary Coil (l=25a.)		Secondary Coil (l=90a.)	
	Litz Wire	Solid Cond.	Litz Wire	Solid Cond.
DC Resistance (Ohms)	.0044	.0022	.00036	.00018
AC Resistance (Ohms)	.011	.0176	.00090	.00144
I^2R_{AC} Loss @ 10K Hz (watts)	6.89	11.0	7.29	11.66

The use of Litz wire at the presently proposed operating frequency of 10KHz results in a 37% or 8.5 watts power savings over the equivalent volume of solid conductors.

1.5.4 Transformer Disturbance Force Calculation

When the transformer is energized and loaded, magnetic fields are established in and around the two windings. If the secondary winding is not centered, the fields interact to produce forces on the windings.

In general, the force exerted ($\vec{F}$) on a current-carrying element in a magnetic field is given by

$$\vec{F} = \int \vec{J} \times \vec{B} \, dV(\text{volume})$$

where $\vec{F}$ is the force, $\vec{J}$ is the current density vector, $\vec{B}$ is the magnetic induction vector, and the integration extends over the volume of the conductor. Typically $\vec{J}$ is proportional to the current in the conductor considered and $\vec{B}$ is proportional to the currents in all the conductors present. For a transformer with two windings, the force (F2) on the secondary has the form

$$F2 = (a_{12})(I_1)(I_2) + (a_{22})(I_2)^2$$

where the a_i are functions of the position of the windings and I_1 and I_2 are the currents in the primary and secondary, respectively. The magnitude of the force is proportional to the products of the rms current values in the windings.

A finite element model of the quasi-magnetostatic field in the transformer was used to predict the $\vec{B}$ field in the windings during the extreme excursions. The $\vec{B}$ field was integrated over the volume of the secondary winding to obtain the maximum disturbance forces. The finite element method was used to obtain solutions of the quasi-static field in the rotary transformer. Maxwell's equations for magnetostatic fields are

$$\vec{\nabla} \cdot \vec{B} = 0$$

$$\vec{\nabla} \times \vec{H} = \vec{J}$$

where $\vec{H}$ is the magnetic field intensity vector (AMP/M). It was assumed that the constituent materials are magnetically linear so

$$\vec{B} = \mu \vec{H}$$

and that the magnetic induction may be obtained from a vector potential, $\vec{A}$, such that

$$\vec{B} = \vec{\nabla} \times \vec{A}$$

The variational form of Maxwell's equations is then

$$\int \Phi = 0,$$

$$\Phi = \frac{1}{2\mu} (\vec{\nabla} \times \vec{A}) * (\vec{\nabla} \times \vec{A}) \, dV$$

$$- \int \vec{A} * \vec{J} \, dv$$

$$+ \int \vec{A} * (\vec{n} \times \vec{H}) dS_{(surface)}$$

where n is the unit outward normal to the surface and the surface integral vanishes at all interior points. On the exterior boundary, the surface integral appears as a boundary condition and is evaluated through the Biot-Savart law,

$$dH = \frac{1}{4\pi r^3} (\vec{J} \times \vec{r}) \, dV$$

integrated over all the conducting elements. Axi-symmetric 4-noded isoparametric elements were used. The known (assumed uniform) current densities are the input sources. Simultaneous linear field equations were solved for the unknown vector potential $\vec{A}$ at the node points. The magnetic induction $\vec{B}$ is given by the curl of the vector potential and was output at the centroid of each element. The force per unit current was obtained by summing the $\vec{J} \times \vec{B}$ components from each element.

The flux leakage inside the cavity of the core is plotted for unit current in the primary, unit current in the secondary, and full load operation (Figures 5, 6, and 7 respectively). Only one half the cavity is shown in these plots (see sketch below) with the conducting area shaded.

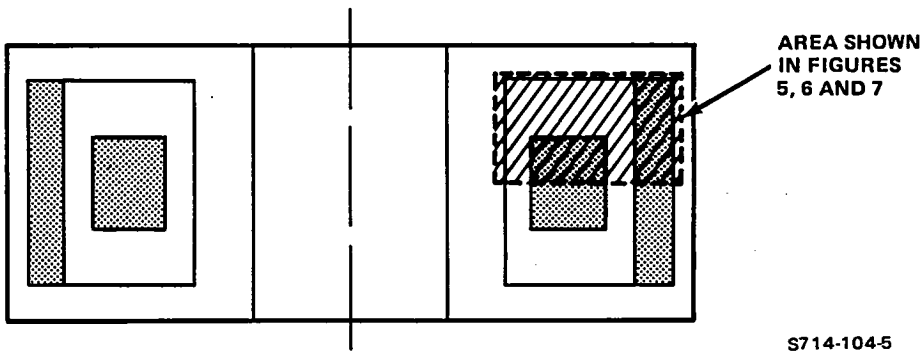

The axial component of leakage due to current in the primary winding was estimated by a hand calculation based on the relative reluctances of the air and ceramic core paths. This leakage prediction is plotted for comparision on the map of the field due to current in the primary (Figure 5). (Additional details of the force calculations are contained in Appendix 2).

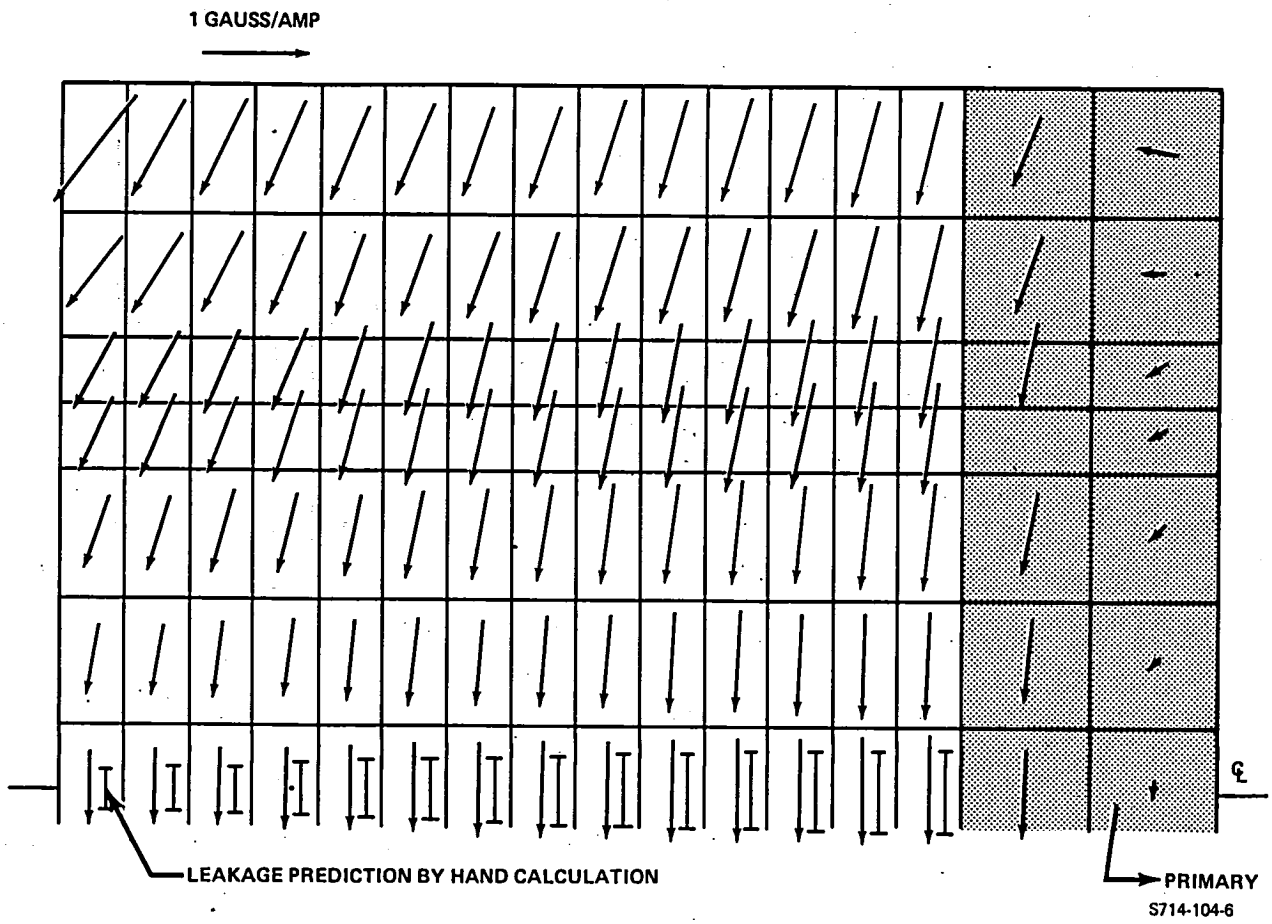

Figure 5
Flux Leakage Due to Unit Current in Primary

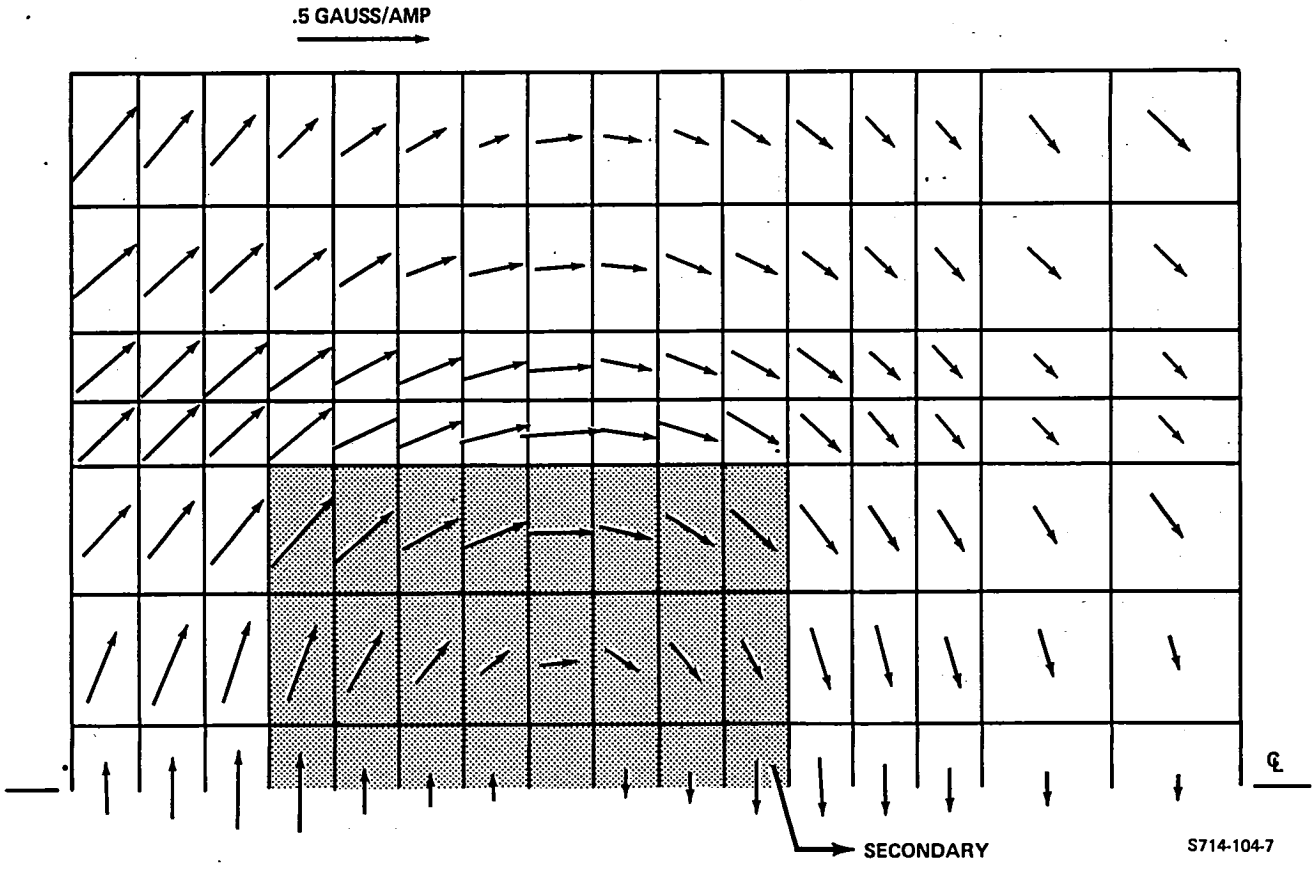

Figure 6
Flux Leakage Due to Unit Current in Secondary

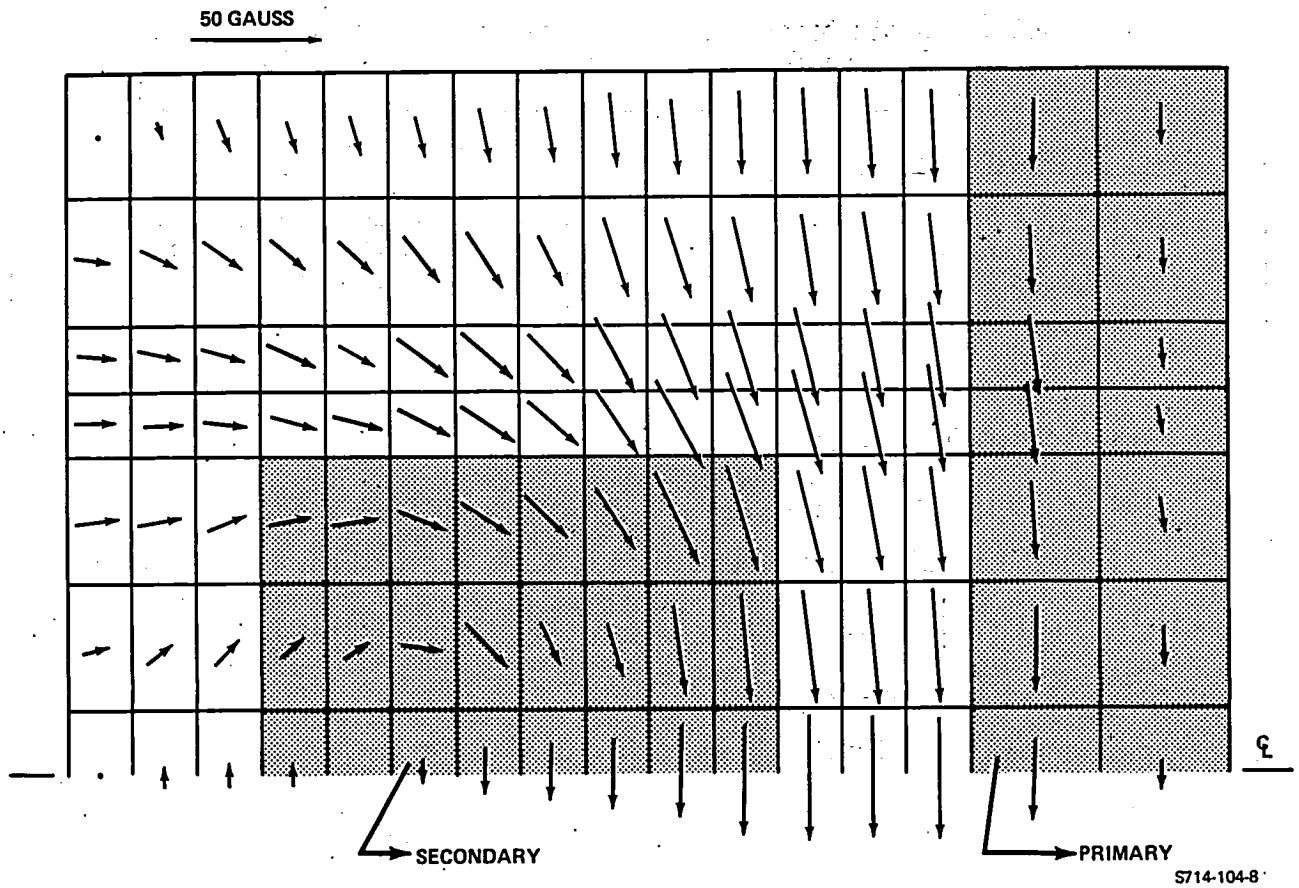

Figure 7
Flux Leakage at Full Load

The disturbance force amplitude predicted by the finite element model with the transformer operating at full load conditions are shown in Table V. The direction of the forces generated are always in a direction to oppose the relative motion between elements.

TABLE V - Disturbance Forces for Transformer at Full Load
Full Load as Predicted by Finite Element Model

Secondary Standard Coil Motion	Force/Torque, Direction
+/- .22 inch, Axial	+ .00244 pounds, Axial
+/- .20 inch, Radial	+ .00124 pounds, Radial
+/- .75 degrees, Tilt	+ .00053 inch-pounds, Tilt

1.5.5 Transformer Equivalent Circuit

The equivalent circuit for the transformer, operating at 10KHz, is derived using the same calculation methods as those described in Appendix 1. For ease of application, all transformer parameters (Table VI) are transferred to the primary side of the 3.5 to 1 ratio, "ideal" transformer. The transformer equivalent circuit is shown in Figure 8.

Table VI - Transformer Parameters

Parameter	Notation	Value
Magnetizing Inductance	LM	3.53 mh
Leakage Inductance	L_1 and L_2	4.4 μh (each)
Primary AC Resistance	R_1	.011 ohm
Secondary AC Resistance		
on secondary side	-	.00090 ohm
on primary side	R_2	.011 ohm
Core Loss Resistor	R_C	1600 ohms

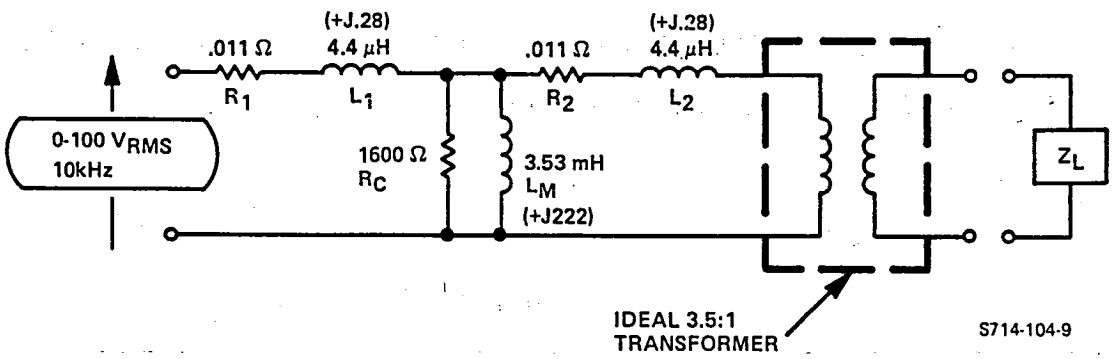

Figure 8
Transformer Equivalent Circuit

1.5.6 Transformer Performance and Weight Summaries Electrical

Working with the equivalent circuit derived in paragraph 1.5.5, and adjusting the load impedance (Z_L) to .315 ohms to obtain approximately 2500 watts output power level with 100 volts rms, 10KHz excitation, the electrical performance of Table VII is obtained.

TABLE VII - Transformer Electrical Performance Values

Parameter	Performance
Input Current	25.57 /-9.2° amps
Load Voltage	28.08 /-8.2° volts
Load Current	89.15 /-8.2° amps
Input Power	2524.1 watts
Load Power	2503.6 watts
Efficiency	99.2%
Primary Winding Power Loss	7.2 watts
Secondary Winding Power Loss	7.1 watts
Core Power Loss	6.2 watts

Disturbance Forces

The forces generated between the two transformer elements while supplying the 2500 watts output power are presented in Table V.

Weight

The transformer weight breakdown is shown in Table VIII.

Table VIII - Transformer Weight Breakdown

Part	Weight (pounds)
Ferrite Core	9.4
Primary Coil	1.5
Secondary Coil	1.0
Support Posts	0.1
Total	12.0

1.5.7 Frequency Selection

Assuming an operating frequency in the 5 to 15 KHz range as established in paragraph 2.5, the transformer design and performance parameters are relatively insensitive to the frequency selected. Therefore, the selection was conceded to the electronics section where significant tradeoffs existed and where the 10KHz baseline frequency was chosen.

The parameters considered in the tradeoff process are assessed as follows:

1) Disturbance Forces:

The disturbance forces are a function of the product of the ampere-turns (NI) in each of the two coils. Under loaded conditions, the currents are dictated by the excitation voltage and power requirements independent of frequency. The turns have been reduced to minimum practical numbers for optimum leakage inductance, also becoming independent of frequency. The disturbance forces are then independent of the frequency selected.

2) Weight:

The diameters and lengths of the transformer cores are determined by the coil areas required to obtain high efficiency, the required coil motions and clearances needed for low disturbance forces, and the self-imposed inner diameter constraint. The outer wall of the core is sized to the practical minimum and the remaining core sections are sized for uniform cross sectional areas. The transformer weight is, therefore, independent of frequency.

3) Power Loss:

Contributors to transformer power losses include the core loss due to eddy currents, hysteresis in the ferrite core, and the winding I^2R losses. The core loss, for a fixed mechanical configuration, decreases inversely with frequency to the 1.6 power (core loss::$K/f^{1.6}$). The skin effect in copper conductors causes the AC winding resistance to increase with frequency to approximately the 0.9 power. These two partially offsetting contributors result in a total power loss relatively insensitive to frequency as shown in Figure 9.

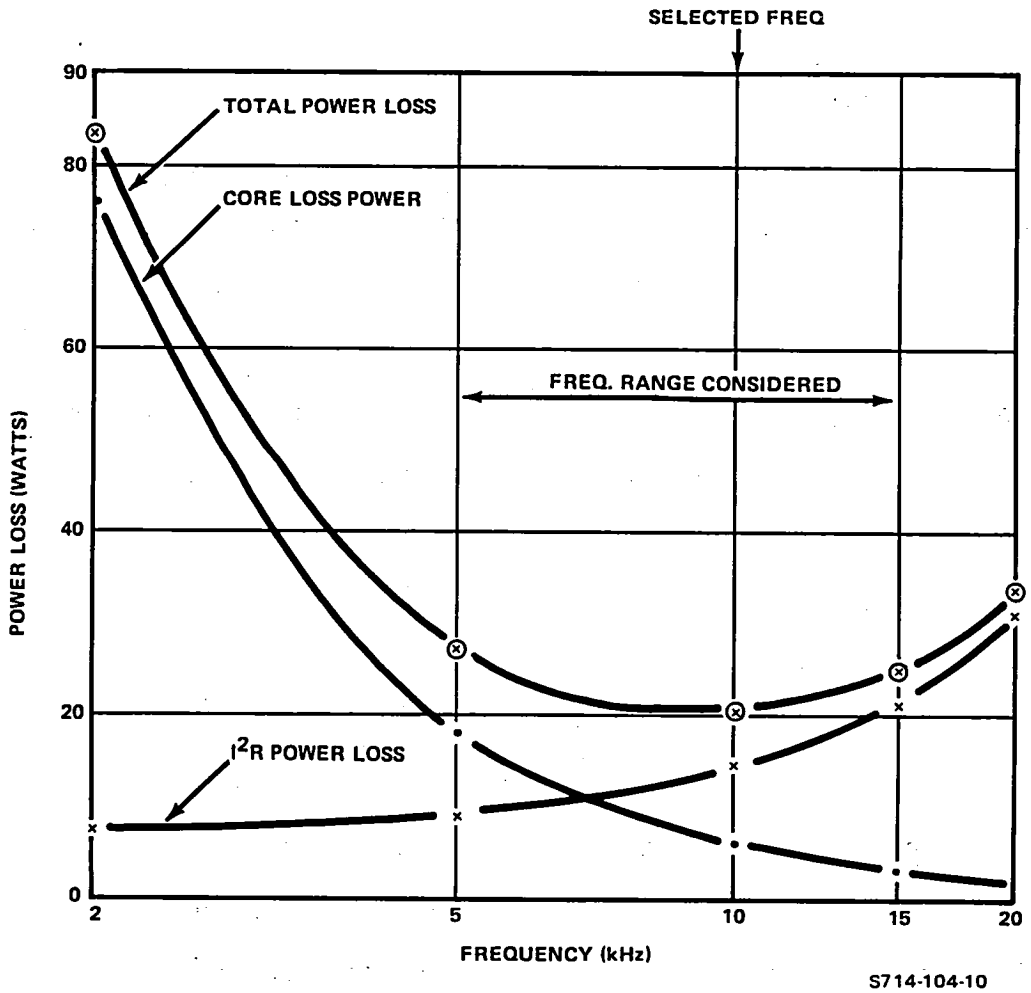

Figure 9
Transformer Power Loss Versus Frequency

PART II - ELECTRONICS DESIGN

2.1.0 Introduction

This section documents the electronics associated with the transmission of power across a gap in a non-contacting manner. The design of the rotary transformer is discussed in Part I of this report.

The design priorities specified by the Statement of Work were:

1) High efficiency.
2) Low weight.
3) Low EMI.

And, implied is:

4) Reliability.

Because both the input and output voltage is to be DC, and, in addition, a rotary transformer is to be included, then the design task is the design of a converter.

2.2.0 Topology Considerations

Various drive techniques for power conversion were considered. In the area of buck/boost/flyback topology, or switched energy pumping, the contenders were the full-wave and the half-wave drives, and the "Cuk" converter. The more recently developed "Cuk" converter was chosen as the better representative of these types of topology because of the low input and output ripple currents possible.

It should be recognized that, in any of these converters where it is possible to sacrifice weight for efficiency, the magnetics power losses can be made much smaller than the semi-conductor power losses. Examining the Cuk, half-wave, and full-wave drives from this viewpoint, the Cuk and half-wave drives appear equal in losses, while the full-wave bridge has higher losses because of voltage drops across two "on" devices. These observations are first-order, with second-order effects difficult to assess without actual prototyping of each converter. The first priority is low losses and thus the full-wave drive is eliminated.

The half-wave and Cuk converters, with equal losses, were next considered relative to weight and reliability. Two power switches must be controlled in the half-wave drive. This adds parts count and the existence of the hazard of having two switches on at the same time. It seems that the Cuk converter has the potential for higher reliability because only one power switch need be controlled (the second switch is a free-wheeling diode).

In examining the weight of these converters it is found that the large DC current inductors in the Cuk converter render this device heavier than the half-wave converter by perhaps a factor of two. Therefore, if the decision was made at this point, the half-wave converter would probably have been chosen based upon lower weight. However, the half-wave converter has a problem associated with regulation of the power delivered to the user.

If the converter were to achieve 80% efficiency, then at 2500 watts output power, converter losses would be 625 watts. Some of this loss is in resistive (copper) losses. Such resistance causes voltage drops which means that without some kind of regulation, the delivered bus voltage will be worse than the normal 24 to 32 volt bus. A ground-rule adopted in this design effort was to attempt to deliver power with no attributes worse than the original bus. The planned solution in the Cuk converter is to feed-forward the incoming bus voltage and control the transistor switch duty cycle thus compensating for input line variations in an absolutely stable manner (feed-forward rather than feed-back). By adding line regulation, a margin to accomodate load caused variations has been created. The Cuk converter has inherently low input ripple currents at any duty cycle of the switch.

Applying this technique, or any technique of regulation to the half-wave drive, results in modulation of the ON/OFF time ratio of the switches with resulting high input current pulsing. This pulsing (EMI) must be removed by adding a high-current input filter. The absence of such filtering inductors in the half-wave drive is why it originally presented lower weight. If the half-wave drive gains the weight of an additional EMI filter then the Cuk converter seems the better choice from the standpoint of simplicity and reliability.

2.3.0 Basic Operation of the Cuk Converter

A simple version of the Cuk converter is shown in Figure 10(a). With no current through L1 and no voltage across C, Q1 turns on. Current rises exponentially in L1. Q1 turns off. The current reached in L1 at turn-off now flows into C with the negative end of C clamped to ground by D1. A voltage is developed on C. Q1 turns on. Because of the voltage on the capacitor, Q1 reverse biases D1 thereby turning D1 off. Again, energy builds in L1 but now energy also exists in C. Load current builds through the load with C's charge supplying the energy and the current controlled by the L2-C-R circuit. As the repeating cycle reaches steady state, the waveforms of Figure 11 are generated.

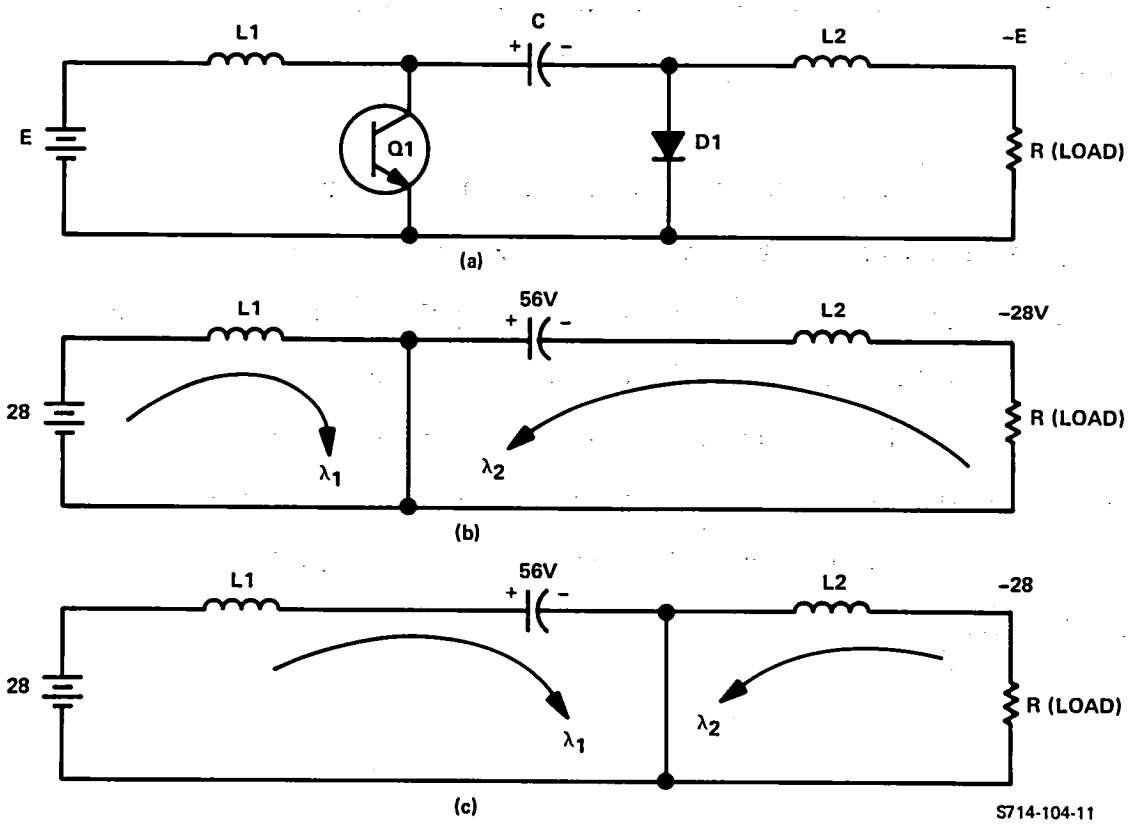

Figure 10
Cuk Converter Operation

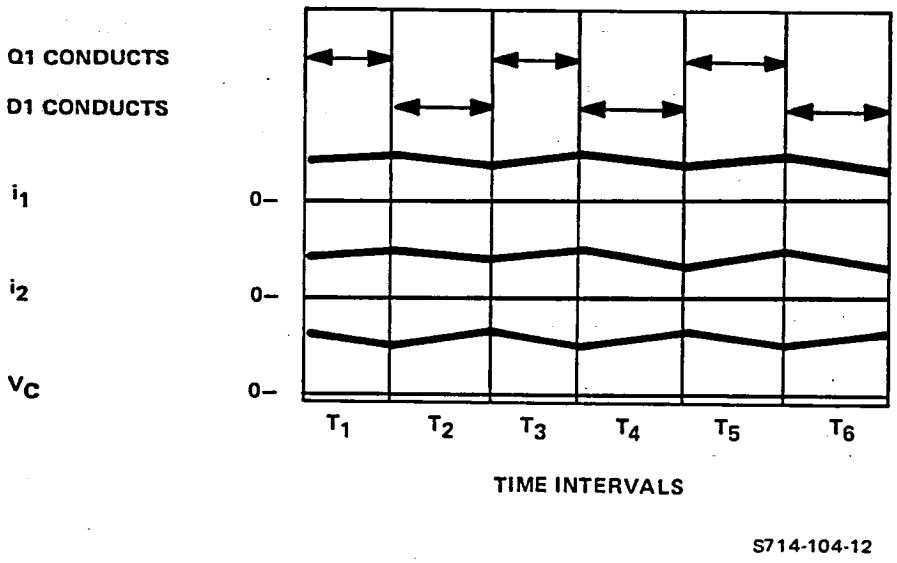

Figure 11
Waveforms

Although this simple version will be modified for the ASPS application, there are several characteristics to observe. When Vout=Vin, the duty cycle must be 0.5. The transistor and diode each conduct twice the load current for a half period. The charge voltage on the capacitor is twice Vout, and this voltage is both the off-state transistor collector voltage and the reverse diode voltage.

The ratio of Vout/Vin is a function of duty cycle such that Vout/Vin=D/(1-D). (See derivation in Figure 12). When D=.5 then Vout/Vin=-1.

From figure 10 (b) and (c), the capacitor current is i_2 when Q1 is on (T_{on}) and i_1 when Q1 is off (T_{off}). For a steady state condition to exist; $i_2 * t_{on} = i_1 * t_{off}$ (Eqn 1)

The duty cycle of Q1 is $\frac{t_{on}}{t_{on} + t_{off}} = D$

or $t_{off} = \frac{t_{on} * (1-D)}{D}$

so (Eqn 1) is $i_2 * t_{on} = i_1 \frac{t_{on} * (1-D)}{D}$

or $i_1 = i_2 * \frac{D}{1-D}$

At 100% efficiency $P_{in} = P_{out}$, $i_1 E = i_2^2 R$

or $i_2 * \frac{D}{1-D} E = i_2^2 R$

$\frac{D}{1-D} E = i_2 * R$

but $i_2 * R = -V_{out}$

thus $\frac{V_{out}}{E} = \frac{-D}{1-D}$

Figure 12
Voltage Transfer Ratio

2.3.1. Modification of Simple Circuit for AVS

The previous simple circuit has two problems. First, a negative voltage is produced. Second, a voltage step-up is desired in order to reduce the current in the long lines passing from the pedestal through the gimbals to the payload plate. A transformer will nicely solve both problems. The sequence of steps to take in introducing the transformer is depicted in figure 13.

In Figure 13(a), we have replaced the single capacitor with two capacitors. To maintain the same capacitance, each individual unit will be twice the value of the single unit. Also, to have the same total voltage of twice E, each unit will be charged to E. Note that this is also the same total stored energy.

The next step (Figure 13(b)) is to introduce an inductor to ground at the midpoint of the two capacitors. This can be done because otherwise there is no definition of what the midpoint voltage will be. With the inductor in place, then the midpoint voltage must average about ground as shown in Figure 13(d).

The final step is to consider the inductor a primary winding of a transformer, and to add the secondary winding as in Figure 13(c). Note that the transformer has inverted polarity which allows the diode to be reversed and provides a positive output voltage.

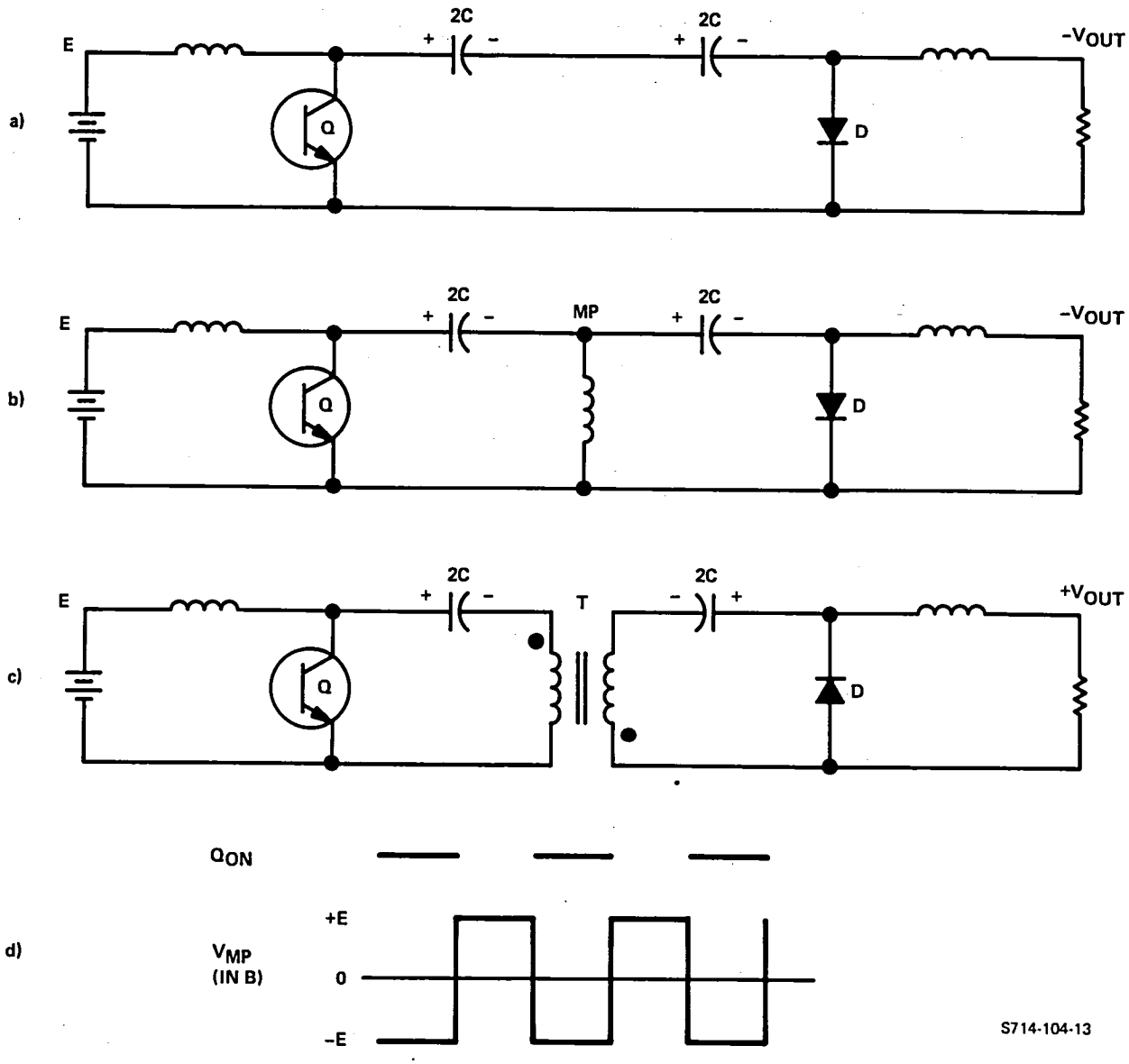

Figure 13
CUK Modification

The proposed layout of the converter for use in AVS is shown in Figure 14. The Cuk transformer is a step-up transformer which is followed by the rotary transformer which is a step-down transformer. In this way, the long line current is reduced for lower losses. A ratio of four is used after considering voltage breakdown stresses of the flex capsules used to pass wires through gimbal pivots with minimum torques. Long-line currents of twenty-five amperes are anticipated.

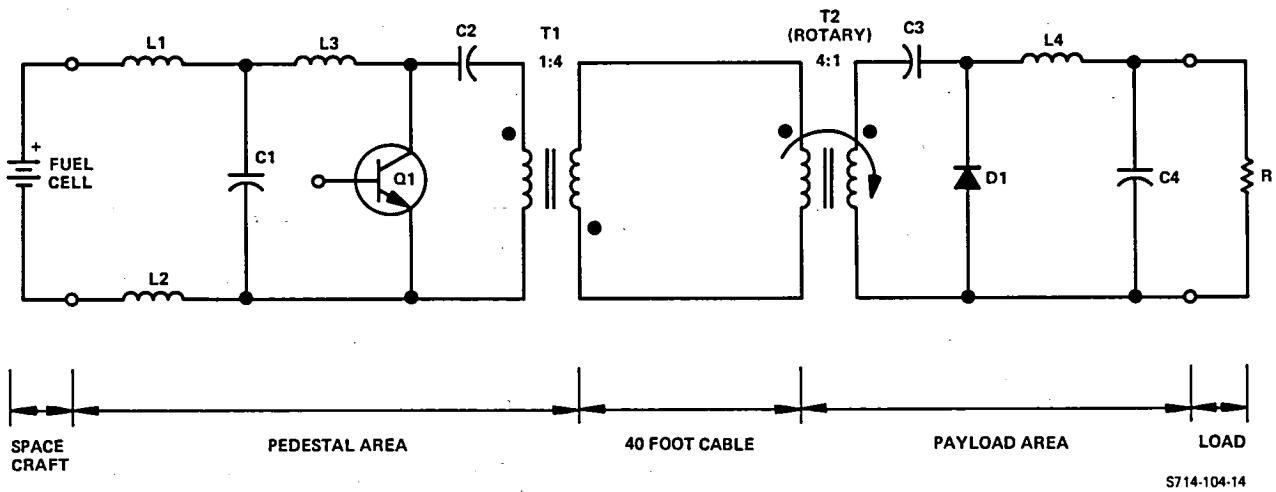

Figure 14
General Layout

2.4.0 Computer Design Programs

It was desired to study tradeoffs of converter weight and power losses as the operating frequency is changed. If the design problem were only that of choosing the converter component values, then manual calculations might be appropriate. However, in addition to component values, magnetic designs were involved for the EMI inductors, the Cuk inductor, and the step-up transformer. The magnetic designs themselves involve tradeoffs in the area of core weight, operating flux density, and wire cross section. Considering the magnitude of this task, computer solutions appeared necessary.

Design programs that include built-in optimization routines deny the designer vision into the sensitivities within the problem. Preferred is a large amount of output data where the designer can see a broad area of the design alternatives, and can then base his decisions on this information. In the case of the Cuk converter, this philosophy dictated two programs - one that produced the large quantity of data, and the other a final summary of the design results after entry of designer decisions. The first was titled "CUK.DES" and the latter "CUK.SUM" (for summary). Both programs are described in this section.

2.4.1 Design Program "CUK.DES"

The program "CUK.DES" produced output data at the six frequencies of 5, 10, 15, 25, 45, and 100 KHz. Converter components are identified by the labels shown in Figure 14.

2.4.1.1 EMI Filter Component Values

The filter formed by L1, L2, and C1 must reduce the triangular input ripple current to magnitudes acceptable to MIL-STD-461A. At the frequencies of concern, the allowed currents, reduced by 12 dB for design margin, are shown in Table IX.

TABLE IX - EMI Requirements

Freq (Hz)	Current (amp)
5K	.079
10K	.0125
25K	.005
45K	.00089
100K	.0004

The next step was to establish a design guideline concerning the amount of input ripple allowed after the EMI filter. This guideline was to design for peak-to-peak input ripple of 10% of the maximum load current.

Because 1000 microfarad tantalum foil capacitors have a reasonably small volume and weight, and because the capacitor ripple current for C1 was small (not demanding ultra low ESR), this value was selected for C1. (This could have have been a later tradeoff if L1, L2 designs proved too large).

The value of L1 and L2 were computed as shown in Figure 15. The resulting equation is located at [1430] in Figure 16, Program Listing 1. (In this report, listing line number references will appear as a number in brackets, as seen above.)

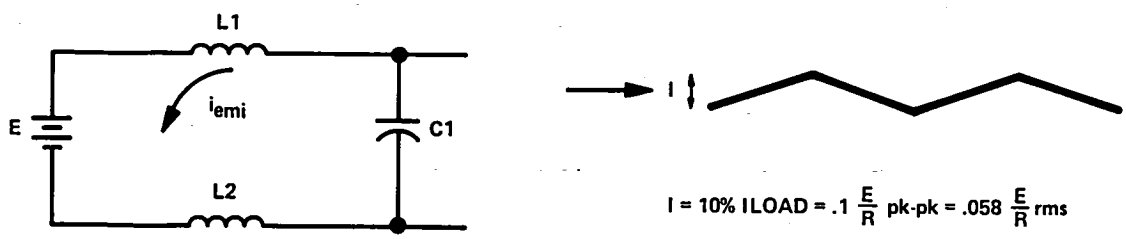

RIPPLE CURRENT, I, CAUSES VOLTAGE RIPPLE ON C1 WHICH PRODUCES CURRENT (CONDUCTED EMISSIONS) BACK THRU THE POWER LEADS, LIMITED BY L1 AND L2 ($R_{FUEL\ CELL} = 0$)

$$V_C = i_C X_C = \frac{.058\ E/R}{WC1} = \frac{.058\ E}{WRC}$$

$$i_{emi} = \frac{V_C}{X_{L1} + X_{L2}} = \frac{V_C}{2X_{L1}} = \frac{V_C}{2WL1} = \frac{.058\ E}{2W^2\ R\ L1\ C1} = \frac{.029\ E}{W^2\ R\ L1\ C1}$$

LET i_{emi} ALLOWED = A(J) FROM TABLE 1 WITH J = FREQUENCY

$$A(J) = \frac{.029\ E/R}{(2\pi f)^2\ L_1\ C_1}$$

$$L_1 = L_2 = \frac{.029\ E/R}{(2\pi f)^2\ C1\ A(J)}$$

S714-104-15

Figure 15
Calculation of L1, L2

```
!HCO 4M

0900 REM PROGRAM SAVED UNDER "CUK.DES"
1000 OPEN FILE (1), "CUKDAT"
1010 PRINT FILE (1), "*************************************************"
1020 PRINT FILE (1), "*CUK COMPONENT SELECTIONS     T.GUNDERMAN 10/9/82 *"
1025 PRINT FILE (1), "*REVISION 14-20 DEC 82                          *"
1030 PRINT FILE (1), "*************************************************"
1040 PRINT FILE (1)
1050 DIM A(6)
1050 PRINT "WHAT IS INPUT VOLTAGE";
1070 INPUT E
1080 PRINT "WHAT IS LOAD RESISTANCE";
1090 INPUT R
1100 PRINT "WHAT IS STEP-UP TURNS RATIO";
1110 INPUT N
1120 PRINT "WHAT IS MAX WEIGHT OF EMI FILTER INDUCTOR";
1130 INPUT R7
1140 PRINT "WHAT IS MAX WEIGHT OF CUK INDUCTOR";
1150 INPUT R8
1160 PRINT "WHAT IS MAX WEIGHT OF CUK TRANSFORMER";
1170 INPUT R9
1180 PRINT "NAME PRACTICAL LIMIT ON PARALLEL WIRES";
1190 INPUT K9
1200 PRINT FILE (1)
1210 PRINT FILE (1)
1220 PRINT FILE (1), "CORE MATERIAL IS METGLASS"
1230 PRINT FILE (1)
1240 PRINT FILE (1)
1250 PRINT FILE (1)
1260 PRINT FILE (1), "SPECIFIED VOLTAGE=";E;" AT LOAD R=";R;" OHMS."
1270 PRINT FILE (1), "SPECIFIED MAX NUMBER OF TURNS ON L'S & T =";K9
1280 REM DETERMINE ALL COMPONET VALUES
1290 REM FIRST READ EMI INPUT CURRENT LIMITS
1300 FOR J=1 TO 6
1310   READ A(J)
1320 NEXT J
1330 DATA .079, .0125, .005, .0022, .00099, .0004
1340 FOR J=1 TO 6
1350   IF J=1 THEN LET F=5000
1360   IF J=2 THEN LET F=1000
1370   IF J=3 THEN LET F=15000
1380   IF J=4 THEN LET F=25000
1390   IF J=5 THEN LET F-45000
1400   IF J=6 THEN LET F=100000
1410   PRINT FILE (1), "CONVERTER DESIGN FOR";E*E/R;"WATTS AT";F;" KHZ"
1420   LET C1=.001
1430   LET L1=(.029*E/R)/((2*3.14159*F)^2*C1*A(J))
1440   LET L2=L1
```

Figure 16
Program Listing 1
(Sheet 1 of 2)

```
1450   LET L3=R/(.2*F)
1460   LET L4=L3
1470   LET C2=2/(.4*F*R)
1480   LET C3=C2
1490   LET C4=.25*E/(F*R)
1500   PRINT FILE (1),"EMI CAPACITOR PREDEFINED AS 1000 MICROFARADS."
1510   PRINT FILE (1),"EMI INDUCTORS EACH ARE";L1*1000000;" MICROHENRIES."
1520   PRINT FILE (1),"CUK CAPACITORS EACH ARE";C2*1000000;" MICROFARADS."
1530   PRINT FILE (1),"CUK INDUCTORS EACH ARE";L3*1000;" MILLIHENRIES."
1540   PRINT FILE (1),"OUTPUT CAPACITOR VALUE IS";C4*1000000;"MICROFARADS."
1550   PRINT FILE (1)
1560   PRINT FILE (1)
1570   PRINT FILE (1)
1580   PRINT FILE (1)
1590   GOSUB 2570                                          (see figure 28)
1600   PRINT FILE (1)
1610   PRINT FILE (1)
1620   PRINT FILE (1)
1630   GOSUB 2670                                          (see figure 28)
1640   REM NOW PRESENT SELECTION OF INDUCTORS FOR EMI AND CUK INDUCTORS
1650   LET W2=R7
1660   LET W1=W2/10
1670   LET L=L1
1680   LET I=E/R
1690   PRINT FILE (1)," 12 "
1700   PRINT FILE (1),"CHOOSE EMI INDUCTOR WEIGHT FROM ATTRIBUTE LIST BELOW"
1710   GOSUB 1880                                          (see figure 23)
1720   LET W2=R8
1730   LET W1=W2/10
1740   LET L=L3
1750   PRINT FILE (1)," 12 "
1760   PRINT FILE (1),"CHOOSE CUK INDUCTOR WEIGHT FROM ATTRIBUTE LIST BELOW"
1770   GOSUB 1880                                          (see figure 23)
1780   LET Y2=R9
1790   LET Y1=Y2/10
1800   PRINT FILE (1)," 12 "
1810   PRINT FILE (1),"CHOOSE CUK TRANSFORMER WEIGHT FROM ATTRIBUTE LIST BELOW"
1820   GOSUB 2180                                          (see figure 28)
1830   PRINT FILE (1)," 12 "
1840   PRINT FILE (1)," 12 "
1850 NEXT J
1860 CLOSE FILE (1)
1870 STOP
*
```

Figure 16
Program Listing 1
(Sheet 2 of 2)

2.4.1.2 Cuk Inductor Value Selection

The design rule given in 2.4.1.1 of 10% load pk-pk ripple current at both input and output furnished the necessary criteria to size L_3, and L_4. This computation is shown in Figure 17 and the final equation appears in Figure 16 [1450].

L_3 gains energy during period $\frac{1}{2F}$ when Q1 is on (50% duty cycle)

$$e = L_3 \frac{di}{dt} \qquad 2E = L_3 \frac{I}{1/2F} = 2F * L_3 * \Delta I$$

$$L_3 = \frac{E}{2F * \%I} \quad \text{but } \Delta I - .1 * I_{DC} = .1 * E/R$$

$$L_3 = \frac{E}{2F * (.1E/R)} = \frac{R}{.2F} \text{ and } L_4 = L_3$$

Figure 17
Calculation of L3, L4

2.4.1.3 Cuk Capacitor Value Selection

The ground-rule leading to the selection of C_2 and C_3 was the allowed ripple voltage on the capacitor. The importance of this voltage is that it increases the collector voltage of Q1 as well the reverse voltage on D1. Voltage stresses on large geometry power devices is a critical stress and for this reason the guideline was to design for 20% pk-pk of the normal DC charge voltage. This lead to the calculations of Figure 18 whose final equation is found in Figure 16 [1470].

Allow 10%* Droop on C_2 and C_3 at 50% Duty Cycle

$$i = C_2 \frac{dv}{dt} \qquad C_2 = \frac{i\Delta t}{\Delta v} = \frac{E/R}{2F(.1E)} = \frac{15}{FR}$$

$$C_2 = C_3$$

*for a combined droop of 20%

Figure 18
Calculation of C_2, C_3

2.4.1.4 Output Capacitor Value Selection

The value of C_4 was determined when the allowed pk-pk output ripple was specified. This output ripple was 100 mv. pk-pk. The calculations are found in Figure 19 whose final equation is found in Figure 16 [1490].

Allow .1 volt output ripple on C_4 as a result of i_{ripple}

$$i = C_4 \frac{dv}{dt} \qquad C_4 = \frac{i\Delta t}{\Delta v}$$

$i_{pk\text{-}pk} = .1\ E/R$ and during $\frac{1}{2F}$ period $I_{avg.} = .05\ E/R$

$$C_4 = \frac{.05\ E/R - 1/2F}{.1} = \frac{.25\ E}{FR}$$

Figure 19
Calculation of C_4

2.4.1.5 Program Operation

Figure 20, Program Listing 2, shows the designer inputs to the program, with underlined items being keystrokes. After receiving these inputs, the program computed, at each of the six frequencies, each of the inductor and transformer designs at 10 different core weights and for four operating fractions of the material's saturating flux density. The selection of Metglass as the core material was made.

```
WHAT IS INPUT VOLTAGE? 28
WHAT IS LOAD RESISTANCE? .31
WHAT IS STEP-UP TURNS RATIO? 4
WHAT IS MAX WEIGHT OF EMI FILTER INDUCTOR? 5
WHAT IS MAX WEIGHT OF CUK INDUCTOR? 5
WHAT IS MAX WEIGHT OF CUK TRANSFORMER? 2
NAME PRACTICAL LIMIT ON PARALLEL WIRES? 10
```

Figure 20
Program Listing 2

Program Listing 1 (Figure 16) designed the magnetics by the use of two subroutines discussed in the following two sections. Program Listing 3, Figure 21, shows the output data produced for 10KHz. The program summarizes the component values before listing the various magnetic designs.

In Program Listing 3 (Figure 21) the column labeled 'X' is a normalized core dimension which is explained in paragraph 2.4.6.1. The columns PL1 and PL2 are the number of wires in parallel to make each turn. Actually, Litz wire or wire strip, keeping the same specified wire area, was used in the final design.

The desired core weights are marked with an asterisk in Listing 3 (Figure 21) and represent the designer's choice of the available designs. Involved here was the idea that a saving of a pound of weight (perhaps 5% of the total) would be made if it cost but a small fraction of the total power loss. Also considered was whether the particular component's power loss relative to its size (weight) would result in too high a temperature rise, and whether the resulting air gap of the inductors was reasonable from a fringing viewpoint.

```
CONVERTER DESIGNED FOR 2529.0323 WATTS AT 10000 KHZ
EMI CAPACITOR PREDEFINED AS 1000 MICROFARADS.
EMI INDUCTORS EACH ARE 53.079316 MICROHENRIES.
CUK CAPACITORS EACH ARE 1612.9032 MICROFARADS.
CUK INDUCTORS EACH ARE .155 MILLIHENRIES.
OUTPUT CAPACITOR VALUE IS 2258.0645 MICROFARADS.

FOR THE CUK CAPACITOR (C2, C3) OF 1612.9032 MICROFARADS.
A TOTAL OF 54 UNITS ARE REQUIRED FOR EACH CAP.
POWER LOSS IS .90646317 WATTS EACH (C2 AND C3)
EACH 30 MICROFARAD CAP HAS A RIPPLE CURRENT OF 1.6726404 AMPS
  (11.4 AMPS ARE ALLOWED)
THE WEIGHT OF C2 AND C3 IS 4.752 POUNDS EACH

CHOOSE EMI INDUCTOR WEIGHT FROM ATTRIBUTE LIST BELOW
FREQ= 10000 HZ
GAP IS IN MILLICENTIMETERS AND RESISTANCE IS IN MILLIOHMS
```

Figure 21
Program Listing 3
(Sheet 1 of 4)

WT	GAP	X	TURNS	PRL	RES	P-CU	P-FE	P-GAP	P-TOT
CORE OPERATING AT .2 TIMES B-MAX									
1.5	1429.00	1.93	72.00	1.00	44.43	362.47	0.21	0.55	363.23
2.0	1179.61	2.12	53.00	3.00	12.00	97.89	0.23	0.50	98.61
2.5	1016.56	2.29	43.00	4.00	7.87	64.17	0.25	0.46	64.88
3.0	900.21	2.43	36.00	5.00	5.60	45.67	0.27	0.43	46.37
3.5	812.30	2.56	31.00	7.00	3.62	29.57	0.29	0.41	30.27
4.0	743.11	2.67	27.00	9.00	2.57	20.94	0.30	0.39	21.63
4.5	686.99	2.78	24.00	10.00	2.14	17.43	0.31	0.38	18.11
5.0	640.39	2.88	22.00	10.00	2.03	16.54	0.33	0.37	17.24
CORE OPERATING AT .4 TIMES B-MAX									
1.0	468.13	1.68	39.00	2.00	10.51	85.76	0.35	0.63	86.73
1.5	357.25	1.93	26.00	5.00	3.21	26.18	0.40	0.55	27.12
2.0	294.90	2.12	20.00	8.00	1.70	13.85	0.46	0.50	14.81
2.5	254.14	2.29	17.00	10.00	1.24	10.15	0.54	0.46	11.15
3.0	225.05	2.43	14.00	10.00	1.09	8.88	0.56	0.43	9.87
3.5	203.07	2.56	12.00	10.00	0.98	8.01	0.58	0.41	9.00
4.0	185.78	2.67	11.00	10.00	0.94	7.68	0.65	0.39	8.73
4.5	171.75	2.78	10.00	10.00	0.89	7.26	0.70	0.38	8.34
5.0	160.10	2.88	9.00	10.00	0.83	6.77	0.71	0.37	7.85
CORE OPERATING AT .6* TIMES B-MAX									
0.5	330.27	1.34	44.00	1.00	18.83	153.59	0.42	0.79	154.79
1.0	208.06	1.68	22.00	4.00	2.96	24.19	0.52	0.63	25.33
1.5	158.78	1.93	15.00	8.00	1.16	9.44	0.60	0.55	10.59
2.0*	131.07	2.12	12.00	10.00	0.82	6.65	0.72	0.50	7.87*
2.5	112.95	2.29	10.00	10.00	0.73	5.97	0.81	0.46	7.24
3.0	100.02	2.43	9.00	10.00	0.70	5.71	0.96	0.43	7.10
3.5	90.26	2.56	8.00	10.00	0.65	5.34	1.05	0.41	6.80
4.0	82.57	2.67	7.00	10.00	0.60	4.89	1.05	0.39	6.34
4.5	76.33	2.78	6.00	10.00	0.53	4.36	0.99	0.38	5.73
5.0	71.15	2.88	6.00	10.00	0.55	4.51	1.21	0.37	6.08
CORE OPERATING AT .8 TIMES B-MAX									
0.5	185.78	1.34	29.00	2.00	6.20	50.61	0.54	0.79	51.94
1.0	117.03	1.68	15.00	6.00	1.35	10.99	0.69	0.63	12.31
1.5	89.31	1.93	11.00	10.00	0.68	5.54	0.89	0.55	6.97
2.0	73.73	2.12	9.00	10.00	0.61	4.99	1.08	0.50	6.57
2.5	63.53	2.29	7.00	10.00	0.51	4.18	1.04	0.46	5.68
3.0	56.26	2.43	6.00	10.00	0.47	3.81	1.09	0.43	5.33
3.5	50.77	2.56	5.00	10.00	0.41	3.34	1.03	0.41	4.78
4.0	46.44	2.67	5.00	10.00	0.43	3.49	1.30	0.39	5.19
4.5	42.94	2.78	5.00	10.00	0.44	3.63	1.59	0.38	5.60
5.0	40.02	2.88	4.00	10.00	0.37	3.01	1.25	0.37	4.63

*See paragraph 2.4.1.5

Figure 21
Program Listing 3
(Sheet 2 of 4)

CHOOSE CUK INDUCTOR WEIGHT FROM ATTRIBUTE LIST BELOW
FREQ= 10000 HZ
GAP IS IN MILLICENTIMETERS AND RESISTANCE IS IN MILLIOHMS

WT	GAP	X	TURNS	PRL	RES	P-CU	P-FE	P-GAP	P-TOT
CORE OPERATING AT .2 TIMES B=MAX									
3.0	2628.76	2.43	130.00	1.00	101.07	824.57	0.41	1.27	826.24
4.0	2170.00	2.67	98.00	2.00	41.93	342.08	0.46	1.15	343.69
5.0	1870.05	2.88	79.00	3.00	24.27	198.03	0.50	1.07	199.61
6.0	1656.02	3.06	66.00	5.00	12.93	105.49	0.54	1.01	107.03
7.0	1494.29	3.22	57.00	6.00	9.80	79.92	0.58	0.96	81.45
8.0	1367.01	3.37	51.00	8.00	6.87	56.07	0.63	0.91	57.62
9.0	1263.78	3.50	45.00	9.00	5.61	45.74	0.65	0.88	47.27
10.0	1178.05	3.63	41.00	10.00	4.76	38.85	0.69	0.85	40.38
CORE OPERATING AT .4 TIMES B=MAX									
2.0	861.16	2.12	73.00	2.00	24.79	202.25	0.73	1.45	204.43
3.0	657.19	2.43	49.00	4.00	9.52	77.70	0.85	1.27	79.82
4.0	542.50	2.67	38.00	6.00	5.42	44.21	0.99	1.15	46.36
5.0	467.51	2.88	31.00	9.00	3.18	25.90	1.11	1.07	28.08
6.0	414.00	3.06	27.00	10.00	2.64	21.58	1.27	1.01	23.85
7.0	373.57	3.22	24.00	10.00	2.47	20.19	1.42	0.96	22.56
8.0	341.75	3.37	21.00	10.00	2.26	18.47	1.47	0.91	20.86
9.0	315.94	3.50	19.00	10.00	2.13	17.38	1.57	0.88	19.83
10.0	294.51	3.63	18.00	10.00	2.09	17.05	1.77	0.85	19.67
CORE OPERATING AT .6* TIMES B=MAX									
1.0	607.56	1.68	82.00	1.00	44.20	360.63	0.87	1.83	363.32
2.0	382.74	2.12	42.00	3.00	9.51	77.57	1.14	1.45	80.17
3.0	292.08	2.43	29.00	7.00	3.22	26.28	1.38	1.27	28.92
4.0	241.11	2.67	23.00	10.00	1.97	16.06	1.65	1.15	18.86*
5.0	207.78	2.88	19.00	10.00	1.75	14.29	1.85	1.07	17.21
6.0	184.00	3.06	16.00	10.00	1.57	12.79	1.96	1.01	15.75
7.0	166.03	3.22	15.00	10.00	1.55	12.62	2.38	0.96	15.95
8.0	151.89	3.37	13.00	10.00	1.40	11.43	2.39	0.91	14.73
9.0	140.42	3.50	12.00	10.00	1.35	10.98	2.60	0.88	14.46
10.0	130.89	3.63	11.00	10.00	1.28	10.42	2.72	0.85	13.99
CORE OPERATING AT .8 TIMES B=MAX									
1.0	341.75	1.68	54.00	1.00	29.11	237.49	1.14	1.83	240.45
2.0	215.29	2.12	29.00	5.00	3.94	32.14	1.60	1.45	35.18
3.0	164.30	2.43	20.00	10.00	1.55	12.69	1.87	1.27	15.83
4.0	135.62	2.67	16.00	10.00	1.37	11.17	2.23	1.15	14.55
5.0	116.88	2.88	14.00	10.00	1.29	10.53	2.72	1.07	14.32
6.0	103.50	3.06	12.00	10.00	1.18	9.59	2.92	1.01	13.52
7.0	93.39	3.22	11.00	10.00	1.13	9.25	3.34	0.96	13.55
8.0	85.44	3.37	10.00	10.00	1.08	8.80	3.60	0.91	13.31
9.0	78.99	3.50	9.00	10.00	1.01	8.23	3.67	0.88	12.78
10.0	73.63	3.63	8.00	10.00	0.93	7.58	3.57	0.85	11.99

*See paragraph 2.4.1.5

Figure 21
Program Listing 3 (Sheet 3 of 4)

CHOOSE CUK TRANSFORMER WEIGHT FROM ATTRIBUTE LIST BELOW
FREQ= 10000 HZ
RESISTANCE IS IN MILLIOHMS

WT	'X'	N1	N2	PL1	PL2	PRW-1	PWR-2	P-FE	P-TOTL
CORE OPERATING AT .2* OF B=MAX									
1.00	1.34	6.00	24.00	5.00	1.00	5.14	6.42	5.41	16.97
1.50	1.53	4.00	16.00	10.00	2.00	1.96	2.45	8.12	12.53*
2.00	1.68	3.00	12.00	10.00	4.00	1.62	1.01	10.82	13.45
2.50	1.82	3.00	12.00	10.00	4.00	1.74	1.09	13.53	16.36
3.00	1.93	2.00	8.00	10.00	8.00	1.23	0.39	16.24	17.86
3.50	2.03	2.00	8.00	10.00	9.00	1.30	0.36	18.94	20.60
4.00	2.12	2.00	8.00	10.00	10.00	1.36	0.34	21.65	23.35
4.50	2.21	2.00	8.00	10.00	10.00	1.41	0.35	24.36	26.12
5.00	2.29	2.00	8.00	10.00	10.00	1.46	0.37	27.06	28.89
CORE OPERATING AT .4 OF B=MAX									
0.50	1.06	4.00	16.00	5.00	1.00	2.72	3.40	9.89	16.01
1.00	1.34	3.00	12.00	10.00	2.00	1.28	1.61	19.78	22.67
1.50	1.53	2.00	8.00	10.00	5.00	0.98	0.49	29.68	31.15
2.00	1.68	2.00	8.00	10.00	6.00	1.08	0.45	134.83	136.36
2.50	1.82	2.00	8.00	10.00	7.00	1.16	0.42	127.61	129.18
3.00	1.93	2.00	8.00	10.00	8.00	1.23	0.39	122.00	123.62
3.50	2.03	2.00	8.00	10.00	9.00	1.30	0.36	117.44	119.11
4.00	2.12	2.00	8.00	10.00	10.00	1.36	0.34	113.64	115.34
4.50	2.21	2.00	8.00	10.00	10.00	1.41	0.35	110.38	112.15
5.00	2.29	2.00	8.00	10.00	10.00	1.46	0.37	107.55	109.38
CORE OPERATING AT .6 OF B=MAX									
0.50	1.06	3.00	12.00	6.00	1.00	1.70	2.55	21.11	25.36
1.00	1.34	2.00	8.00	10.00	4.00	0.86	0.54	42.23	43.62
1.50	1.53	2.00	8.00	10.00	5.00	0.98	0.49	144.74	146.21
2.00	1.68	2.00	8.00	10.00	6.00	1.08	0.45	134.83	136.36
2.50	1.82	2.00	8.00	10.00	7.00	1.16	0.42	127.61	129.18
3.00	1.93	2.00	8.00	10.00	8.00	1.23	0.39	122.00	123.62
3.50	2.03	2.00	8.00	10.00	9.00	1.30	0.36	117.44	119.11
4.00	2.12	2.00	8.00	10.00	10.00	1.36	0.34	113.64	115.34
4.50	2.21	2.00	8.00	10.00	10.00	1.41	0.35	110.38	112.15
5.00	2.29	2.00	8.00	10.00	10.00	1.46	0.37	107.55	109.38
CORE OPERATING AT .8 OF B=MAX									
0.50	1.06	2.00	8.00	10.00	2.00	0.68	0.85	36.16	37.69
1.00	1.34	2.00	8.00	10.00	4.00	0.86	0.54	159.97	161.36
1.50	1.53	2.00	8.00	10.00	5.00	0.98	0.49	144.74	146.21
2.00	1.68	2.00	8.00	10.00	6.00	1.08	0.45	134.83	136.36
2.50	1.82	2.00	8.00	10.00	7.00	1.16	0.42	127.61	129.18
3.00	1.93	2.00	8.00	10.00	8.00	1.23	0.39	122.00	123.62
3.50	2.03	2.00	8.00	10.00	9.00	1.30	0.36	117.44	119.11
4.00	2.12	2.00	8.00	10.00	10.00	1.36	0.34	113.64	115.34
4.50	2.21	2.00	8.00	10.00	10.00	1.41	0.35	110.38	117.15
5.00	2.29	2.00	8.00	10.00	10.00	1.46	0.37	107.55	109.38

Figure 21
Program Listing 3 (Sheet 4 of 4)

2.4.1.6 Air-Gapped Inductor Design Subroutine

Program Listing 1, Figure 16, calls to an inductor design subroutine (figure 28) to determine inductor characteristics for a given weight, DC current, and frequency. When manually designing inductors, a common approach is to determine the sizing from an equation relating the product of window area with core cross-sectional area. This technique places the designer in the vicinity of a possible solution but requires iteration since it is not an exact solution to the multi-dimensional problem. In some past computer driven solutions, a table of vendor core shapes within the program would allow a multiple design process to choose an adequate design.

The approach taken here, as well as in the transformer subroutine, to be described in the next section, was similar to the vendor catalog approach except the core dimensioning was normalized to a standard form factor. This allowed more of a one to one comparison which was not manufacturer dependent.

2.4.1.6.1 Standard Geometry

The standard C-Core geometry with all dimensions related to the 'stack' height "x" is shown in Figure 22. From these dimensions all needed geometry relationships were calculated as also shown in Figure 22.

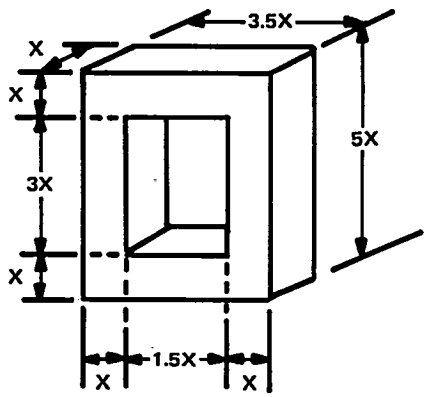

VOLUME: 13 x^3
AC: X^2 (CORE CROSS SECTION)
WA: 4.5 X^2 (WINDOW AREA)
MLT: 10 X (MEAN TURN LENGTH)
LC: (CORE LENGTH)

S714-104-16

Figure 22
Normalized Core

The subroutine used is shown in Program Listing 4, figure 23. Note that there are two nested loops - first in Z [1950] and then in W [1980].

```
!HCO 1M

1880 REM AIR GAPPED INDUCTOR SELECTION
1890 PRINT FILE (1),"FREQ=";F;"HZ"
1900 PRINT FILE (1),"GAP IS IN MILLICENTIMETERS AND RESITANCE IS IN MILLIOHMS"
1910 PRINT FILE (1)
1920 PRINT FILE (1),"WT    GAP    X    TURNS":
1930 PRINT FILE (1), TAB(37);"PRL    RES    P-CU    P-FE    P-GAP    P-TOT"

1940 PRINT FILE (1)
1950 FOR Z=.2 TO .8 STEP .2
1960  PRINT FILE (1),"CORE OPERATING AT ";Z;" TIMES B-MAX"
1970  PRINT FILE (1)
1980  FOR W=W1 TO W2 STEP W2/10
1990   LET X=EXP(LOG(34.9*W/7.3)/3)
2000   LET N1=L*I/*X*X*Z*1.6*.0001 )
2004   LET G=.4*3.14159*N1*I*.0001/(Z*1.6)
2006   LET F1=1+(G/(X*X))*LOG(6*X/G)
2008   LET N1=F1*N1
2010   IF N1 1 THEN GOTO 2140
2020   LET N1=INT(N1)
2030   LET P=36.1*X*X/N1
2040   LET P=INT(P)
2050   IF P|K9 THEN LET P=K9
2060   IF P 1 THEN GOTO 2140
2080   LET R1=.00032*X*N1/P
2090   LET P1=I*I*R1
2100   LET B3=(.4*3.14159*N1*.1*I*.0001/2)/(G+13*X/2000)
2110   LET P2=(W*454/1000)*.0044*F/1000*(B3/.01) 1.87
2115   LET P3=.0775*X*G*F*(.05*Z*1.6) 2
2120   PRINT FILE (1),USING "++.+",W;
2130   PRINT FILE (1),USING "++++++.++",1000*G;X;N1;P;1000*R1;P1;P2;P3;P1+P2+P3
2140  NEXT W
2150  PRINT FILE (1)
2160 NEXT Z
2170 RETURN
*
```

Figure 23
Program Listing 4

2.4.1.6.2 Determining "x" From Weight

Because the program is driven in increments of weight, this will be determined in terms of "x" as shown in Figure 24. After determining "x" for a particular weight, the geometric constants in Figure 22 can be determined.

$W = V * D$; where V = volume; D = density

$W = 13 * x^3 * D$ but if W is in lbs and D in gm/cm^2, then

$454 * W = 13 * x^3 * D$

$x^3 = 34.9\ W/D$

$x = \sqrt[3]{34.9\ W/D}$ with x in cm

in program [1990]

Note: D of Metglass = 7.3

Figure 24
Deriving "x" From Weight

2.4.1.6.3 Number of Turns

The method of computing the required number of turns for a required inductance using a given weight core at a given DC current is shown in Number of Turns, Figure 25. Notice that the loop parameter "z" is introduced as that fraction of B-Max at which the core will operate. For inductors with little AC induction, it is normally optimum to operate at high values of "z". In transformer designs however, high B-operating raises core losses (because of high AC induction) and it is not readily apparent where the trade off between core and copper losses takes place.

Because a gap is to exist in this design, fringing will occur and this modifies the number of turns as shown in the calculation lines re-entering the core. This is included in the computations.

Assuming that $\mu rDC >> 10000$

$$B_{DC} = \frac{.4\pi * N * I_{DC}\, 10^{-4}}{Gap} \quad \text{Tesla} \quad \text{(Eqn 1)}$$

$$\text{also } L = \frac{.4\pi * N^2 * A_C * 10^{-8}}{Gap} \quad \text{Henry} \quad \text{(Eqn 2)}$$

Solve (Eqn 1) for gap and put into (Eqn 2)

$$L = \frac{N * A_C * B_{DC} * 10^{-4}}{I_{DC}} \quad \text{(Eqn 3)}$$

$$N = \frac{L * I_{DC} * 10^4}{A_C * B_{DC}} \qquad \text{but } A_C^2 = X^2 \text{ and } B_{DC} = Z * B_m$$

$$N = \frac{L * I * 10^4}{X^2 * Z * B_m} \text{ same as [2000] } (B_m = 1.6 \text{ T for Metglass}) \quad \text{(Eqn 4)}$$

$$\text{from (Eqn 1) } Gap = \frac{.4\pi * N * I_{DC} * 10^{-4}}{1.6 * Z} \text{ same as [2004]} \quad \text{(Eqn 5)}$$

$$F = 1 + \frac{Gap}{X^2} * L_n * \frac{(21)}{Gap} \text{ fringing factor} \quad \text{(Eqn 6)}$$

(1 = coil length = 3X)

$$N_{Corrected} = N * F \quad \text{(Eqn 7)}$$

Figure 25
Number of Turns

2.4.1.6.4 Number of Wires to Parallel

In order to reduce copper losses, a wire size larger than is practical to wind on a bobbin was required. This was accomplished in the program by computing [2030], (figure 23), how many AWG 10 wires could be supported by the window area after dividing by the required number of turns. The number of parallel turns was then modified [2050], (figure 23), to be no more than a practical limit which was a keyboard input to the program.

2.4.1.6.5 Power Losses

Power loss calculations are shown in Figure 26. Copper loss is found by first determining the coil resistance. Next the AC flux density is computed in order to find the core loss. The equation for core loss was computed from the data in Figure 27.

In addition to the copper and core losses, there exists a "gap loss", or more properly a loss caused by the effect of the air gap on flux lines re-entering the core. This was included in the computations, but the result was small because the AC induction was small. In addition, the equation used pertains to a standard iron wound core. The Metglass core, although wound in strips, is of a material much like ferrites where particle separations cause an effective distributed air gap (between particles) and the true gap-loss may be even smaller than predicted.

$R_{\#10} = 32\mu\Omega/cm$; MLT = 10x $\quad R_{Coil} = 320 * 10^{-6} * Nl/P$

Loss $C_u = PI = I * I * R_{Coil}$ [2090]

$$B_{AC} = \frac{.4\pi * N * (1/2) * 10^{-4}}{Gap + \frac{13\,x}{2000}} \Delta I \text{ [2100] } (r = 2000\ L_{core} = 13x)$$

$$Loss_{Core} = P_2 = (W * 454/1000) * (.0044\ F/1000) * (B_{AC}/.01)^{1.87}$$

$$Loss_{Gap} = P_3 = .0775 * GF * (.05 * Z * 1.6)^2 \quad \text{[2115]}$$

Figure 26
Loss Calculations

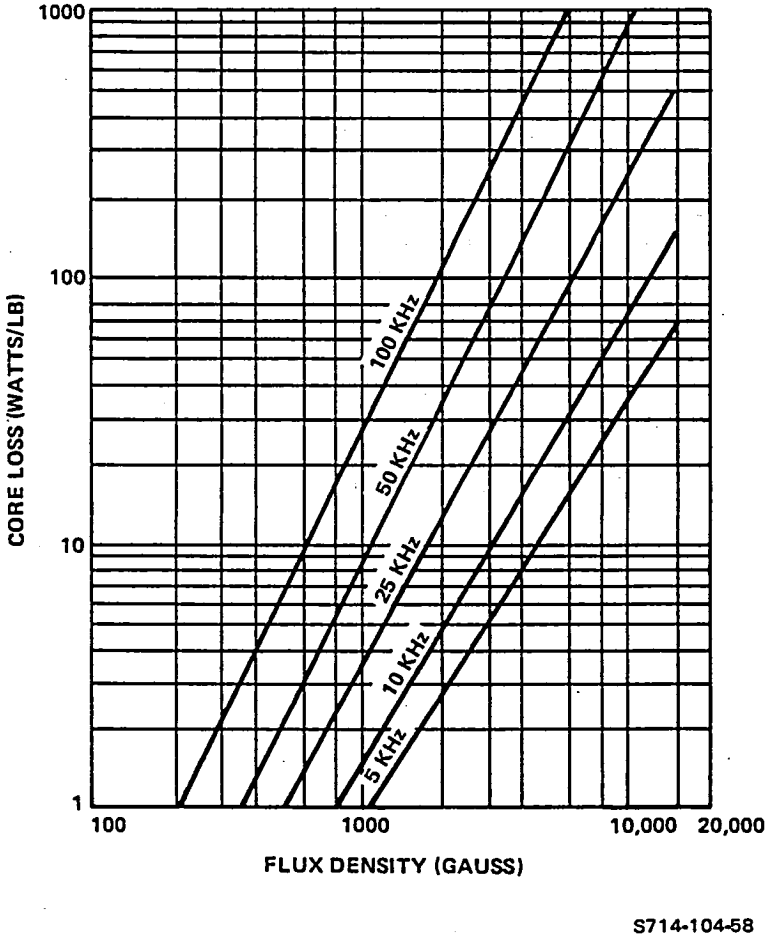

Figure 27
Core Loss of Metglass

2.4.1.7 Transformer Design Subroutine

The transformer design subroutine is shown in Program Listing 5, figure 28. The calculations follow the same pattern as those of the inductor design. The geometry was again standardized but, in this case, an 'E' core configuration (shown in "E" Core Dimensions, Figure 29) was chosen because the transformer had high AC induction and the 'E' core better contains the coil fields. The complete calculations follow.

```
!HCO 2M

2180 REM E-CORE TRANSFORMER SELECTION
2190 PRINT FILE (1),"FREQ=";F;"HZ"
2200 PRINT FILE (1),"RESITANCE IS IN MILLIOHMS"
2210 PRINT FILE (1)
2220 PRINT FILE (1),"    WT    'X'    N1    N2    PL1    PL2";
2230 PRINT FILE (1), TAB(53);"PWR-1  PWR-2  P-FE  P-TOTL"
2240 PRINT FILE (1)
2250 FOR Z=.2 to .8 STEP .2
2260  PRINT FILE (1),"CORE OPERATING AT ";Z;"OF B-MAX"
2270  PRINT FILE (1)
2280  FOR W=Y1 TO Y2 STEP Y2/10
2290   LET X=EXP(LOG(W*17.46/7.3)/3)
2300   LET N1=E*10000/(4*Z*1.6*2*X*X*F)
2310   IF N1 2 THEN LET Z1=E*10000/(4*1.6*2*X*X*F)
2320   IF N1|=2 THEN LET Z1=Z
2330   IF N1 2 THEN LET N1=2
2340   LET N1=INT(N1)
2350   LET N2=N*N1
2360   LET A1=4.5*X*X
2370   LET A1=A1*.5*.75*.6
2380   LET A2=A1
2390   LET W1=A1/N1
2400   LET W2=A2/N2
2410   LET W1=INT(W1/.056)
2420   IF W1|K9 THEN LET W1=K9
2430   LET W2=INT(W2/.056)
2440   IF W2|K9 THEN LET W2=K9
2450   IF W1=- THEN GOTO 2530
2460   IF W2=0 THEN GOTO 2530
2470   LET R1=.0000327*N1*12*X/W1
2480   LET R2=.0000327*N2*12*X/W2
2490   LET P1=I*I*R1
2500   LET P2=I*I*R2/(N*N)
2510   LET P3=26*X*X*X*7.3*.000001*F*.0044*(Z1/.01) 1.87
2520   PRINT FILE (1),USING "+++++.++",W;X;N1;N2;W1;W2;P1;P2;P3;P1+P2+P3
2530  NEXT W
2540  PRINT FILE (1)
2550 NEXT Z
2560 RETURN
2570 LET N3=INT((C2+.00003)/.00003)
2580 LET I3=E/(N3*R)
2590 LET P4=I3*I3*.006*N3
2600 LET W3=N3*.000
2610 PRINT FILE (1),"FOR THE CLK CAPACITOR (C2,C3) OF ";C2*1000000;" LFD,"
2620 PRINT FILE (1),"A TOTAL OF ";N3;" UNITS ARE REQUIRED FOR EACH CAP."
2630 PRINT FILE (1),"POWER LOSS IS ";P4;" WATTS EACH (C2 & C3)"
2640 PRINT FILE (1),"EACH 30 LFD CAP HAS A RIPPLE CURRENT OF ";I3;" AMPS"
2650 PRINT FILE (1),"   (11.4 AMPS ARE ALLOWED)"
2660 PRINT FILE (1),"THE WEIGHT OF C2&C3 IS ";W3;" POUNDS EACH"
2670 LET C4=.25*E/(F*R)
2680 RETURN
```

Figure 28
Program Listing 5

a. Generalized Geometry

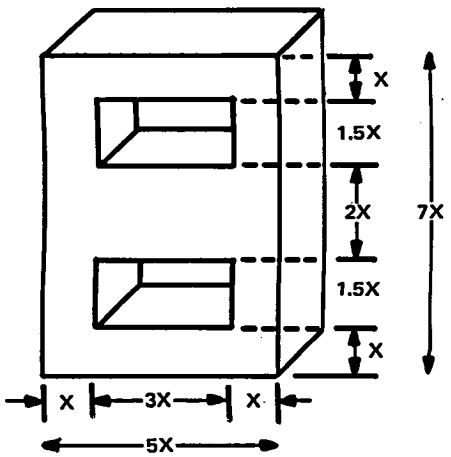

CHARACTERISTICS: VOLUME = 26 X^3
AW = 4.5 X^2
AC = 2 X^2
MWL = 12 X

S714-104-17

Figure 29
"E" Core Dimensions

b. Finding X from Weight

$V * D = W$

$26 * X^3 * D = W * 454$ (W in lbs)

$X^3 = \frac{17.46 * W}{D}$ Metglass D = 7.3 gm/cm^3

$X = \sqrt[3]{17.46\ W/D}$

Same as line [2290] X = E * P (Log(W * 17.46/7.3)/3)

c. Number of Primary Turns

Faraday's Law: $N = \frac{Ep * 10^4}{4 * B * A_c * f}$ Let operating Flux Density = Z * Bm

$$N = \frac{E * 10^4}{4 * Z * B_m * 2^2 * x * F}$$

Same as line [2300] with B_m = 1.6 Tesla

N1 = E * 10000/(4 * Z * 1.6 * 2 * X * X * F)

d. Primary Turns Decisions

If N1 < 2 turns, N1 = 2 turns and the operating flux density is recalculated for future use in the core loss calculations. Thus:

[2310] If N1<2, then Z1 = E * 10000/(4 * 1.6 * 2 * X * X * F)

[2320] If N1 >= 2, then Z1 = Z

[2330] If N1 < 2, then N1 = 2

e. Secondary Turns

'N' was an input variable representing the step-up turns ratio.

[2350] N2 = N * N1

f. Number of Parallel Wires

Area of Primary wires = .5 W * (.75) * (.6) (utilization factor) (winding factor); A1 = .5(4.5 * x^2) * (.75) * (.6) = (lines [2360] and [2370])

Area of Secondary (A2)1 = A1; (line [2380])

Primary Parallel (W1) = A1/(N1 * (.056); .056 cm is diameter of #10 AWG wire)

Secondary Parallel (W2) = A2/(N2 * .056)

g. Winding Resistances

R1 = (.0000327 * N1 * 12 * X)/W1 (12 * X is MLT)

R2 = (.0000327 * N2 * 12 * X)/W2

h. Copper Loss

P3 = P1 + P2 = (I * I * R1) + ((I/N) * (I/N) * R2)

i. Core Loss

Same as in Figure 26.

2.4.2 Summary Program "CUK.SUM"

Entry to the summary program listing is shown in "CUK.SUM" Entry, Figure 30. The summary program listing is given in Program Listing 6, Figure 31. In this case the designer specifies the selected core weights of the magnetics after he has considered the data from "CUK.DES". The calculations use the same equations and subroutines of "CUK.DES". One output summary page is prepared at the requested frequency. Typical output for 10 KHz is given in Figure 32. Summaries for several frequencies, based on the designer selected core weights as shown circled in the output sheets of Appendix A are listed in Appendix B.

Although the design equations will not be converted again, it is desirable to describe the structure of this program. Rather than be driven by nested loops, "CUK.SUM" steps through the various components building the output image array C (x, y). Each output line is represented by x, while each line contains columns in y. The assignments of x and y are shown in Tables X and XI.

```
INPUT E,R,N,F? / ? 28,.31,4,10000
MAX NUMBER OF PARALLEL TURNS? 10
WHAT IS W and Z FOR L1 (and L2)? 2,.6
WHAT IS W and Z FOR L3 (and L4)? 4,.6
WHAT IS W and Z FOR TRANSFORMER? 1,.2
STOP AT 2410
*
```

Figure 30
"CUK.SUM" Entry

```
0500 REM PROGRAM SAVED UNDER "CUK.SUM"
1000 OPEN FILE (1),"CLKDAT"
1010 FOR N=1 TO 10
1020  PRINT FILE (1)
1030 NEXT N
1040 PRINT FILE (1),**********************************************************"
1050 PRINT FILE (1),"* CLK CONVERTER DESIGN PROGRAM  T.GUNDERMAN 10/7/82 *"
1055 PRINT FILE (1),"* REVISION 8-20DEC82                                  *"
1060 PRINT FILE (1),"**********************************************************"
1070 PRINT FILE (1)
1080 PRINT FILE (1)
1090 PRINT FILE (1)
1100 DIM A(6),BS(22),C(11,11)
1110 PRINT "INPUT E,R,N,F";
1115 INPUT E,R,N,F
1120 PRINT "MAX NUMBER OF PARALLEL TURNS";
1140 INPUT K9
1150 PRINT FILE (1), "CONVERTER DESIGNED FOR";INT(E*E/R);" WATTS"
1160 PRINT FILE (1), "AT A FREQUENCY OF";F/1000;" KHZ"
1170 PRINT FILE (1)
1180 PRINT FILE (1)
1190 PRINT FILE (1),"CORE MATERIAL IS METGLASS"
1200 PRINT FILE (1),"MAX ALLOWED + TURNS IN COILS=";K9
1210 PRINT FILE (1)
1212 PRINT FILE (1),"L AND C VALUES GIVEN IN MICROHENRIES AND MICROFARADS"
1214 PRINT FILE (1)
1220 PRINT FILE (1)," -   VALUE    WEIGHT    TURNS-1    TURNS-2";
1230 PRINT FILE (1), TAB(51);"PARL-1    PARL-2    GAP    PWE-CU";
1240 PRINT FILE (1), TAB(96);"PWR-FE    PWR-GAP    PWR-TOTL"
1250 PRINT FILE (1)
1260 REM DETERMINE ALL COMPONENT VALUES
1270 REM FIRST READ EMI INPUT CURRENT LIMITS
1280 FOR J=1 TO 6
1290  READ A(J)
1300 NEXT J
1310 DATA .079,.0125,.025,.0022,.00009,.0004
1320 IF F=5000 THEN LET J=1
1330 IF F=10000 THEN LET J=2
1340 IF F=15000 THEN LET J=3
1350 IF F=25000 THEN LET J=4
1360 IF F=50000 THEN LET J=5
1370 IF F=100000 THEN LET J=6
1380 IF J|6 THEN PRINT "UNALLOWED FREQUENCY--RE TRY"
1390 IF J|6 THEN GOTO 1110
1400 LET C1=.001
1410 LET L1=(.029*E/R)/((2*3.14159*F) 2*C1*A(J))
1420 LET L2=L1
1430 LET L3=R/(.2*F)
1440 LET L4=L3
1450 LET C2=2/(.4*F*R)
1460 LET C3=C2
```

Figure 31
Program Listing 6 (Sheet 1 of 4)

```
1470 REM COMPUTE C1
1480 LET C(1,1)=C1
1490 LET C(1,2)=.2
1500 LET C(1,10)=0
1510 REM COMPUTE L1,L2
1520 PRINT "WHAT IS W & Z FOR L1(&L2)";
1530 INPUT W,Z
1540 LET L=L1
1550 LET I=E/R
1560 GOSUB 2450
1570 LET C(2,1)=L1
1580 LET C(2,2)=W
1590 LET C(2,3)=N1
1600 LET C(2,5)=P
1610 LET C(2,7)=G
1620 LET C(2,8)=P1
1630 LET C(2,9)=P2
1640 LET C(2,10)=P3
1645 LET C(2,11)=P1+P2+P3
1650 FOR J=1 TO 11
1660  LET C(3,J)=C(2,J)
1670 NEXT J
1680 REM COMPUTE C2(&C3)
1690 GOSUB 2810
1700 LET C(4,1)=C2
1710 LET C(4,2)=W3
1720 LET C(4,11)=P4
1730 FOR J=1 TO 11
1740  LET C(5,J)=C(4,J)
1750 NEXT J
1760 REM COMPUTE L3(&L4)
1770 PRINT "WHAT IS W & Z FOR L3 (&L4)";
1780 INPUT W,Z
1790 LET L=L3
1800 GOSUB 2450
1810 LET C(6,1)=L3
1820 LET C(6,2)=W
1830 LET C(6,3)=N1
1840 LET C(6,5)=P
1850 LET C(6,7)=G
1860 LET C(6,8)=P1
1870 LET C(6,9)=P2
1880 LET C(6,10)=P3
1885 LET C(6,11)=P1+P2+P3
1890 FOR J=1 TO 11
1900  LET C(7,J)=C(6,J)
1910 NEXT J
1920 REM COMPUTE TRANSFORMER
1930 PRINT "WHAT IS W & Z FOR TRANSFORMER";
1940 INPUT W,Z
1950 GOSUB 2580
```

Figure 31
Program Listing 6 (Sheet 2 of 4)

```
1955 IF W2 1 THEN GOTO 2040
1960 LET C(8,2)"W
1970 LET C(8,3)=N1
1980 LET C(8,4)=N2
1990 LET C(8,5)=W1
2000 LET C(8,6)=W2
2010 LET C(8,8)=P1+P2
2020 LET C(8,9)=P3
2030 LET C(8,11)=P1+P2+P3
2040 REM COMPUTE C4
2050 LET C(11,1)=.25*E/(F*R)
2060 LET C(11,2)=.2*C(11,1)/.001
2070 REM COMPUTE XISTOR PWR DISSIPATION
2080 READ V1,V2,T1
2090 DATA .75,1.5,.000002
2100 LET C(9,11)=E*E*T1*F*2/R+((2*E*V1/R+.2*EV2/R))*(.5-T1*F)
2110 REM COMPUTE DIODE PWR DISSIPATION
2120 READ V3,T2
2130 DATA 1,.000001
2140 LET C(10,11)=2*E*E*T2*F/R+2*E*V3*(.5-T2*F)/R
2150 REM CREATE OUTPUT FILE
2160 LET B5="C1L1L2C2C3L3L4T1Q1D1C4"
2170 FOR J=1 TO 11
2175  LET C(J,1)=C(J,1)*1000000
2180  PRINT FILE (1),B5(2*J-1,2*J);"  ";
2190  FOR K=1 TO 11
2200   PRINT FILE (1),USING "++++.++++",C(J,K);
2210   PRINT FILE (1),"  ";
2220  NEXT K
2230  PRINT FILE (1)
2240 NEXT J
2250 PRINT FILE (1)
2260 LET W=0
2270 LET L=0
2280 FOR K=1 TO 11
2290  LET W+W+C(K,2)
2300  LET L=L+C(K,11)
2310 NEXT K
2320 PRINT FILE (1),"TOTAL CONVERTER COMPONENT WEIGHT=";W;" POUNDS."
2330 PRINT FILE (1),"TOTAL CONVERTER POWER LOSS=";L;" WATTS."
2340 PRINT FILE (1),"PWR LOSS W/O SEMI'S";L-C(9,11)-C(10,11);"WATTS."
2350 PRINT FILE (1),"CONVERTER EFFICIENCY=";(E*E/R)/(E*E/R+L)*100;" %."
2360 PRINT FILE (1)
2370 PRINT FILE (1)
2380 PRINT FILE (1),"Q1 VCE=";V1;" VBE=";V2;= T RISE=FALL=";T1*1000000;"US."
2390 PRINT FILE (1),"D1 V ON=";V3;" T RISE=FALL=";T2*1000000;"US."
2400 CLOSE FILE (1)
2410 STOP
2420 REM
2430 REM
2440 REM
```

Figure 31
Program Listing 6 (Sheet 3 of 4)

```
2450 REM AIR GAPPED INDUCTOR SELECTION
2460 LET X=EXP(LOG(34.9*W/7.3)/3)
2470 LET N1=L*I/(X*X*Z*1.6*.0001)
2472 LET G=.4*3.14159*N1*I*.0021/(2*1.6)
2473 LET F1=1+(G/(X*X))*LOG(6*X/G)
2474 LET N1=F1*N1
2480 LET N1=INT(N1)
2485 IF N1 1 THEN GOTO 2570
2490 LET P=36.1*X*X/N1
2500 LET P=INT(P)
2510 IF P|K9 THEN LET P=K9
2530 LET R1=.00032*X*N1/P
2540 LET P1=I*I*R1
2550 LET B3=(.4*3.14159*N1*.1*I*.0001/2)/(G+13*X/2000)
2560 LET P2=(W*454/1000)*.0044*F/1000*(B3/.01) 1.87
2565 LET P3=.0775 *X*G*F*(.05*Z*1.6) 2
2570 RETURN
2580 REM E-CORE TRANSFORMER SELECTION
2590 LET X=EXP(LOG(W*17.46/7.3)/3)
2600 LET N1=E*1000/(4*Z*1.6*2*X*X*F)
2610 IF N1 2 THEN LET Z1=E*10000/(4*1.6*2*X*X*F)
2620 IF N1|=2 THEN LET Z1=Z
2630 IF N1 2 THEN LET N1=2
2640 LET N1=INT(N1)
2650 LET N2=N*N1
2660 LET A1=4.5*X*X
2670 LET A1=A1*.5*.75*.6
2680 LET A2=A1
2690 LET W1=A1/N1
2700 LET W2=A2/N2
2710 LET W1=INT(W1/.056)
2720 IF W1|K9 THEN LET W1=K9
2730 LET W2=INT(W2/.056)
2740 IF W2|K9 THEN LET W2=K9
2745 IF W2 1 THEN GOTO 2800
2750 LET R1=.0000327*N1*12**/W1
2760 LET R2=.0000327*N2*12**/W2
2770 LET P1=I*I*R1
2780 LET P2=I*I*R2/(N*N)
2790 LET P3=26*X*X*X*7.3*.000001*F*.0044*(Z1/.01) 1.87
2800 RETURN
2810 LET N3=INT((C2+.00003)/.00003)
2820 LET I3=E/(N3*R)
2830 LET P4=I3*I3*.006*N3
2840 LET W3=N3*.088
2850 RETURN
8
```

Figure 31
Program Listing 6 (Sheet 4 of 4)

```
**********************************************************
* CUK CONVERTER DESIGN PROGRAM      T.GUNDERMAN 10/7.82 *
* REVISION 9-3JAN83                                     *
**********************************************************
```

CONVERTER DESIGNED FOR 2529 WATTS
AT A FREQUENCY OF 10 KHZ

CORE MATERIAL IS METGLASS
MAX ALLOWED # TURNS IN COIL5= 10

L AND C VALUES GIVEN IN MICROHENRIES AND MICROFARADS

	VALUE	WEIGHT	TURNS-1	TURNS-2	PARL-1	PARL-2	GAP	PWE-CU	PWR-FE	PWR-GAP	WR-TOTL
C1	1000.0000	0.2000	0.0000	0.0000	0.0000	0.0000	0.0000	0.0000	0.0000	0.0000	0.0000
L1	53.0793	2.0000	12.0000	0.0000	10.0000	0.0000	0.1311	6.6492	0.7220	0.4967	7.8679
L2	53.0793	2.0000	12.0000	0.0000	10.0000	0.0000	0.1311	6.6492	0.7220	0.4967	7.8679
C2	1612.9032	4.7520	0.0000	0.0000	0.0000	0.0000	0.0000	0.0000	0.0000	0.0000	0.9065
C3	1612.9032	4.7520	0.0000	0.0000	0.0000	0.0000	0.0000	0.0000	0.0000	0.0000	0.9065
L3	155.0000	4.0000	23.0000	0.0000	10.0000	0.0000	0.2411	16.0568	1.6507	1.1513	18.8587
L4	155.0000	4.0000	23.0000	0.0000	10.0000	0.0000	0.2411	16.0568	1.6507	1.1513	18.8587
T1	0.0000	1.5000	4.0000	16.0000	10.0000	2.0000	0.0000	4.4106	8.1187	0.0000	12.5294
Q1	0.0000	0.0000	0.0000	0.0000	0.0000	0.0000	0.0000	0.0000	0.0000	0.0000	92.3548
D1	0.0000	0.0000	0.0000	0.0000	0.0000	0.0000	0.0000	0.0000	0.0000	0.0000	168.3613
C4	2258.0645	0.4516	0.0000	0.0000	0.0000	0.0000	0.0000	0.0000	0.0000	0.0000	0.0000

TOTAL CONVERTER COMPONENT WEIGHT= 23.655613 POUNDS.
TOTAL CONVERTER POWER LOSS= 328.51171 WATTS.
PWR LOSS W/O SEMI'S 67.79558 WATTS.
CONVERTER EFFICIENCY= 88.503704 #.

Q1 VDC= .6 VBE= 1.5 T RISE=FALL= .5 MICROSECONDS.
D1 V ON= 1.6 T RISE=FALL= .5 MICROSECONDS.

Figure 32
Typical Program Output for 10KHz

Table X CUK.SUM Output Lines

X	Component
1	EMI Capacitor (C1)
2, 3	EMI Inductor (L1, L2)
4, 5	Cuk Capacitors (C2, C3)
6, 7	Cuk Inductor (L3, L4)
8	Cuk Transformer (T1)
9	Diode (D1)
10	Transistor (Q1)
11	Output Capacitor (C4)

Table XI CUK.SUM Columns

Y	Meaning
1	Value
2	Weight
3	Turns-2 (primary of transformer)
4	Turns-2 (secondary of transformer)
5	Parl-1 (wires in parallel winding 1)
6	Parl-2 (parallel in transformer secondary)
7	Gap (for inductors)
8	Pwr-cu (copper loss)
9	Pwr-fe (core loss)
10	Pwr-gap (gap loss in inductors)
11	Pwr-totl (sum of above losses)

2.5.0 Operating Frequency Selection

2.5.1 Efficiency vs. Weight

2.5.1.1 As specified in paragraph 2.1.0, both efficiency and weight are important parameters of the AVS converter. However, as determined from the CUK.SUM program, efficiency and weight are affected oppositely by frequency. Therefore, a compromise was required in the selection of the converter's operating frequency.

2.5.1.2 It should be noted here that the CUK.SUM program assumes that the switching power transistor in the AVS converter will be bipolar rather than the popular MOSFET counterpart. The significance of bipolar versus MOSFET is that, as indicated in Frequency Tradeoffs, Figure 33 (circle graph), the power transistor accounts for approximately half of the total converter power loss. For high current levels, bipolar transistors operate more efficiently at low frequencies than MOSFETs; whereas the MOSFETs operate more efficiently than bipolars as high frequencies. Therefore, the CUK.SUM program is biased towards lower operating frequencies. Justification of bipolar for the power transistor is based on the frequency constraints of the rotary transformer and a comparison of MOSFET vs Bipolar power losses (refer to paragraph 2.6.1). It should also be noted that the CUK.SUM program does not include copper and structural weight in the weight computation. Therefore, the computed weights for different frequencies are to be used as a relative measure.

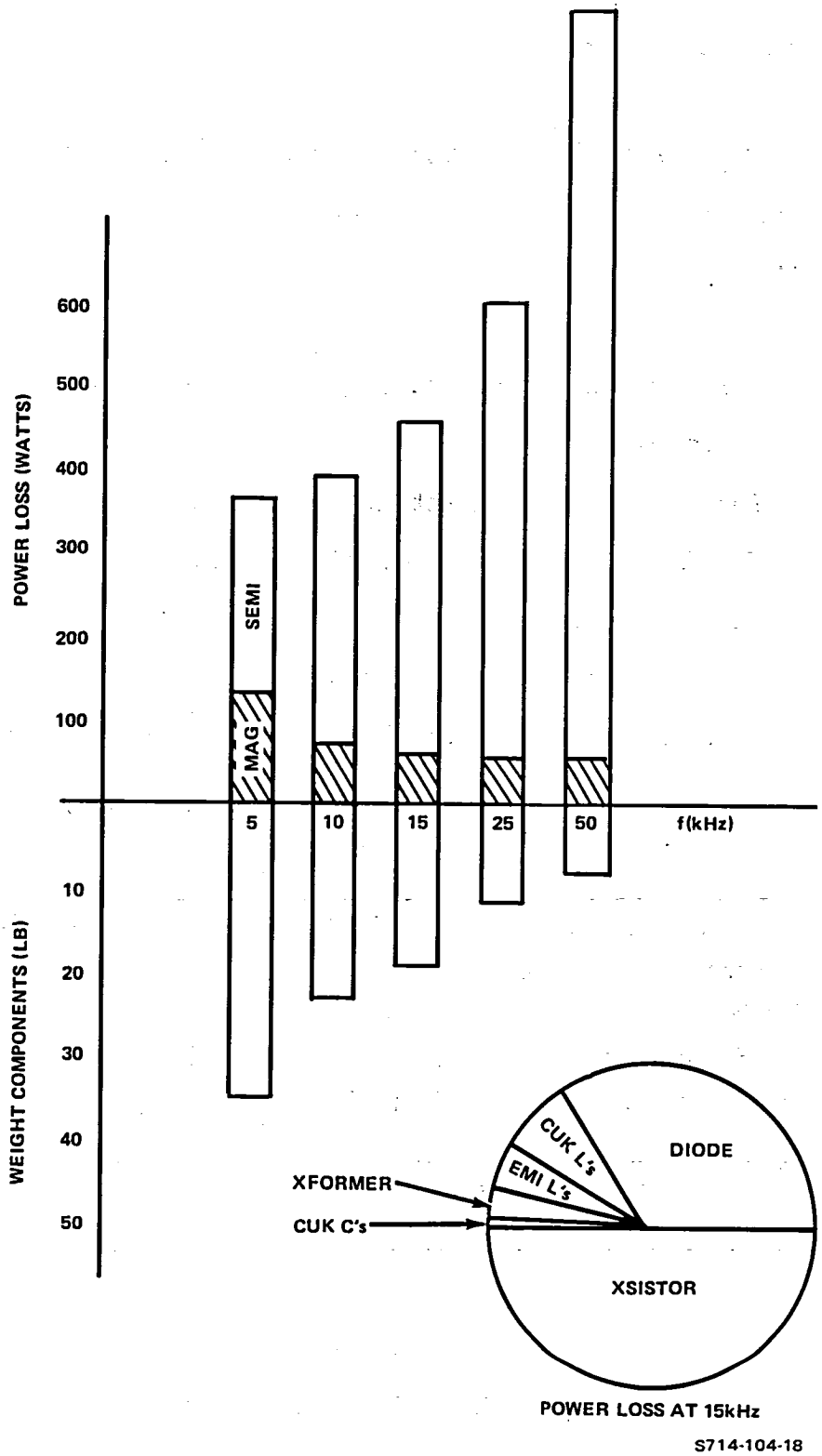

Figure 33
Frequency Tradeoffs

2.5.2 Analysis of CUK.SUM Data

2.5.2.1 Data provided by the CUK.SUM program for various operating frequencies is summarized in 5KHz to 15KHz Tradeoffs, Figure 34. From the figure it can be seen that:

- o For good converter efficiency, a low operating frequency is desirable.
- o For low converter weight, a high operating frequency is desirable.
- o For frequencies lower than 10KHz the increase in converter weight becomes excessive.
- o For frequencies greater than 15KHz, the increase in converter power loss (hence decrease in efficiency) becomes excessive.

Parameter	5KHz	10KHz	15KHz
Converter Power Loss	307W	329W	349W
Transformer Power Loss		20W	
Net Power Loss		349W	
Net Efficiency		87.8%	
Converter Weight*	53lbs	24lbs	18lbs
* Transformer weight is not affected by frequency.			

Figure 34
5KHz to 15KHz Tradeoffs

2.5.2.2 From the above observations, the converter operating frequency range is preferred to be from 10KHz to 15KHz.

2.5.3 Rotary Transformer Consideration

2.5.3.1 As an integral part of the AVS converter, the rotary transformer figures into the overall converter efficiency and must therefore be considered in the determination of the operating frequency.

2.5.3.2 From the rotary transformer design portion of this report, it was shown that the transformer operating frequency is limited to frequencies below 20KHz due to excessive power loss caused by "skin effect" at high frequencies.

2.5.4 Frequency Selection

2.5.4.1 From paragraphs 2.5.2 and 2.5.3 the frequency range from which the operating frequency will be selected is from 5KHz to 15KHz. The chosen frequencies to select from are 5, 10 and 15KHz. Figure 34 shows that the significant trade-off in this regime is the weight assessment.

2.5.4.2 From Figure 34, in choosing between 5 and 10KHz, the significantly greater weight with little increase in converter efficiency makes the 10KHz frequency preferable. Also from Figure 34, in choosing between 10 and 15KHz, the significantly better efficiency with a reasonable sacrifice in weight gain makes the 10KHz frequency preferable.

Therefore in the interest of maximizing converter efficiency while maintaing a reasonable converter weight, the operating frequency for the AVS converter was chosen to be 10KHz.

2.6.0 Component Selection

The requirements of the basic AVS converter components shown in Figure 13(c) far exceed the capability of currently available components. The inductors and transformer can be tailor made for the converter; however, the transistor, diode and capacitors must be selected from what is available off-the-shelf. The following paragraphs document the selection of available components that, when connected in parallel, will meet the requirements of the converter.

2.6.1 Power Transistor

2.6.1.1 Transistor Requirements

2.6.1.1.1 The power transistor must be capable of switching 200 Amps at a 10KHz rate and have a minimum breakdown voltage of 100V. The transistor must also be fast switching and have a low effective ON state impedance to minimize power loss.

2.6.1.2 Technology Selection - MOSFET vs Bipolar

2.6.1.2.1 The advantages of MOSFET over bipolar technology are faster switching speeds and lower power loss. The primary disadvantage of MOSFET

technology is a significantly lower current switching capability. MOSFETs are generally limited to less than 30 Amps. Eight MOSFETS connected in parallel would be required to achieve the required current capability of the converter.

2.6.1.2.2 As mentioned in paragraph 2.6.1.2.1, at this time, the primary advantage of bipolar technology is a greater current switching capability. However, although there are bipolar transistors capable of switching 200 Amps, none are capable of efficiently switching 200 Amps at a 10KHz rate. Three paralleled bipolar transistors with lower current capability but faster switching speeds would be required to meet the current switching requirements.

2.6.1.2.3 The MOSFET transistor power loss can be approximated as follows:

Eq. 2.6.1: $$P_{Loss} = PAC + PDC$$

PAC is transitional power loss and PDC is steady state power loss. Assuming a linear transient response, then PAC is the same as that for the bipolar transistor power loss equation developed in Figure 36: (see Figure 35 for switching diagram.)

Eq. 2.6.2: $$PAC = 2\,E^2 t_t\,F/R$$

PDC Loss occurs within $\frac{1}{F}$ for a period of $1/2(\frac{1}{F} - t_t)$ and dissipates I^2R_{DS} power during that time (R_{DS} is the drain to source ON resistance):

$$PDC = [(1/2)(1/F - t_t)/(1/F)](I^2R_{DS})$$

Eq. 2.6.3: $PDC = 2(E/R)^2\,R_{DS}$, for $t_t << 1/F$ and $I = 2E/R$

For E = 28V, R = .31 Ohms, and F = 10KHz, the MOSFET power loss equation is:

Eq. 2.6.4: $$P_{Loss} = 50.6 * 10^6\,t_t + 16 * 10^3\,R_{DS}$$

2.6.1.2.4 A possible MOSFET selection is the International Rectifier IFR 150. With 8 IRF 150s connected in parallel, the resultant DC resistance in the ON state is .007 ohms with a switching speed of 200 nsec. Using the approximated power loss equation, the resultant loss is 124 watts.

2.6.1.2.5 The bipolar transistor power loss equation (see Figure 35 for switching diagram) developed in Figure 36 was:

$$P_{Loss} = 2\ t_t\ F\ \frac{E^2}{R} + (.5 - Ft_t)\left(\frac{2E\ Vce}{R} + \frac{.2VbeE}{R}\right)$$

Eq. 2.6.5 $$P_{Loss} = 2t_tF\ \frac{E^2}{R} + EV_{CE}/R = \frac{.1EV_{VE}}{R},\ \text{for } ft_t \quad .5$$

For E = 28V, R = .31 Ohms, and F = 10KHz, the bipolar power loss equation is:

Eq. 2.6.6 $$P_{Loss} = 50.6 * 10^6\ t_t + 90.3\ V_{CE} + 9.3\ V_{BE}$$

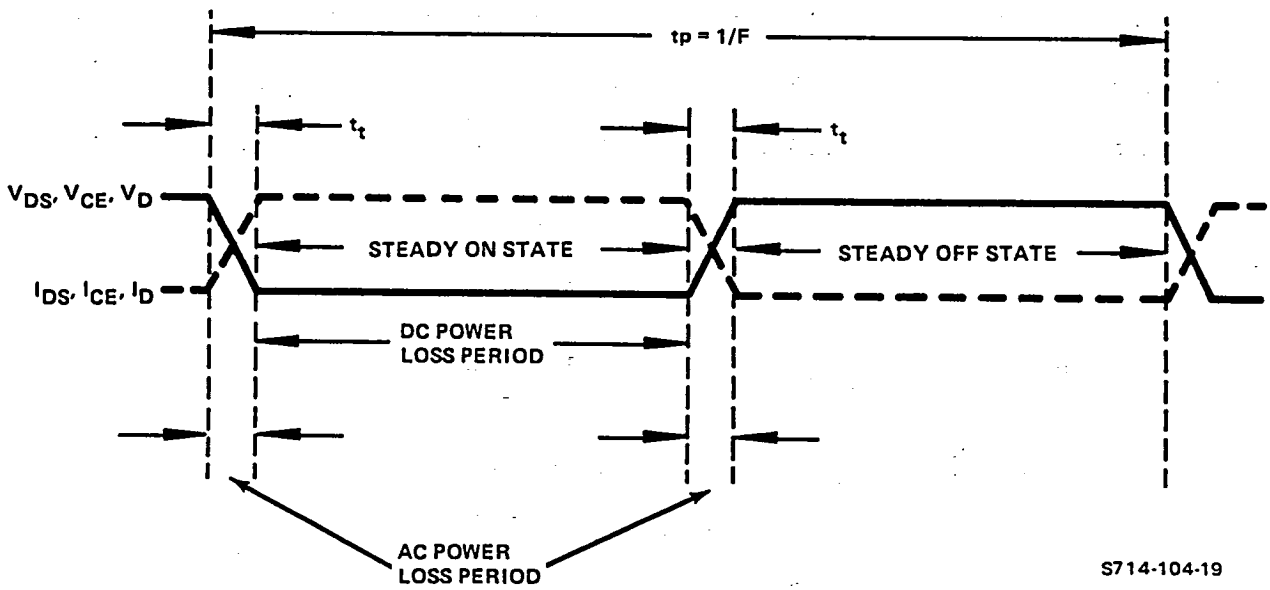

Figure 35
Device Switching Diagram

Transistor:

$$P_{Total} = P_{Col} + P_{Base} = (P_{Col} + P_{Base})AC + (P_{Col} + P_{Base})DC$$

$$P_{CAC} = \frac{1}{2} V_{CE} * \frac{1}{2} I_C = \frac{1}{2} (2E) * \frac{1}{2} \frac{2E}{R} = \frac{E^2}{R}$$

(Use $B_{Forced} = 10$)

$$P_{BAC} = \frac{1}{2} V_{BE} * \frac{1}{2} I_B = \frac{1}{2} V_{BE} * \frac{1}{2} * 1 \qquad \frac{2E}{R} = \frac{.05\ V_{BE} * E}{R}$$

$$P_{CDC} = V_{CESAT} * I_C = V_{CE} * \frac{2E}{R}$$

$$P_{BDC} = V_{BE} * I_B = V_{BE} * \frac{.2E}{R}$$

If t_p = period, $f = \frac{1}{t_p}$, $t_{transition} = t_r = t_f = t_t$

Then transition occurs twice each t_{twide} or

$$P_{AC} = \frac{2t_t}{t_p} \left[\frac{E^2}{R} + \frac{.05\ V_{BE}E}{R} \right] \qquad 2t_t * F * \frac{E^2}{R}$$

DC power is dissipated during t_p for $.5\ t_p - t_t$

$$P_{DC} = \frac{.5t_p - t_t}{t_p} \left[\frac{2E * V_{ce}}{R} + \frac{.2V_{BE} * E}{R} \right]$$

and $\frac{.5 * t_p - t_t}{t_p} = .5 - F * t_t$ [same as Listing 6 line 2100]

Diode

With same reasoning as above

$$P_{Diode} = \frac{2t_t}{t_p} \left[\frac{1}{2} * V_D * \frac{1}{2} I_D \right] + \frac{.5t_p - t_t}{t_p} [V_{DS} * I_{Load}]$$

$$= \frac{2\ t_t}{t_p} \left[\frac{E^2}{R} \right] + (.5 - Ft_t) \left[\frac{2EVd}{R} \right]$$

[same as Listing 6 line 2140]

Figure 36
Semiconductor Dissipation

2.6.1.2.6 A possible bipolar transistor selection is the Power Tech PT - 4500. With three PT - 4500s connected in parallel, the resultant VCE saturation voltage is .6 VDC with a switching speed of 500 nsec and a V_{BE} of 1.1V. Using the approximated power loss equation, the resultant loss is 90 watts.

2.6.1.2.7 The MOSFET voltage drive circuitry requires an insignificant amount of power. However, the bipolar current drive circuitry will require approximately 30 watts. Therefore, the resultant power losses of the MOSFET and bipolar transistor examples given in paragraphs 2.6.1.2.4 and 2.6.1.2.6 are about the same. These power loss calculations are rough approximations and have omitted other significant factors in the total switching losses. However, the calculations do provide a good comparison of MOSFET relative to bipolar transistor power loss.

2.6.1.2.8 From the preceding comparison of paralleled MOSFETs versus paralleled bipolar transistors, the bipolar transistor was selected on the basis of minimizing the number of converter components thus minimizing weight, size, and complexity of the converter. The Power Tech PT-4500 bipolar transistor was selected for the AVS converter.

2.6.1.3 Transistor Selection

Although two paralleled PT-4500s will meet the requirements of the converter, a third PT-4500 is desirable. Besides the obvious advantages of increasing converter efficiency and decreasing stress on the individual transistors, an additional advantage is lower net base drive current. The transistor gain is a nonlinear function of collector current. By adding a third transistor, the current gain is doubled. For two paralleled transistors,

where each will have a collector current of 100 Amps, the minimum current gain is 10 with a resultant maximum base current of 20 Amps. For the three paralleled transistors, where each will have a collector current of 67 Amps, the minimum current gain is 20 with a resultant maximum base current of 10 Amps.

Therefore, in the interest of efficiency and reliability, three parallel PT-4500 transistors are specified in the AVS converter design.

The Westinghouse D7 ST401010 has comparable specifications to the Power Tech device and would be a viable second source.

2.6.2 Power Diode

2.6.2.1 Diode Requirements

2.6.2.1.1 The power diode must be capable of conducting 200 Amps at a 10 KHz rate and have a minimum breakdown voltage of 100V. The diode must also be fast switching and have a low effective ON state impedance to minimize power loss.

2.6.2.2 Analysis of Diode Power Loss

2.6.2.2.1 The power loss equation developed in Figure 35 was:

$$P_{Loss} = \frac{2t_t}{t_p}\left[\frac{E^2}{R}\right] + (.5 - F\,t_t)\left[\frac{2E\,V_D}{R}\right]$$

For E = 28VDC, F = 10 KHz, $t_p = \frac{1}{F}$, R = .31 and assuming Ft_t .5, the diode power loss equation is:

Eq. 2.6.7: $$P_{Loss} = 50.6t_t + 90.3V_D$$

2.6.2.2.2 A possible diode selection is the Westinghouse R-6020422PSYA. The t_t is 500 nsec and V_D is 1.6 V. Using the approximated power loss equation, the resultant loss is 170 watts. Paralleling three diodes will reduce V_D to .9V resulting in a power loss of 107 watts. The power savings of paralleling three diodes will improve the converter efficiency by approximately 2%.

2.6.2.3 Diode Selection

2.6.2.3.1 The Westinghouse R6020422PSYA diode was selected for the AVS converter. As indicated in paragraph 2.6.2.2.2, paralleling three diodes as opposed to using a single diode will yield a significantly better converter efficiency. Paralleling diodes will also decrease stress on the individual diodes. Therefore, in the interest of efficiency and reliability, three parallel diodes are specified for the AVS converter.

2.6.3 Capacitor

2.6.3.1 Capacitor Requirements

2.6.3.1.1 The capacitor must have a minimum value of 1613 microfarads with breakdown voltage of at least 100V and be capable of 100 AMPs of alternating current at a 10 KHz rate. The capacitor must also have low series resistance to minimize power loss. Lastly, it must be non-polarized.

2.6.3.2 Selection

2.6.3.2.1 There are no capacitors available that meet all the requirements specified in paragraph 2.6.3.1.1. Paralleling of several low loss, high current handling capacitors such as polypropylene, teflon, polystyrene and polysulfone capacitors is required. The metallized polypropylene capacitor is the best choice for low series resistance and high current handling capability.

2.6.3.2.2 Fifty-four, paralleled, Sprague 735P306X9100YVL capacitors are specified for the AVS converter. The selected capacitor is a metallized-polypropylene, 30 microfarads, 100 V dc. With 54 Sprague capacitors connected in parallel, the resultant net capacitance is 1620 microfarads.

2.6.3.2.3 The selected capacitor is specified to have a worst case series resistance (ESR) of 6 milliohms for a ripple current of 11.4 AMPS rms at 85°C. Since each of the paralleled capacitors will handle 1/54 of the 100 AMP alternating current, 6 milliohms will be assumed to be the worst case series resistance for each of the paralleled capacitors. The net power loss for the parallel configuration is:

$$P_{Loss} = 54 * (100/54)^2 (.006) = 1.1W$$

2.7.0 Drive Circuitry

2.7.1 The drive circuitry causes the power transistor to alternately switch between saturation and cut off states at a 10KHz rate with a nominal 50% duty cycle. The drive circuitry also provides over current protection, current balance, and duty cycle adjustment.

2.7.2 The drive circuitry, as shown in Drive Circuitry Block Diagram, Figure 37, is made up of the following sections:

- o Clock Generator
- o Duty Cycle Control
- o Power Drive
- o Current Balance
- o Over Current Protection

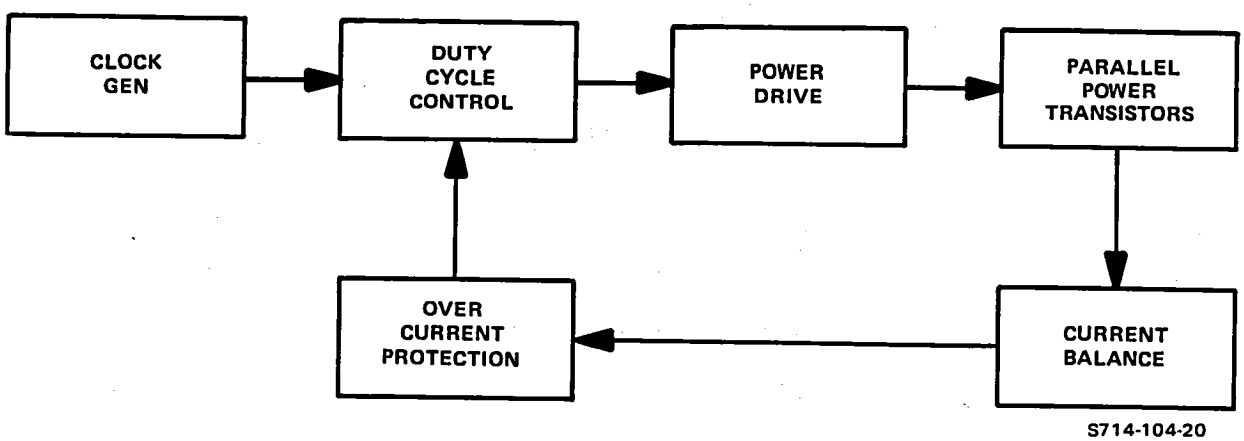

Figure 37

Drive Circuitry Block Diagram

Since the drive circuitry is powered by a single 28V supply, a nominal +14VDC reference voltage is provided in order to operate the circuitry away from the supply limits. In the following circuit descriptions all voltage levels mentioned are referenced to the +14V reference level unless otherwise specified.

2.7.2.1 Clock Generator

2.7.2.1.1 Function

The clock generator output is a 10KHz triangle wave that is used by the duty cycle control circuitry. A schematic of the clock generator is provided in Figure 38.

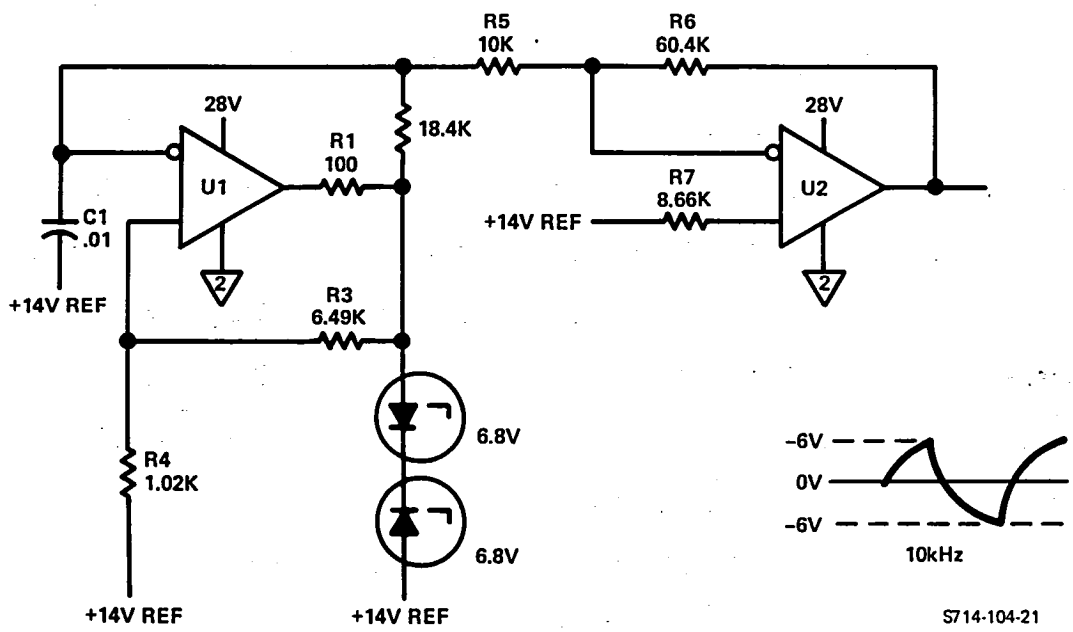

Figure 38

Clock Generator Schematic Diagram

2.7.2.1.2 Circuit Description

Operational Amplifier U1 is used as a comparator that compares the voltage across the capacitor C1 with the regenerative feedback voltage across Resistor R4. U1 output voltage is clamped to +14V reference via two back-to-back zener diodes that limit the saturation voltages to +/- 7.4 VDC. Resistors

R3 and R4 were selected to provide a regenerative feedback voltage of +/- 1 VDC. The Operational Amplifier will alternately charge and discharge capacitor C1 from +1 to -1 VDC as follows:

Assume voltage across C1 to be 0V and the Operational Amplifier output voltage to be 7.4V. The voltage at the non-inverting input of the Operational Amplifier will be 1V, and the inverting input will be zero volts. The Operational Amplifier output will remain at 7.4V until the inverting input voltage exceeds the noninverting input voltage. C1 will charge (at a rate set by the Operational Amplifier output voltage, value of R2, and value of C1) toward the Operational Amplifier output voltage. However, once the charge on C1 exceeds 1V, the Operational Amplifier changes state such that the output voltage switches to -7.4V. The regenerative feedback voltage consequently becomes -1V and C1 discharges towards -7.4V. Once C1 voltage drops below -1V, the Operational Amplifier will again change state to a +7.4V output and C1 will charge up again and the cycle repeats. U2 Operational Amplifier circuitry buffers the voltage across C1 with a gain of 6.

Equations for the clock generator are as follows:

Eq. 2.7.1: $$V_{Triangle} = \begin{cases} -50.4e^{-t/RC} + 44.4;\ 0 \leq + \leq 1/(2F) \\ +50.4e^{-(t-1/(2F)/RC} - 44.4;1/2F \leq + \leq 1/F \end{cases}$$

Eq. 2.7.2: $$F = \frac{1.866}{RC}$$

Eq. 2.7.3: $$t = -\ RC\ \ln\left(\frac{44.4 - Vout}{50.4}\right),\ 0 \leq t \leq \frac{1}{2F}$$

Eq. 2.7.4: $$t = -\ RC\ \ln\left(\frac{44.4 + Vout}{50.4} + \frac{1}{2F},\ \frac{1}{2F} \leq t \leq \frac{1}{F}\right.$$

2.7.2.2 Duty Cycle Control

2.7.2.2.1 Function

The duty cycle control circuitry converts the clock generator signal into separate ON and OFF commands with adjustable duty cycle for the power drive circuitry. A schematic of the duty cycle control circuitry is provided in Figure 39.

2.7.2.2.2 Circuitry Description

U2 and U3 are comparators that compare the triangle wave voltage level to a reference voltage. During normal converter operation, U2 output is high for triangle wave levels less than -V1 (see Wave Forms in Figure 39), and U3 output is high for triangle wave levels greater than +V1. For levels between -V1 and +V1, both U2 and U3 outputs are low which results in a dead zone. The dead zone is necessary for the power drive circuitry which contains a transistor bridge.

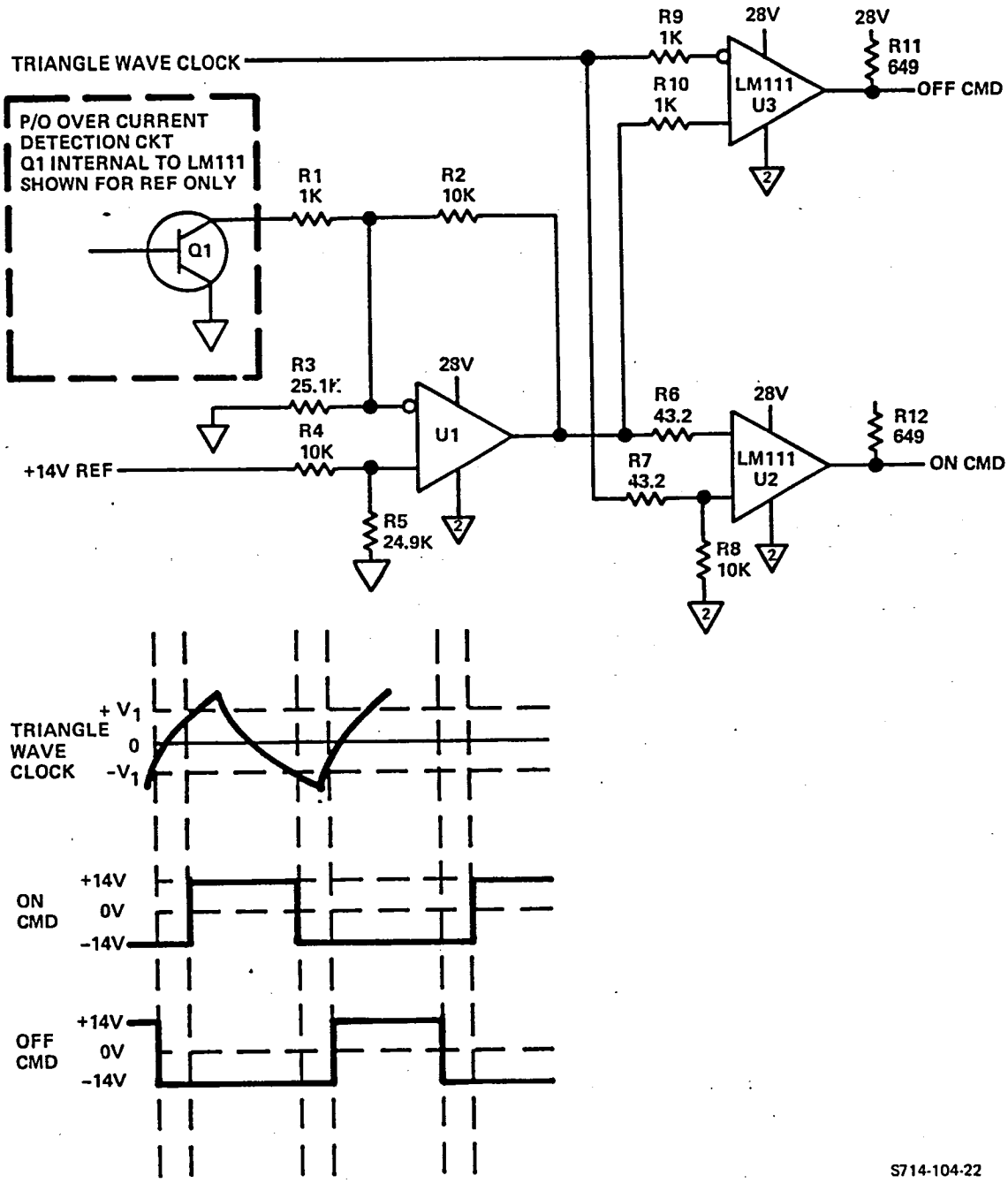

Figure 39
Duty Cycle Control Schematic Diagram

U2 output high commands the power transistors ON; U3 output high commands the power transistors OFF. In the event of an over current condition, Q1 is commanded ON forcing U1 output to go hard over positive which, in turn, forces U2 to go low and U3 to go high. Equations for the Duty Cycle Control circuitry are:

U1 Output: $\left[\left\{\frac{R5}{R4 + R5} * \frac{R2 + R3}{R3}\right\} - 1\right]$ 14, Q1 OFF

Eq. 2.7.5: $V_{U1} = \left[\frac{R5}{R4 + R5} * \frac{R2 + R1//R3}{R1//R3}\right] - 1$ 14, Q1 ON

U2 Trip Point:

Eq. 2.7.7.6: $V_{Triangle} = V_{U1} + (V_{U1} + 14)\frac{R7}{R8} = +V1$

U3 Trip Point:

Eq. 2.7.7: $V_{Triangle} = V_{U1} = -V1$

The dead zone voltage is derived from the period of time required to drive a pair of transistors in the power drive bridge from saturation into cut-off, and from the rate of change of the triangle wave voltage. The dead zone period must be kept to a minimum in order to maintain control of the transformer driven by transistor bridge in the power drive circuitry. The dead zone time period is selected to be .25 microseconds.

+V1 and - V1 are computed as follows:

Let: t_0 - time at which $V_{Triangle} = 0V$

t_1 - time at which $V_{Triangle} = -V1$

t_2 - time at which $V_{Triangle} = +V1$

for -V1 (using equation 2.7.3):

Eq. 2.7.10: $$t_0 - t_1 = -RC * \ln\frac{44.4 + V1}{50.4}$$

for +V1 (using equation 2.7.3):

Eq. 2.7.11: $$t_0 + t_2 = - RC * \ln\frac{44.4 - V1}{50.4}$$

Subtracting Equation 2.7.10 from 2.7.11

Eq. 2.7.12: $$t_2 + t_1 = - RC * \ln\frac{44.4 - V1}{50.4} + RC * \ln\frac{44.4 + V1}{50.4}$$

Substituting in values (i.e., $(t_1 + t_2) = .25\ \mu s$, $C = .01\ \mu F$, and $R = 18.4K$) and solving for V1:

Eq. 2.7.13: $$+V = .03V$$
$$-V = -.03V$$

Resistors R7 and R8 are computed as follows:

From Eq. 2.7.7: $V_{U1} = -V1 = -.03$

From Eq. 2.7.6: $$V_{U1} + (V_{U1} + 14)\frac{R7}{R8} = +V1$$

$$-.03 + (-.03 + 14)\frac{R7}{R8} = .03$$

Solving for R7: $$R7 = \frac{.06}{13.97} R8$$

Select R8 to be 10K, then: R7 = 42.95

Closest available standard value is 43.2 ohms for R7.

2.7.2.3 Power Drive

2.7.2.3.1 Function

The power drive circuitry converts the power transistor ON and OFF commands from the Duty Cycle Control circuitry into base drive current which drives the power transistors. The power drive circuitry schematic diagram is provided in Figure 40.

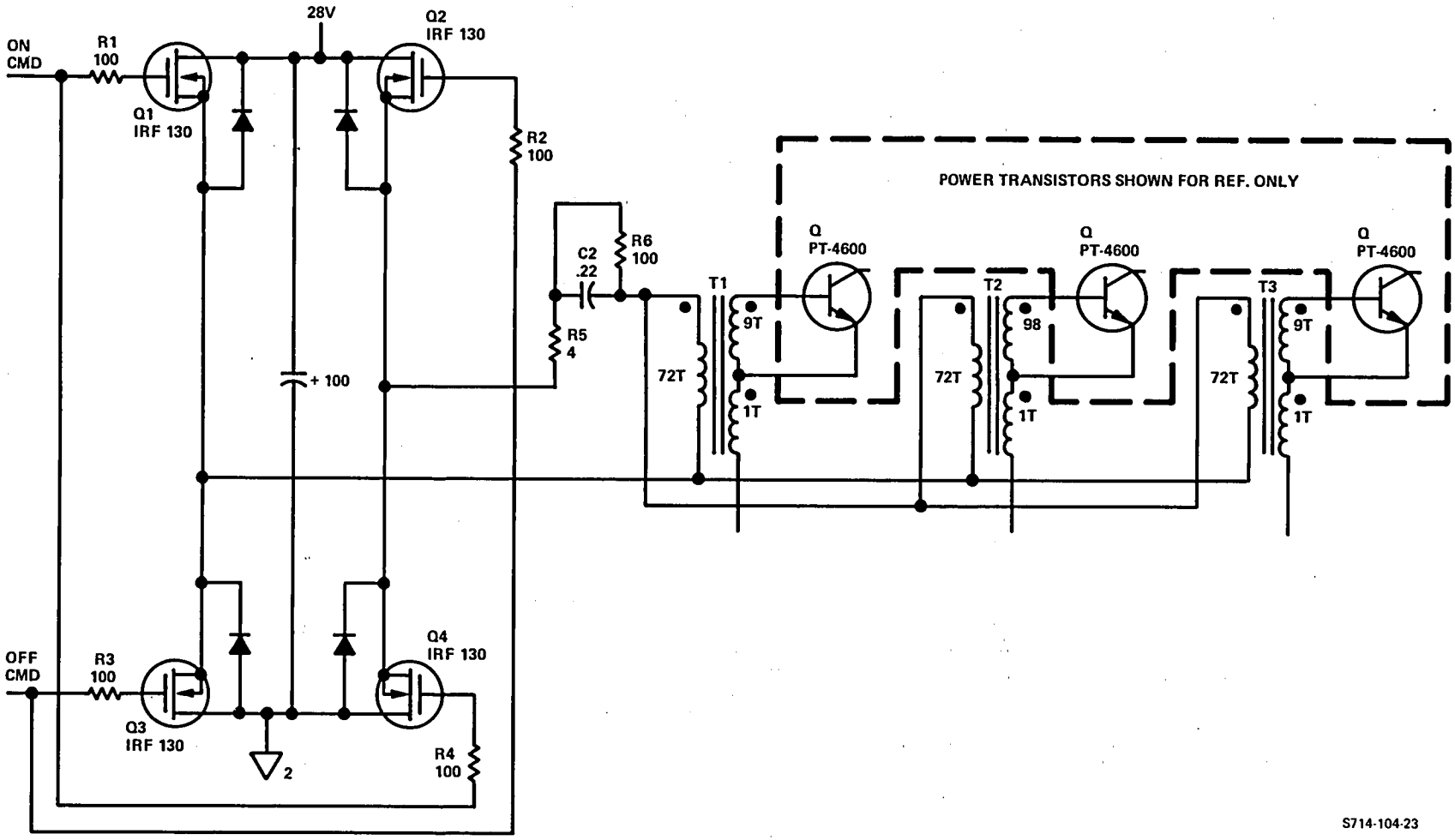

Figure 40
Power Drive Circuitry Schematic Diagram

2.7.2.3.2 Circuit Description

T1, T2 and T3 are used to provide isolation between the power transistors and the drive circuitry. The transformers also provide a regenerative feedback to supplement the drive circuitry during turn-on of the power transistors. Transistors Q1 thru Q4 form a bridge that alternates the current through the 72 turn primary winding to provide bipolar base drive to the power transistors.

Assuming an initial state where transistors Q1 thru Q4 are OFF, the power transistors are OFF, capacitor C2 is charged to -28V and the transformer cores are in a negative saturation state. The power drive circuitry functions as follows:

Cut off to saturation:

Transistors Q1 and Q4 are commanded on by the duty cycle control circuitry which presents an initial voltage of +56V on the paralleled 72 turn primary windings of transformers T1, T2 and T3. The 56V is the combined voltage of the 28V power supply and the initial charge on capacitor C2. The transformers are excited out of negative saturation and an instantaneous positive voltage is impressed on the secondary windings of the transformers which attempts to reach +7V as defined by the turns ratio and the primary voltage. However, the base emitter junction of the power transistors become forward biased and limit the secondary voltage to a maximum of +1.5V. The limited secondary voltage reflects back and limits the primary voltage to a maximum of +12V as defined by the secondary-to-primary turns ratio and the secondary voltage.

Since the primary voltage across the paralleled transformers is now fixed at +12V, the current through each of the primaries can be approxmiated as:

Assuming: R6>>R5, RQ1, RQ2

Then:

Eq. 2.7.14: $i_{pR^I} = \frac{1}{3}\frac{28 - 12}{R6} + \frac{1}{3}\frac{2 * 28 - 12}{R5+RQ1+RQ4} e^{-(t/(R5+RQ1+RQ4)C)}$

where RQ1 and RQ4 are the DC resistances of transistors Q1 and Q4, respectively, and t = 0 at time Q1 and Q4 are switched ON.

For: R5 = 4, R6 = 100, RQ1 = RQ2 = .18, C2 = .22μF

Then:

Eq. 2.7.15: $i_{PRI} = .05 + 3.4e^{-t/(.88 * 10^{-6})}$

The power into each of the primaries is approximated as:

$$P_{IN} = V_{PRI} . I_{PRI}$$

$$P_{IN} = 12\ (.05 + 3.4e^{t/(.88 * 10^{-6})})$$

The power out of the secondaries is ideally equal to the power into the primaries. Therefore, the resultant base current can be approximated as:

$$i_B = P_{IN}/V_{BE}$$

$$i_B = 12\ (.05 + 3.4e^{-t/(.88 * 10^{-6})})/1.5$$

Eq. 2.7.16: $i_B = .4 + 27e^{-t/(.88 * 10^{-6})}$

The instantaneous base current of 27.4 Amps will cause rapid turn-on of the power transistors. When conduction begins, additional current is fed to the power transistors' base via the 1:9 turns ratio windings. Since the base current is transformer fed directly across the base-emitter junction, the current through the single turn winding is equal to the collector current. With a minimum power transistor current gain of 10 as determined from the PT-4500 data sheet and a transformer current gain of one-ninth as determined by

the turns ratio, a resultant current proportional to the collector current is fed back to the power transistors' base with an overall current gain greater than unity. As a result, once the power transistor begins to conduct, it will drive itself into saturation. The net base drive current is the sum of the feedback current through the 1:9 windings and the control current through the 72:9 windings:

Eq. 2.7.17: $$i_B = i_C/9 + .4 + 27\ e^{-t/(.88 * 10^{-6})}$$

When the power transistor achieves saturation no further energy is transfered via the primary windings of the transformers due to the steady state current through the primaries. The energy in the secondary winding at the time transistor saturation occurs becomes the sole source of the power transistor base drive and is dissipated at a rate determined by the inductance of the secondary winding and the DC resistance of the base-emitter junction:

Eq. 2.7.18: $$i_B = I_B\ e^{-(R/L)t}$$

where I_B is base current at time of saturation

R is the base-emitter junction DC resistance

L is the secondary winding inductance

The value of I_B is approximated as:

$$I_B = I_C/9 + .4$$

where I_C is the collector saturation current.

For Ic = 67 Amps, I_B = 7.8 Amps

In order to maintain the power transistor in saturation, the base current must remain greater than one-tenth I_c. For an I_c of 67 Amps, and a current gain of 10, the base current must remain greater than 6.7 Amps. From the PT-4500 data sheet, the DC resistance of the forward biased base-emitter junction is:

$$R = \frac{V_{BE} - .6}{I_C}$$

$R = .01$, for $V_{BE} = 1.5$, $I_C = 67$

From Eq. 2.7.18 and solving for L:

Eq. 2.7.19: $L = Rt/\ln(i_B/I_B)$

For a 50% duty cycle at 10 KHz, the value of t is 50 microseconds. Therefore, the minimum inductance of the transformer secondaries is:

Eq. 2.7.20: $L(MIN) = .01 * 50 * 10^{-6}/\ln(6.7/7.8) = 3.3$ microhenries

Saturation to cut-off:

Transistors Q1 and Q4 are commanded OFF and Q2 and Q3 are commanded ON by the duty cycle control circuitry which presents an initial -56V across the 72 turn primary windings of T1, T2, and T3 transformers. The -56V is the combined voltage of the reversed connection of the 28V power supply and the initial charge on capacitor C2. At the time Q2 and Q3 are switched on, the voltage induced on the secondary will attempt to reverse bias the power transistor base-emitter junction to -7V. However, the base-emitter junction will appear as a very low impedance to the secondary due to the excess carrier charge that accumulates in the power transistor base region during the

saturation state. As a result, the base-emitter voltage will be near zero as the excess carriers discharge through the secondary. Once the excess carriers are depleted, the base-emitter junction voltage will go to a negative value determined by the discharge rate of capacitor C2. Since the secondary voltage is clamped near OV, the primary voltage will also be OV. The voltage across capacitor C2 during the excess carrier withdrawal is approximated as:

Eq. 2.7.21: $$Vc = 28(1 - 2e^{-t/RC})$$

The voltage across capacitor C2 at the time the transistor is driven out of saturation is -13.7V. Once the power transistor is driven into cut-off, the base-emitter junction appears as an open curciut to the secondary. The open on the secondary is reflected to the primary. The primary then appears as an open circuit thus inhibiting any further discharge of capacitor C2. The resultant voltage across the transformer primaries is -41.7V which will drive the transformer cores into negative saturation. When the transformer cores saturate, the primary and secondary windings become virtual shorts. As a result, the power transistors, with the base-emitter junction shorted, will remain in cut off and capacitor C2 will charge to -28V. Once C2 is fully charged, resistor R6 provides a steady state current through the transformer primaries. This maintains the transformer cores in negative saturation thus maintaining the cut off state of the power transistors.

2.7.2.4 Current Balance

2.7.2.4.1 The current balance circuitry assures equal conduction of the three paralleled power transistors thus preventing any one of the transistors from being over stressed. The circuitry also provides a means of sensing the net switched current for over current detection. The current balance circuitry schematic diagram is presented in Figure 41.

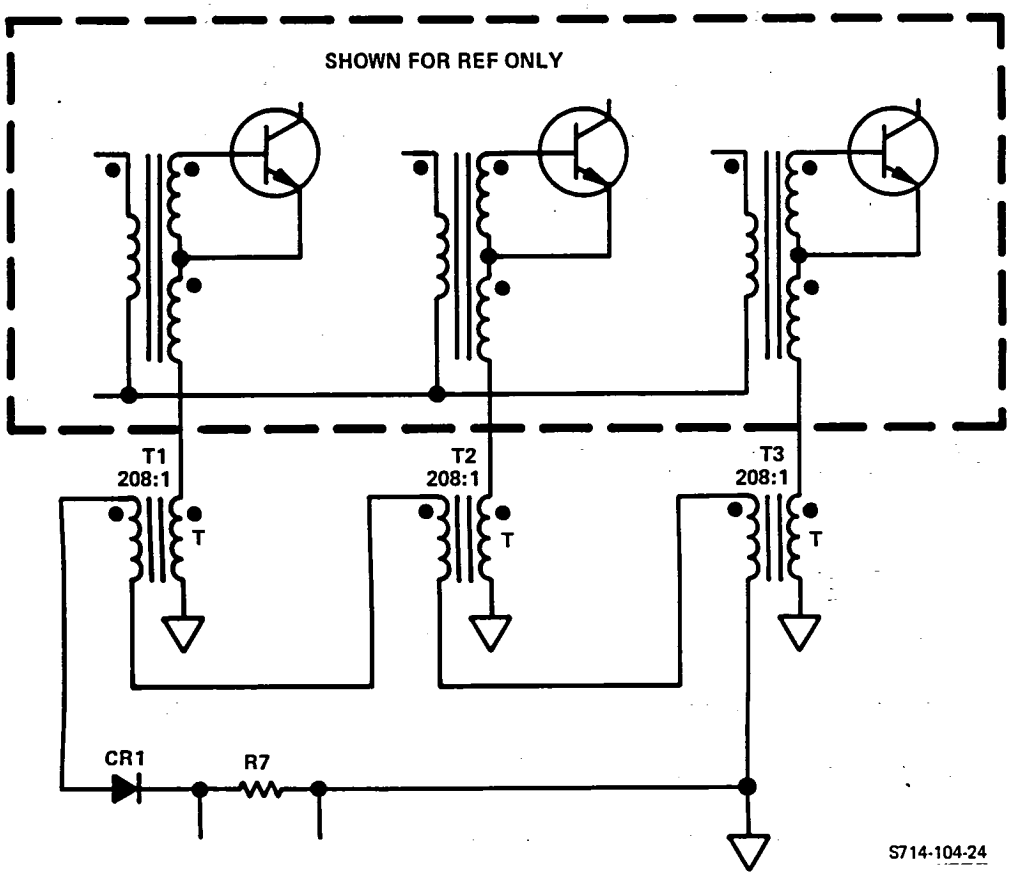

Figure 41
Current Balance Circuitry Schematic Diagram

2.7.2.4.2 Circuit Description

Transformers T1, T2, and T3 are pulse type transformers. The single turn secondaries of transformers T1, T2 and T3 are connected in series with the ground path for respective power transistors. Therefore, the current induced in the transformer primaries will be proportional to the respective transistor collector current. However, since the transformer primaries are connected in series, the resultant net current in each primary will be proportional to the net current conducted by all three transistors. Since the current in each of the primary windings is forced to be identical by virtue of the series loop connection, the current in each of the secondaries will in turn be forced to be identical. Resistor R7 is connected in series with the primary windings to sense the net current conducted by the transistors. The net current as related to the voltage developed across R1 is:

$$Ic = 100V_R$$

2.7.2.5 Over Current Protection

2.7.2.5.1 Function

The over current protection circuitry monitors the net power transistor turn on surge current and if an over current condition occurs, will cause the power transistors to be switched off. The overcurrent protection circuitry schematic diagram is presented in Figure 42.

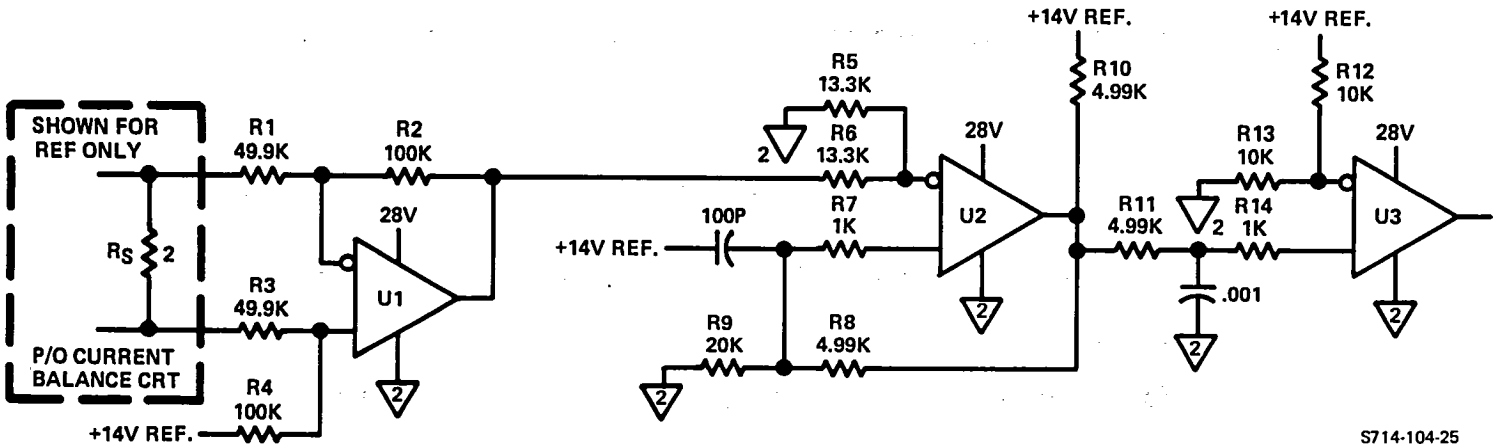

Figure 42
Over Current Circuitry Schematic Diagram

2.7.2.5.2 Circuit Description

Note: In this section only, all voltages are identified with respect to ground.

Resistor R_S is part of the current balance circuitry (see paragraph 2.7.2.4). The voltage developed across R_S is directly proportional to the net current conducted by the power transistors. The voltage across R_S is amplified by a gain of 2 and referenced to the +14V reference voltage by the U1 Operational Amplifier circuitry. The resultant voltage at the output of U1 is

divided by resistors R5 and R6 and presented to the inverting input of comparator U2 at one half the value of the U1 output. The relationship of the voltage applied to U2 inverting input as a function of the net power transistor current is:

$$V_1 = \frac{2(I_C/100)+14}{2} = \frac{I_C}{100} + 7$$

Since the maximum current to be demanded of the converter is to be 100 AMPS, the maximum current to be switched by the power transistors is 200 AMPS. Therefore, the maximum value of V_1 under normal operating conditions will be 9V. The voltage divider network consisting of R8, R9, R10 divides down the +14V reference voltage to set the non-inverting input of U2 to +9.3V. In the event that the net power transistor current exceeds 230 AMPS, the voltage at the inverting input to U2 will exceed the voltage at the non-inverting input to U2 and will cause U2 output to switch low. When U2 switches low, it will ground the R8, R10, R11 junction which effectively grounds the U2 non-inverting input and latches U2 output into the low state. Since the inverting input to U2 cannot be driven lower than ground, U2, when caused to switch low, will remain low until power is removed and reapplied to the converter. When U2 output is high, the voltage presented to U3 non-inverting input is determined by the R8, R9, and R10 voltage divider network which divides the +14V reference voltage. The voltage presented to U3 with U2 output high is 11.7V. The inverting input to U3 is determined by the voltage divider network consisting of R12 and R13 which divides the +14V reference voltage to +7V. U3 is a comparator and its output will be high as long as U2 output is high. In the event that U2 switches low, U2 output effectively applies a ground to the non-inverting input of U3 which causes U3 to switch low. The output of U3 is

used to initiate turnoff of the power transistors and to inhibit subsequent turnon cycles (refer to paragraph 2.7.2.1). Capacitor C1 is provided for initial converter power up to prevent accidental latch up of U2. Capacitor C2 is provided to provide a small delay before commanding the power transistors off. This allows the voltage doubling capacitor in the power drive circuitry sufficient time to charge (refer to paragraph 2.7.2.3).

2.8.0 Transformer/Inductor Specifications

2.8.1 Output Isolation Transformer

2.8.1.1 Requirements

The output isolation transformer must be capable of transferring a 28 Vpeak-to-peak, 10KHz square-wave voltage with a 50% duty cycle to the load with a 1:3.5 step-up turns ratio. As determined by the CUK.DES program, the maximum power to be transferred is 2,529 watts. The transformer design must assure that the core will not saturate and must provide an efficiency of approximately 99.5%. The transformer/inductor schematic is shown in figure 43.

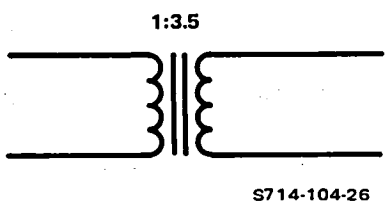

Figure 43
Output Isolation Transformer Schematic Diagram

2.8.1.2 Specifications

General:

Operating Frequency - 100KHz

Duty Cycle - 50%

Response Time - .5 microseconds (Max)

Insulation Breakdown - 100v (Min)

Efficiency - 99% (Min)

Winding Specifics - See Table XII

Table XII. Winding Specifics, Output Isolation Transformer

Winding	Number of Turns	Voltage/ Current Rating	Max DC Resistance	Inductance
Primary	2	40V/100A	.0005	*
Secondary	7	140V/30A	.005	*

*Minimize to meet response time and efficiency specifications.

2.8.2 Base Drive Transformer

2.8.2.1 Requirements

The base drive transformer, as shown in the Base Drive Transformer Schematic Diagram (Figure 44) is to have two primary windings with a common secondary winding. The primary to secondary turns ratios are to be 1:9 and 72:9. The 1:9 turns ratio windings are to transfer 20w of pulsed power at 10KHz, 50% duty cycle. The 72:9 windings are to transfer 360w of pulsed power at 10KHz, 50% duty cycle. The transformer design must provide a response time

of less than .5 microseconds for a step voltage input. The transformer core must not saturate for a step voltage input of 12v on the 72:9 windings within a 60 microseconds period, but may saturate within the 60 microseconds period for an input voltage of 28v. The secondary winding must have an inductance of 4 +/- .7 microhenries. The primary winding of the 1:9 turns ratio must be a single turn winding and capable of conducting a switched current of 100 Amps at a 10KHz rate and 50% duty cycle.

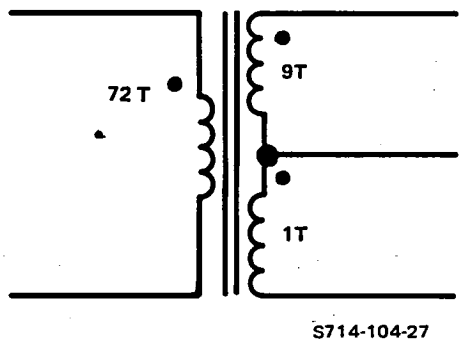

Figure 44
Base Drive Transformer Schematic Diagram

2.8.2.2 Specifications

General:

Operating Frequency	- 10KHz
Duty Cycle	- 50%
Response Time	- .5 microseconds (Max)
Insulation Breakdown	- 100V (Min)
Efficiency	- 99% (Min)
Winding Specifics	- See Table XIII

Table XIII. Winding Specifics, Base Drive Transformer

Winding	Number of Turns	Voltage/ Current Rating	Max DC Resistance	Inductance
Primary	72	70V/4A	.001	*
Primary	1	.50V/100A	.0005	*
Secondary	9	2V/40A	.001	4 uH

*Minimize to meet response time and efficiency specifications.

2.8.3 Current Balance Transformer

2.8.3.1 Requirements

The current balance transformer, as shown in the Current Balance Transformer Schematic Diagram (Figure 45) must have a turns ratio of 200:1. The transformer is to be a pulse type using a 25 +/- 5 microseconds pulse duration. The secondary winding must be a single turn winding and capable of conducting a switched current of 100 Amps at a 10KHz rate, 50% duty cycle.

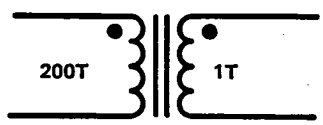

S714-104-28

Figure 45
Current Balance Transformer Schematic Diagram

2.8.3.2 Specifications

General:

Operating Frequency - 10KHz

Duty Cycle - 50%

Response Time - .5 microseconds (Max)

Insulation Breakdown - 100V (Min)

Efficiency - 99% (Min)

Winding Specifics - See Table XIV

Table XIV. Winding Specifics, Current Balance Transformer

Winding	Number of Turns	Voltage/ Current Rating	Max DC Resistance	Inductance
Primary	200	100V/2A	.001	*
Secondary	1	.5V/100A	.0005	*

*Minimize to meet response time and efficiency specifications.

2.8.4 Input Filter Inductor

2.8.4.1 Requirements

The input filter inductor must have an inductance of 43 microhenries and be capable of conducting a DC current of 100 Amps with an AC current of 10 Amps at 10KHz 50% duty cycle.

2.8.4.2 Specifications

Operating Frequency	- 10KHz
Duty Cycle	- 50%
Insulation Breakdown	- 100V
Inductance	- 43 +/- 4 microhenries
Efficiency	- 99% (Min)
DC Current	- 100A
AC Current	- 10A

2.8.5 CUK Inductor

2.8.5.1 The Cuk inductor must have an inductance of 155 microhenries and be capable of conducting a DC current of 100Amps with an AC current of 10Amps at 10KHz, 50% duty cycle.

2.8.5.2 Specifications

Operating Frequency	- 10KHz
Duty Cycle	- 50%
Insulation Breakdown	- 100V
Inductance	- 155 +/- 10 microhenries
Efficiency	- 99% (Min)
DC Current	- 100A
AC Current	- 10A

Appendix 1

Small Scale Model Tests

Appendix 1

Small Scale Model Tests

A1.1 Model Description

The transformer models consisted of existing Ferroxcube pot core sets #6656, made from Ferroxcube 3C8 Manganese-Zinc ferrite material. The coil bobbins, which were also available from another program, were sized such that one bobbin fit into each pot core section. Although this axial positioning of the coils differed from the radial positioning planned for the full scale design, the data obtained are considered quite relevant.

A1.2 Model #1

Model #1 contained coils as follows:

Primary coil: 27 turns, 12 parallel strands, #22AWG wire

Secondary coil: 41 turns, 6 parallel strands, #22 AWG wire for a turns ratio (A:1) of 0.659:1.

Open and short circuit impedance and load tests were performed over a frequency range from 0.3 to 45KHz. The data were fitted to the equivalent circuit shown in Figure A1-1. Results and derived parameters were as shown in Table A1-I.

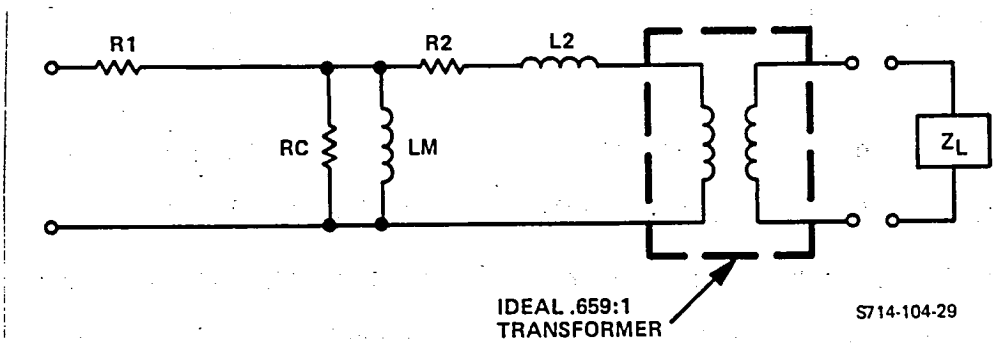

Figure A1-1
Transformer Model #1 Equivalent Circuit

TABLE A1-I - Model #1 Test Results

Freq (KHz)	0.3	1	2	5	10	15	45
R1 (ohms)	.031	.05	.12	.4	.8	1.3	4.7
R2 (ohms)	.063	.11	.23	.8	1.7	2.7	9.4
X2 (ohms)	.24	.79	1.50	3.1	5.1	6.6	10.5
RC (ohms)	240	1060	1880	3200	4180	4850	6500
XM (ohms)	26	84	172	358	750	1175	3800
L2 (mH)	.127	.126	.119	.099	.081	.070	.037
LM (mH)	13.8	13.4	13.7	11.4	11.9	12.5	13.4
*Ratio RAC/RDC	1.04	1.78	3.9	13.3	28	44	157

* Measured and calculated DC resistances (including lead wires) were:

Primary Coil = .03 ohms; Secondary coil = .06 ohms.

A1.3 Model #2

The coils for model #2 were wound with identical primary and secondary windings of 5 turns, 12 parallel strands, #16 AWG wire. Recognizing that the resistance of lead wires would be quite significant with respect to the coil resistance and would distort RAC/RDC ratio calculations, the lead wire was limited to less than 2 inches per coil. The preferred operating frequency range had been narrowed to between 5 and 10KHz. Therefore, only partial data were obtained beyond 10KHz.

Impedance and load tests were again performed. Working with a 1:1 turn ratio, a balanced equivalent circuit could be used with the leakage inductance (L1 and L2) equally attributed to the primary and secondary sides. The equivalent circuit is shown in Figure A1-2. Test result data is shown in Table A1-II.

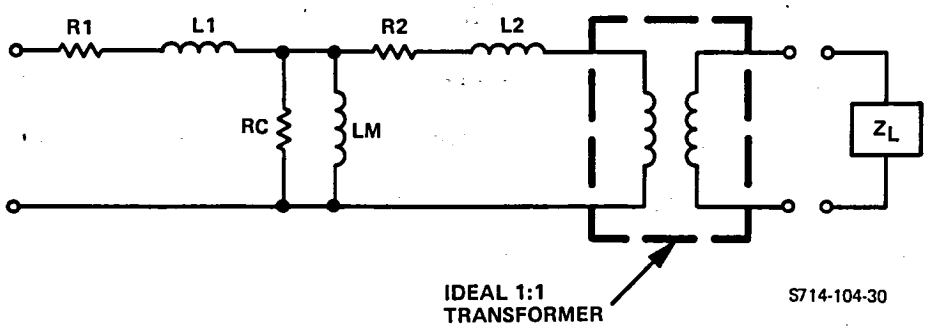

Figure A1-2
Transformer Model #2 Equivalent Circuit

TABLE A1-II - Model #2 Test Results

Freq (KHz)	0.5	1	3	6	10	15	20
R1,R2 (ohms)	.0028	.0043	.0083	.0132	.0201	.0283	.0370
X1,X2 (ohms	.00745	.0140	.0356	.067	.108	.160	.210
RC (ohms)	14	28	100	235	500	-	-
XM (ohms)	1.78	3.35	8.8	14.2	22.8	-	-
L1,L2 (mh)	.00237	.00223	.00189	.00178	.00172	.00170	.00167
LM (mh)	.57	.53	.47	.38	.36	-	-
*Ratio	1.56	2.40	4.64	7.37	11.23	15.81	20.67

* RD/Coil = .00179 ohms

A1.4 Discussion of Results and Additional Tests

A1.4.1 Conductor Skin Effect

One of the principle objective of the tests was to characterize the skin and proximity effects in the copper conductors caused by the tendency of high frequency current to flow only on the conductor surface. This phenomenon

can produce AC series resistance orders of magnitude larger than the DC coil resistance. Since the total transformer losses will consist of 50% to 70% I^2R losses, the skin effect caused resistance increase would have a significant effect on transformer efficiency. The RAC/RDC ratio measured on models #1 and #2 are plotted in Figures A1-3 and A1-4 and are compared to similar curves published by Reuben Lee. Since the total transformer losses will consist of 50% to 70% I^2R losses, this skin effect caused resistance increase would have a significant impact on the transformer efficiency

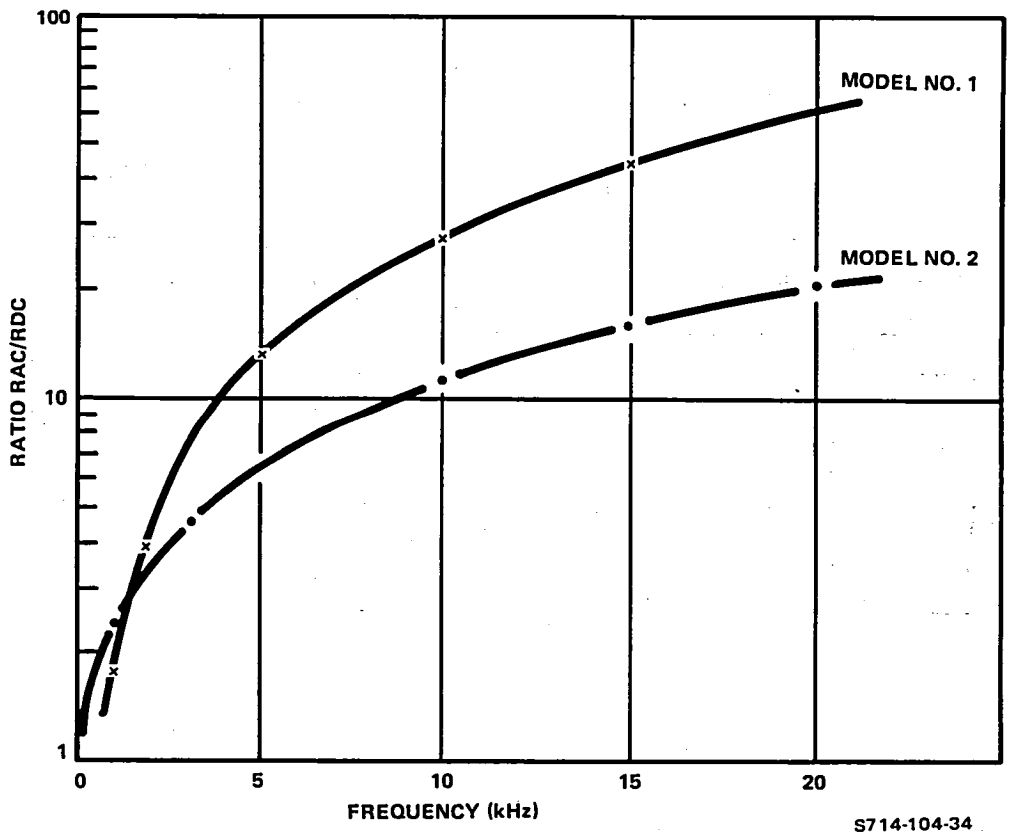

Figure A1-3
RAC/RDC Ratio Vs Frequency, Models #1 and #2

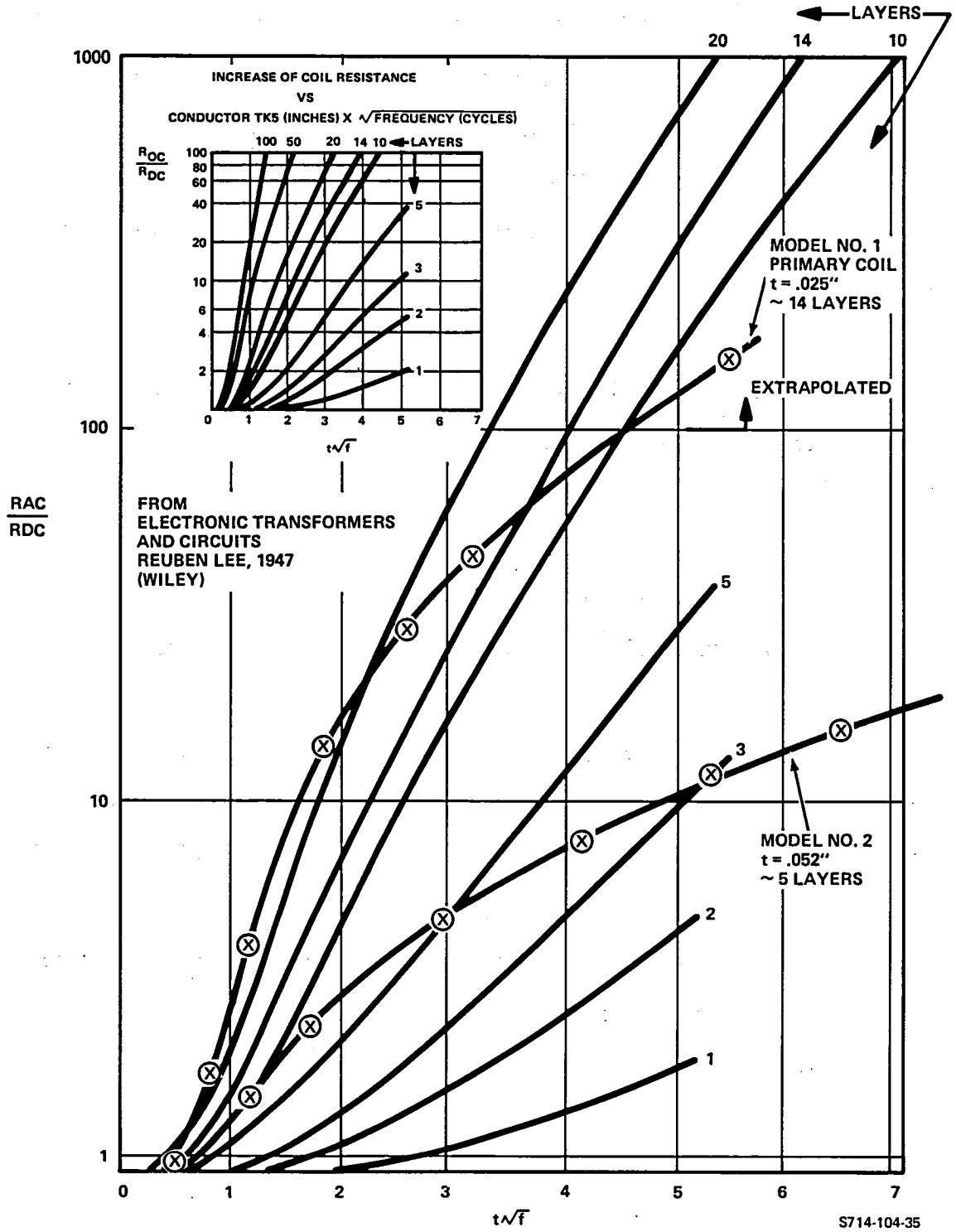

Figure A1-4
RAC/RDC Ratio Curves

To combat the skin effect problem, it is necessary to increase the conductor surface area with minimum increase in the conductor size. This is accomplished by bunching together many strands of fine, film insulated wire, with the constraint that each wire must regularly occupy a position at the surface of the conductor. Wire of this type is known as Litzendraht or, more commonly, Litz wire and consists of a number of separately insulated strands woven together.

To evaluate the Litz wire skin effect reduction capabilities, two versions were obtained and wound into coils as follows:

A. 20 turns, Litz wire - 105 strands, #33 AWG wire
B. 20 turns, Litz wire - 17 strands, #24 AWG wire
C. 20 turns, Solid conductor - 2 strands, #15 AWG wire

The third coil type, using #15 solid conductor, was wound to provide a directly comparable baseline. Test results plotted in Figure A1-5 show RAC/RDC ratio reductions of 4.2 to 1 at 20 KHz and 3.2 to 1 at 10KHz.

The Litz wire, however, requires about two times the volume of equivalent solid conductors. The net reduction in I^2R losses for a fixed coil size is, therefore, about 37% at 10KHz and 53% at 20KHz.

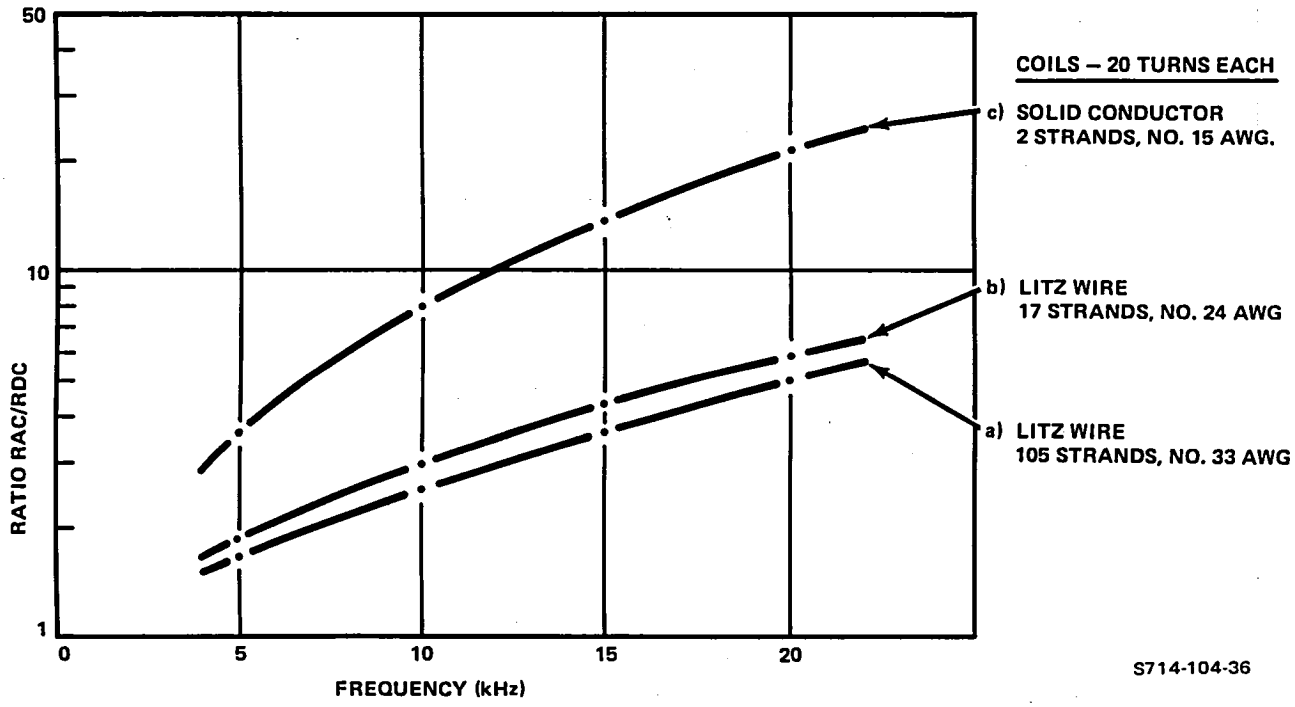

Figure A1-5
RAC/RDC Ratio vs Frequency Litz Wire and Baseline Coils

A1.4.2 Core Loss Measurements and Calculations

Initial correlation between core loss calculated from the material manufacturer's published curves and measured values was very poor. Values were measured up to 6 times the calculated values. However, in discussions with the vendor regarding possible explanations for the large apparent core loss discrepancy, he indicated that he is in the process of revising his core loss curves. A preliminary copy of these new curves (Figure A1-6) was supplied in which the losses increased 1.5 to 2.7 times the previously published values. Correlation, significantly improved, still indicates measured core loss at from 1.3 to 3 times the calculated values.

The core loss calculations are performed by first determining the flux density in the core from the relationship:

$B_{max} = E_{rms} * 10^8/4.44 * f * Np * Ae$

E_{rms} = the rms input voltage in volts

f = the frequency in Hz

Np = the number of primary winding turns

Ae = the effective core area in square centimeters

B_{max} = the flux density in gauss

For model #2 Ae = 7.15 cm^2 and Np = 5 turns

This relationship was verified by comparing a saturation curve performed on the transformer and the corresponding calculated flux levels to the manufacturer's B-H curve.

The knees of the curves coincided within a few percent, confirming the accuracy of the flux density calculations. Then, for a known flux density and operating frequency, the core loss in mw/cm^3 is determined from the manufacturer's Core Loss vs. Flux Density curves.

Measured core loss values may be determined by either of two methods. In the first method, the transformer is loaded and mesurements of input voltage, input current, load voltage, load current and the corresponding phase angles are obtained. From this data, all of the equivalent circuit parameters may be calculated. However, since the core loss is the drop across the core loss resistor (R_C) in the shunt branch, and most of the current flows

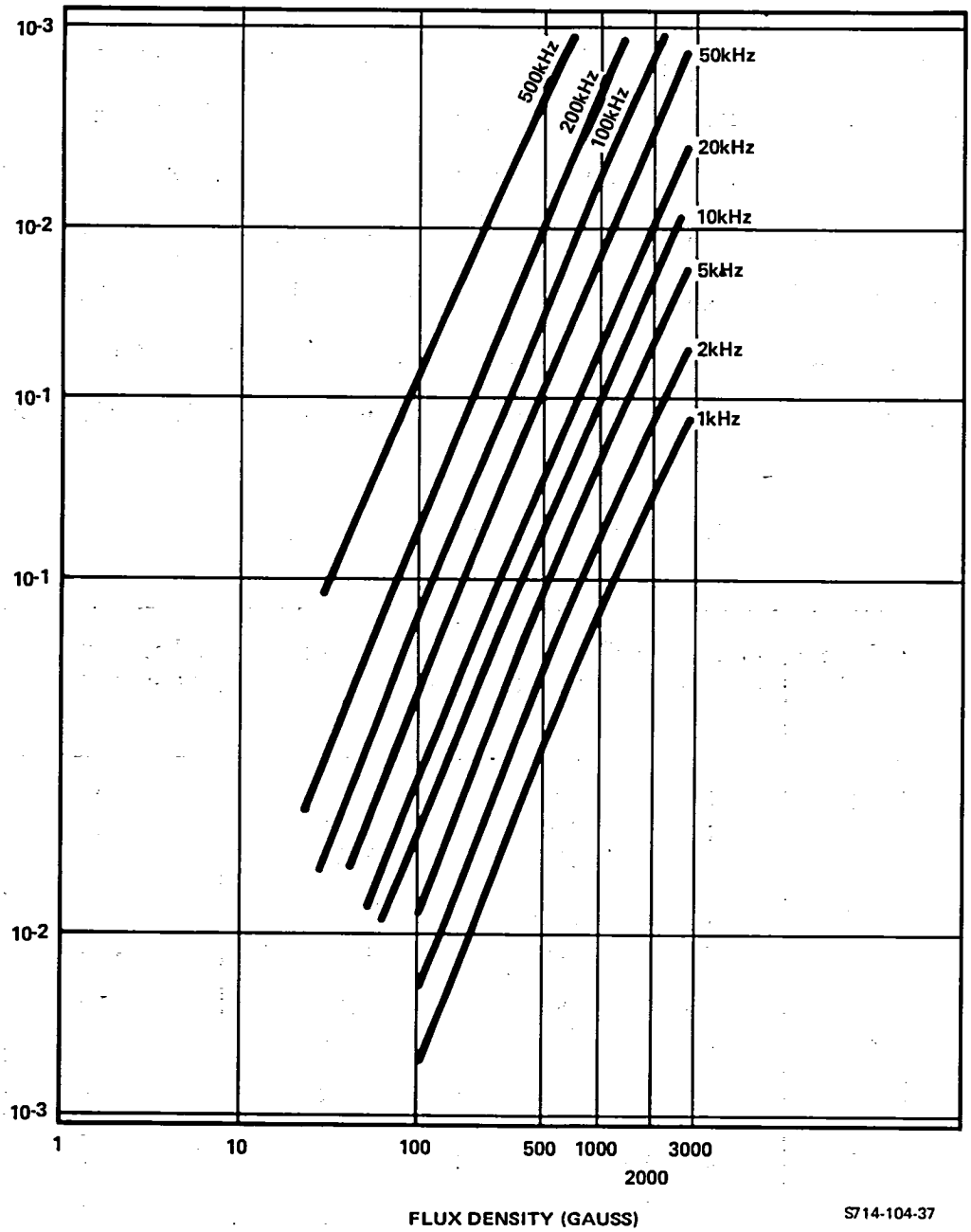

Figure A1-6
Manufacturer's Preliminary Revised Coreloss vs.
Flux Density Curves for 3C8 Material

directly through the series branch, small inaccuracies in the phase angle measurements may produce significant errors in the core loss calculation.

The second method to determine core loss is to excite the transformer primary with the secondary circuit open, and then measure input voltage, current and phase angle. In this method, all current flows through the series equivalent shunt branch and nearly all of the total power loss is attributable to core loss. Core loss was determined using both of these methods yielding reasonably consistant results. The test results, calculated flux density values, and the calculated core loss based on the vendor's revised curves are shown in Table A1-III.

TABLE A1-III - Core Loss Test Results

Freq. (KHz)	E_{RMS} Volts	Test Method *	Calc. B. (gauss)	Meas. Core Loss (watts)	Calc. Core Loss (watts)	Ratio **
1	3	2	1890	.40	.23	1.7
1	3.5	1	2205	.59	.33	1.8
1	5	1	3150	1.73	.74	2.3
3	6	1	1260	.45	.35	1.3
3	10	2	2100	1.82	1.13	1.6
6	6.5	1	683	.29	.19	1.5
6	20	2	2100	4.34	2.74	1.6
10	7	1	441	.24	.11	2.2
10	16	2	1008	2.07	.82	2.5
10	32	2	2016	9.31	4.15	2.2
20	30	2	945	4.43	1.47	3.0

*Test Methods: 1 = Load test; 2 = Open circuit impedance test

**Ratio = Measured Core Loss/Calculated Core Loss.

The remaining discrepancy between measured and calculated core loss values, shown in the last column of Table A1-III, has no obvious explanation. Allowance for a similar error is provided in the transformer design calculations.

A1.4.3 Inductance Calculations and Measurement

A1.4.3.1 Magnetizing Inductance

The magnetizing inductance (L_M) is determined by first calculating the permeances of the ferrite path sections from the relationship

$$P = \mu \frac{A}{L}$$

where the path area (A) and length (L) are in meters and the permeability (μ) is the product of the ferrite relative permeability (μr) and the permeability of a vacuum ($\mu o = 4\pi * 10^{-7}$ webers/ampere turn meter.)

Then, combining the permeances of the individual sections to determine the total path permeance (P_T):

$$P_T = 1/(1/P_1 + 1/P_2 + 1/P_3 + \ldots)$$

and assuming a ferrite relative permeability, ?r = 4700, the total permeance for the pot core set is described as:

$$P_T = 32.3 * 10^{-6} \text{ webers/ampere-turn.}$$

Then for an ideal current sheet winding (a long, thin solenoidal coil consisting of a single layer winding with negligibly small gaps between

successive turns), the inductance will be the total permeance times the turns squared.

$$L = N^2 P_T \text{ henrys. (webers-turn/ampere)}$$

However, as the coil is made shorter and multilayered, the inductance becomes a function of the ratio of length to radius and the winding depth. In reference A-1 (see paragraph A1.6), this relationship is described by the "Nagoaka constant" (Kn)

$$Kn = 1/(1 + .9 \frac{r}{l} + .32 \frac{t}{r} + .84 \frac{t}{l})$$

where r = coil means radius

l = coil axial length

t = coil radial thickness

Inductance is now defined as $L = Kn\ N^2\ P_T$.

Assume .030 wall thicknesses for the coil bobbin; l = .74 inch, r = .83 inch and t = .44 inch. Then, for the Nagoaka constant calculation, Kn = .373

The magnetizing inductance values calculated and measured are shown in table A1-IV.

Table A1-IV - Magnetizing Inductance Values

Magnetizing Inductance Value	Model #1 (N=27)	Model #2 (N=5)
Calculated (ideal current sheet)(mH)	23.55	.808
Calculated (with Nagoaka const.)(mH)	8.78	.301
Measured (average value) (mH)	12.9	.462

Based on the measured inductance values, it appears that the Nagoaka constant applies excessive reduction to the "ideal" inductance and that the constant should be about .56 for this size coil.

A1.4.3.2 Leakage Inductance

Leakage inductance is determined by defining the leakage path as the area inside the core and beyond the primary coil as shown in figure A1-9.

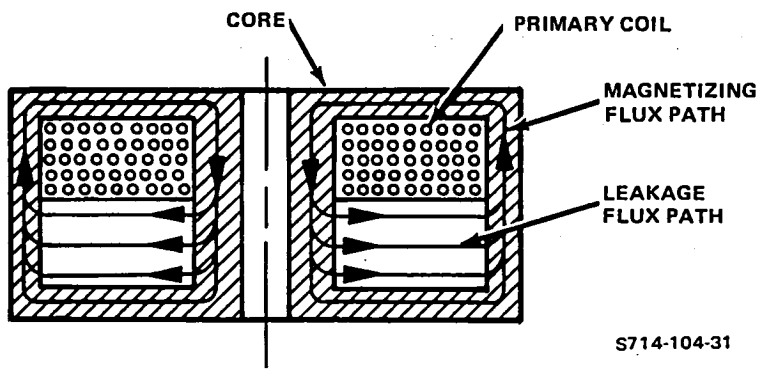

Figure A1-9
Leakage Path

The leakage permeance $P_L = \mu_o * \pi *$ Avg. Dia $* \frac{\text{Axial length}}{\text{Radial length}}$

$$P_L = .264 * 10^{-6} \text{ webers/ampere-turn}$$

For the "ideal" coil the leakage inductance is:

$$L_L = N^2 P_L$$

Including the Nagoaka constant, the leakage inductance is:

$$L_L = Kn\ N^2 P_L$$

The leakage inductance values calculated and measured are shown in table A1-V.

Table A1-V - Leakage Inductance Values

Leakage Inductance Value	Model #1 (N=27)	Model #2 (N=5)
Calculated (ideal current sheet)(mh)	.192	.00660
Calculated (with Nagoaka const.)(mh)	.0718	.00246
Measured (average value)(mh)	.104	.00390

As in the magnetizing inductance case, it appears that a Kn value of .56 is more appropriate than the .373 value derived from the equation. In the transformer design, the Nagoaka constant is applied but is modified based on these test results.

A1.5 Conclusions

The tests performed on the two small scale models and Litz wire coils may be summarized as follows:

1) The AC resistance of a transformer coil using solid conductor magnet wire and operating at 10KHz can easily be ten times the DC resistance value with a corresponding I^2R power loss increase. This phenomenon is due to "skin effect" in the conductor and may partially be eliminated by using woven stranded magnet wire, Litz wire.

2) Measured core losses were up to 6.3 times those calculated using the material vendor's published core loss curves and were 3 times those calculated using his revised curves.

3) The calculation procedure to determine magnetizing and leakage inductances to reasonable accuracy was established.

A1.6 References

A-1 The Theory and Design of Inductance Coils, V.G. Welsby; John Wiley and Sons, Inc. 1960 (p. 44)

Appendix 2

Disturbance Force Calculations

Appendix 2

Disturbance Force Calculations

A2.1 Force Calculation Techniques

The transformer contains a secondary winding which is attached to the magnetically suspended payload and undergoes the same excursions as the payload. When the transformer is energized and loaded, magnetic fields are established around the windings. If the payload is not centered, the fields interact to produce forces on the windings. In general, the force exerted on a current-carrying element in a magnetic field is given by:

$$\vec{F} = \int \vec{J} * \vec{B} \, dv$$

where $\vec{F}$ is the force in Newtons, $\vec{J}$ is the current density vector (amp/M^2), $\vec{B}$ is the magnetic induction vector (w/m^2), and the integration extends over the volume of the conductor. Typically $\vec{J}$ is proportional to the current in the conductor considered and $\vec{B}$ is proportional to the currents in all the conductors present.

For a transformer with two windings, the force on the secondary has the form:

$$F_2 = (a_{12} * i_1 * i_2) + (a_{22} * (i_2)^2))$$

where a_{12} and a_{22} are functions of the position of the windings and i_1 and i_2 are the currents in the primary and secondary, respectively. For

the AC currents considered here, the force consists of a DC component and an AC component with twice the frequency of the input current. The AC portion is well beyond the bandwidth of the suspension system, but the DC portion must be very small with respect to the magnetic bearings capabilities. Its magnitude is proportional to the products of the RMS values of the currents in the windings. A finite element model of the quasi-magnetostatic field in the transformer was used to predict the $\vec{B}$ field in the winding during extreme excursions. The $\vec{B}$ field was integrated over the volume of the secondary winding to obtain the DC component of the maximum disturbance forces.

The finite element method was used to obtain solutions of the quasi-static field in the transformer. Maxwell's equations for magnetostatic fields are:

$$\vec{\nabla} * \vec{B} = 0$$

$$\vec{\nabla} * \vec{H} = \vec{J}$$

where H is the magnetic field intensity vector (amp/M). It was assumed that all the constituent materials are magnetically linear so

$$\vec{B} = \mu\vec{H}$$

and that the magnetic induction may be obtained from a vector potential, A, such that

$$\vec{B} = \vec{\nabla} * \vec{A}$$

The variational form of Maxwell's equations is then

$$\int \Phi = 0,$$

$$\Phi = \int \frac{1}{2\mu} (\vec{\nabla} * \vec{A}) \cdot (\vec{\nabla} * \vec{A}) \, dv$$

$$- \int \vec{A} \cdot \vec{J} \, dV$$

$$+ \int \vec{A} \cdot (\vec{n} * \vec{H}) \, dS$$

where n is the unit outward normal to the surface and the surface integral vanishes at all interior points. On the exterior boundary, the surface integral appears as a boundary condition and is evaluated through the Biot-Savart law,

$$d\vec{H} = \frac{1}{4\pi r^3} (\vec{J} * \vec{r}) \, dV,$$

integrated over all the conducting elements. Axi-symmetric, 4-noded, isoparametric elements were used. The known (assumed uniform) current densities are the input sources. The simultaneous linear field equations were solved for the unknown vector potential A at the node points. The magnetic

induction $\vec{B}$ is given by the curl of the vector potential and was output at the centroid of each element. The force per unit current was obtained by summing the $\vec{J} \times \vec{B}$ components from each elements.

The program also calculates the inductance of the windings. The inductance in a circuit 1 due to the field established by the current in circuit 2 is given by:

$$L_{12} = \frac{1}{i_1} \frac{1}{i_2} \int_1 \vec{J}_1 * \vec{A}_{12} \, \text{dvolume}$$

where $\vec{A}_{12}$ is the vector potential due to the current in circuit 2.

A2.2 Calculation Technique Confirmation

To assess the accuracy of the solution method, two simple air core problems for which exact solutions are known were worked. The test geometrics were a single conducting loop and a seven-turn air core solenoid. The projection on a plane of symmetry of the axi-symmetric finite element model of the single conducting loop is shown in Figure A2-1. The geometry for the solenoid was obtained by extending the axial length of the conducting zone 7 times. Contour maps of the vector potential for both geometries were plotted (Figures A2-2 and A2-3) and a numerical comparison of the exact and finite element solutions is shown in Table A2-I and A2-II. The maximum error in the flux density prediction for these simple geometries is 2 1/2%.

TABLE A2-I - Self Inductance Numerical Comparisons

Case Modeled	Self Inductance	
	Exact	Finite Element
Single Loop	.073 uh	.060 uh
7 Turn Solenoid	1.63 uh	1.51 uh

TABLE A2-II - Flux Density Numerical Comparisons

Distance from E	FLUX DENSITY ON AXIS OF SYMMETRY ($x10^6$ w/m^2)			
	Single Loop		7 Turn Solenoid	
	Exact	Finite Element	Exact	Finite Element
Om	26.11	25.73	144.3	145.3
.005	24.29	24.17	140.2	141.1
.011	19.92	20.21	128.1	128.7
.016	15.04	15.42	109.6	110.2
.023	10.90	11.13	87.8	88.7
.027	7.82	7.91	66.7	67.6
.032	5.64	5.67	49.1	49.7
.057	4.13	4.13	35.9	36.1
.042	3.08	3.07	26.3	26.3
.048	2.34	2.33	19.6	19.5
.053	1.80	1.80	14.9	14.8
.059	1.42	1.41	11.5	11.4

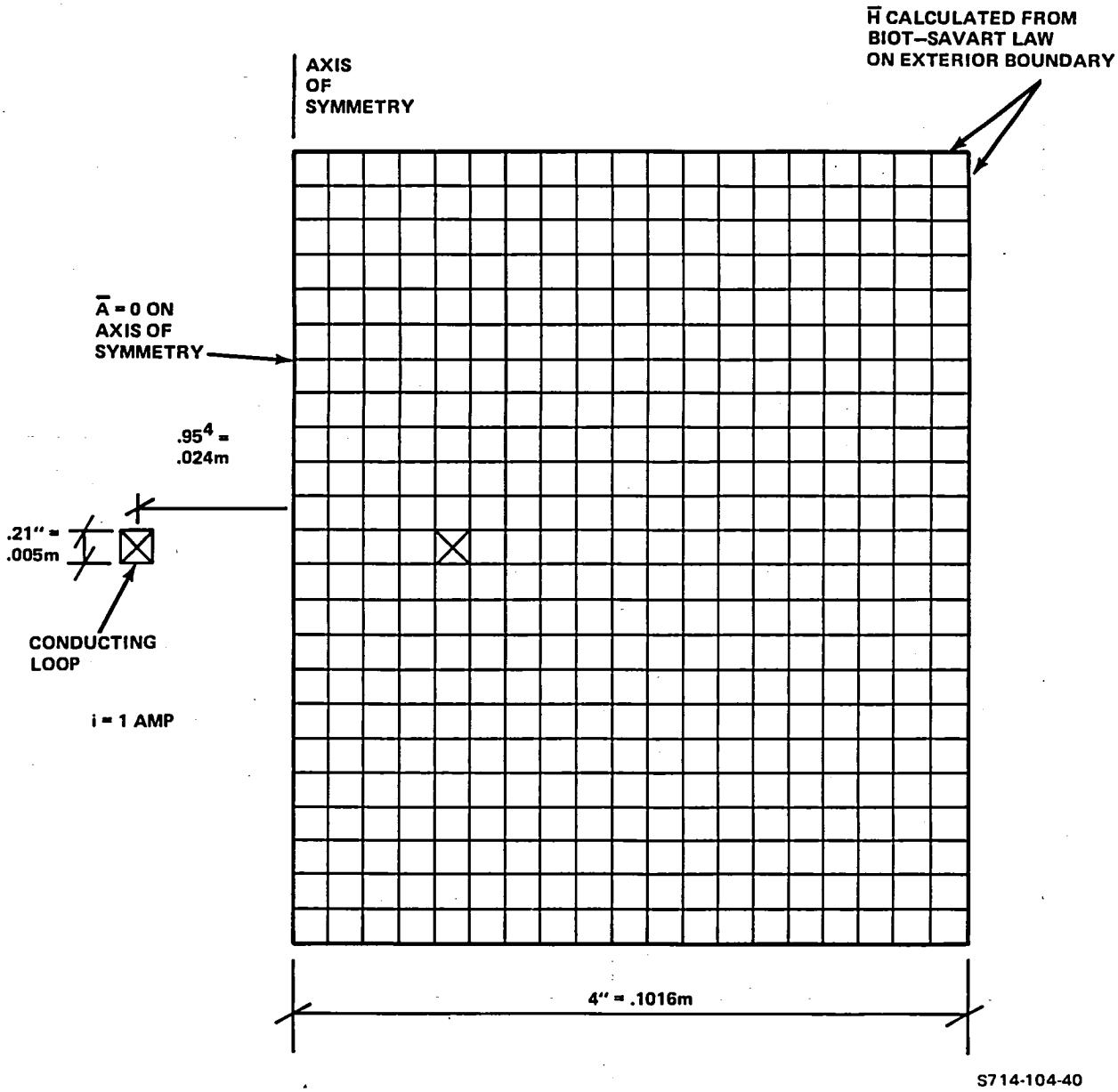

Figure A2-1
Single Conducting Loop
Finite Element Grid

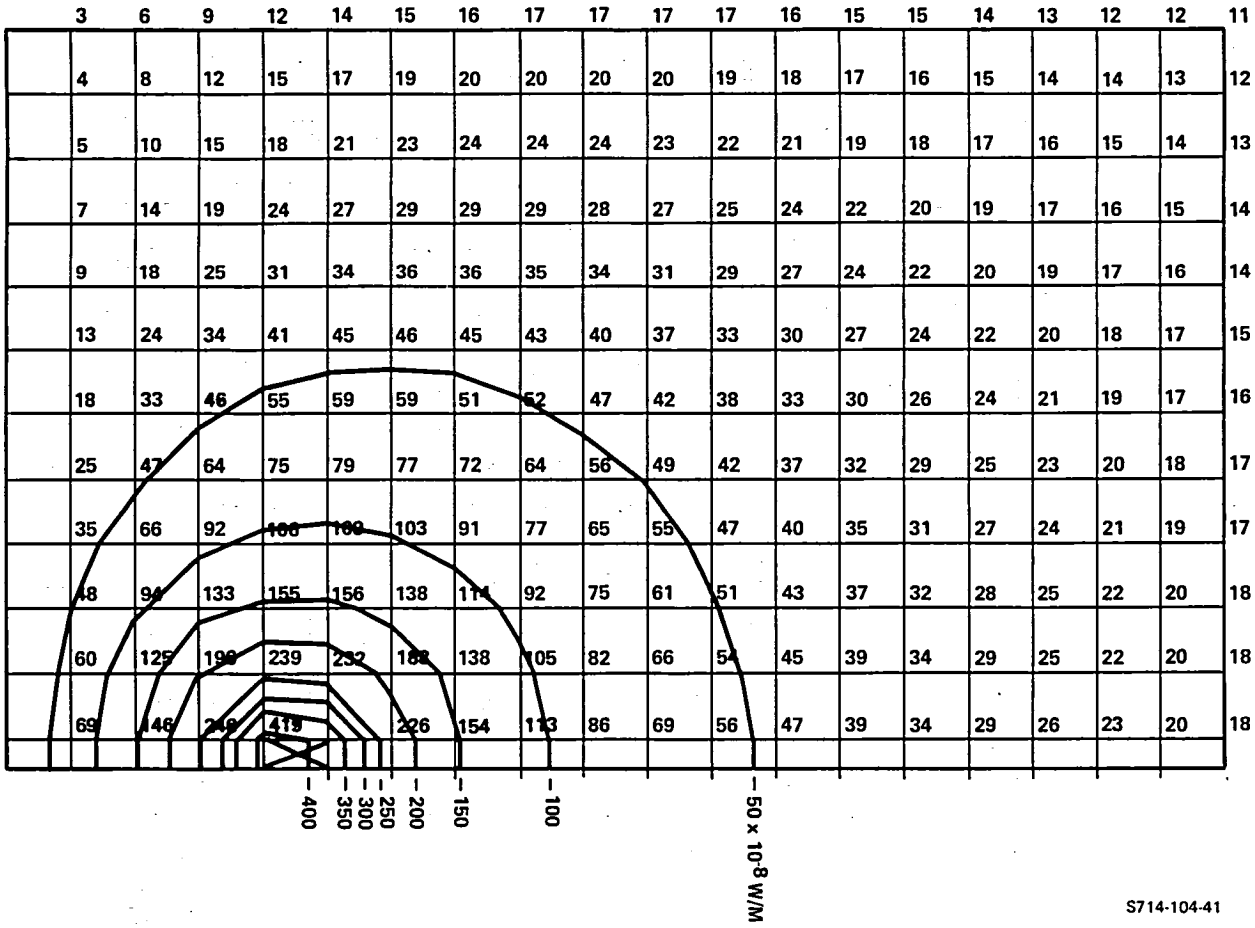

S714-104-41

Figure A2-2
Equipotential Lines Single Conducting Loop

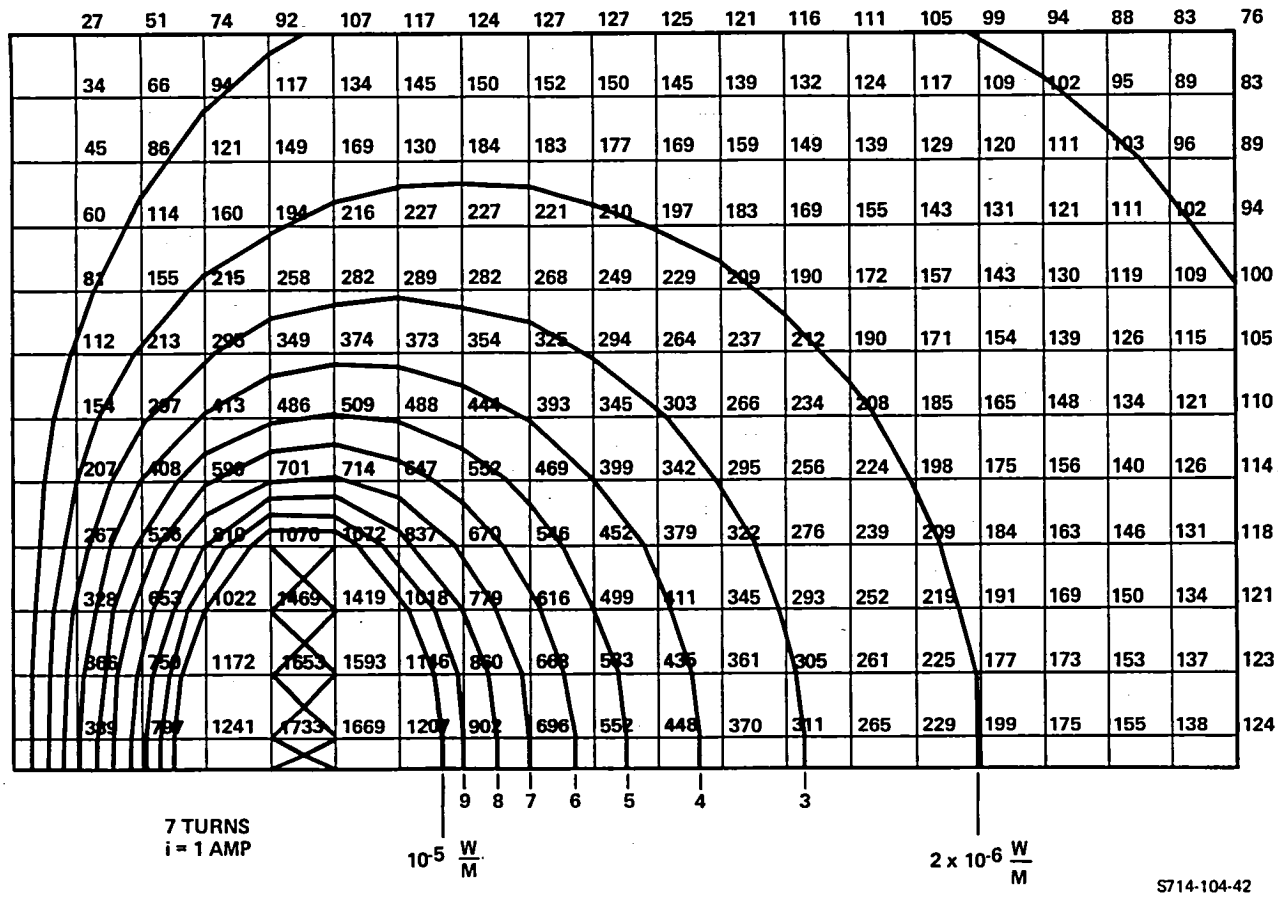

Figure A2-3
Equipotential Lines Solenoid

A2.3 Force Calculations

Several simplifying assumptions are implicit in this solution procedure. It is assumed that the magnetostatic field is applicable although the excitation frequency is 10 KHz. The most significant omissions in this assumption are skin effect in the windings and eddy currents in the core. Skin effect is tacitly neglected by the assumption of uniform current density over the area of the conductors. This is considered appropriate since Litz wire is used for the windings, with 630 and 1995 strands in the primary and secondary, respectively. Eddy currents are considered negligible since the core material is an extremely low loss ferrite. Only magnetic forces were considered. Actually, electric charge forces are also present but they are several orders of magnitude smaller in amplitude. The core material was assumed to be linear but is actually as shown in figure A2-4. This assumption is considered appropriate since the flux density is only on the order of 600-1400 gauss.

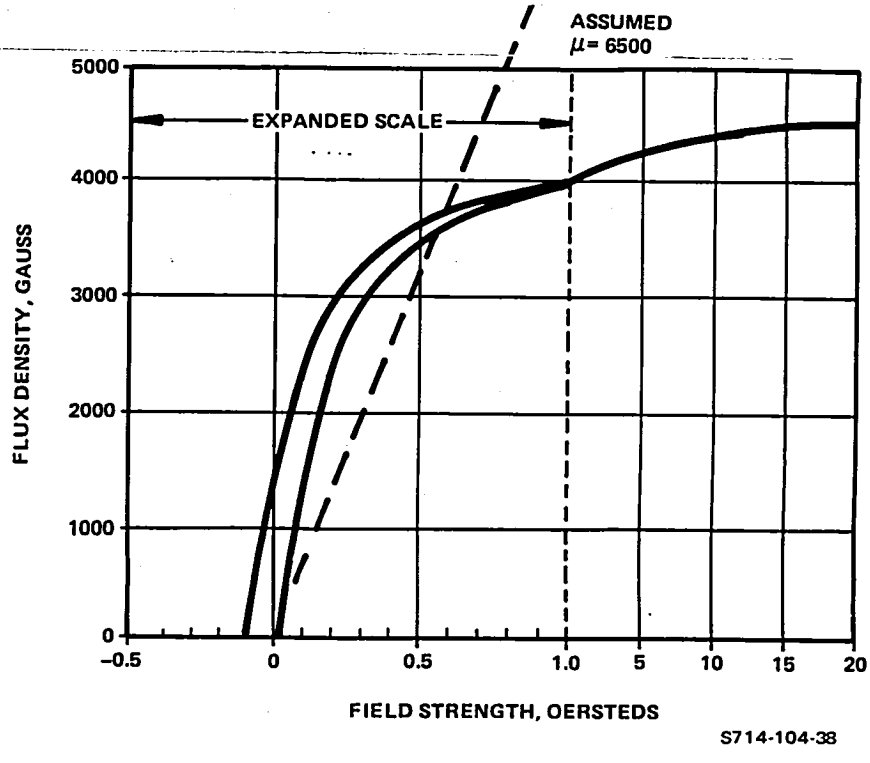

Figure A2-4
Hysteresis Loop

The transformer configuration modeled and the finite element gridwork used are sketched in Figures A2-5 and A2-6, respectively. The core material is ceramic magnetics MN60, with a relative permeability of 6500. The windings were assumed to have a relative permeability of one. There are 7 and 2 turns in the primary and secondary, respectively. The proportions of the secondary and the core cavity were selected to minimize the forces due to motion of the secondary. The flux leakage inside the cavity of the core is plotted for unit current in the primary (Figure A2-7), unit current in the secondary (Figure A2-8), and full load operation (Figure A2-9). Only one half the cavity is shown in these plots and the conducting area is shaded. The axial component of leakage due to current in the primary only was estimated by a hand calculation based on the relative reluctances of the air and ceramic core paths. This leakage prediction is plotted for comparison on the map of the field due to current in the primary only. A summary of the inductances and DC force amplitudes predicted by the model is shown in Tables A2-III through A2-V.

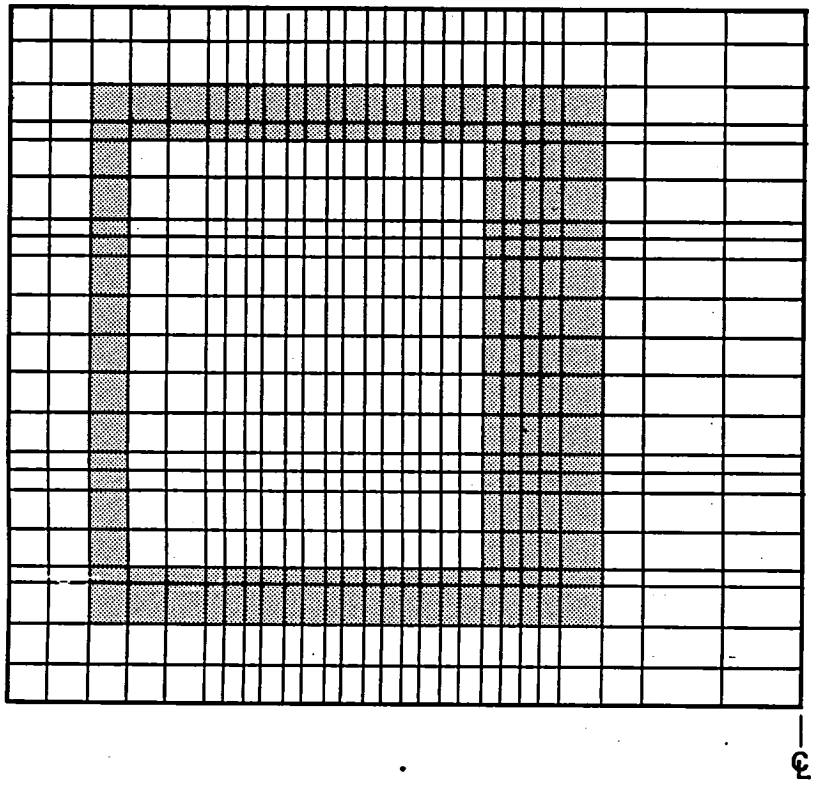

Figure A2-5
Finite Element Grid

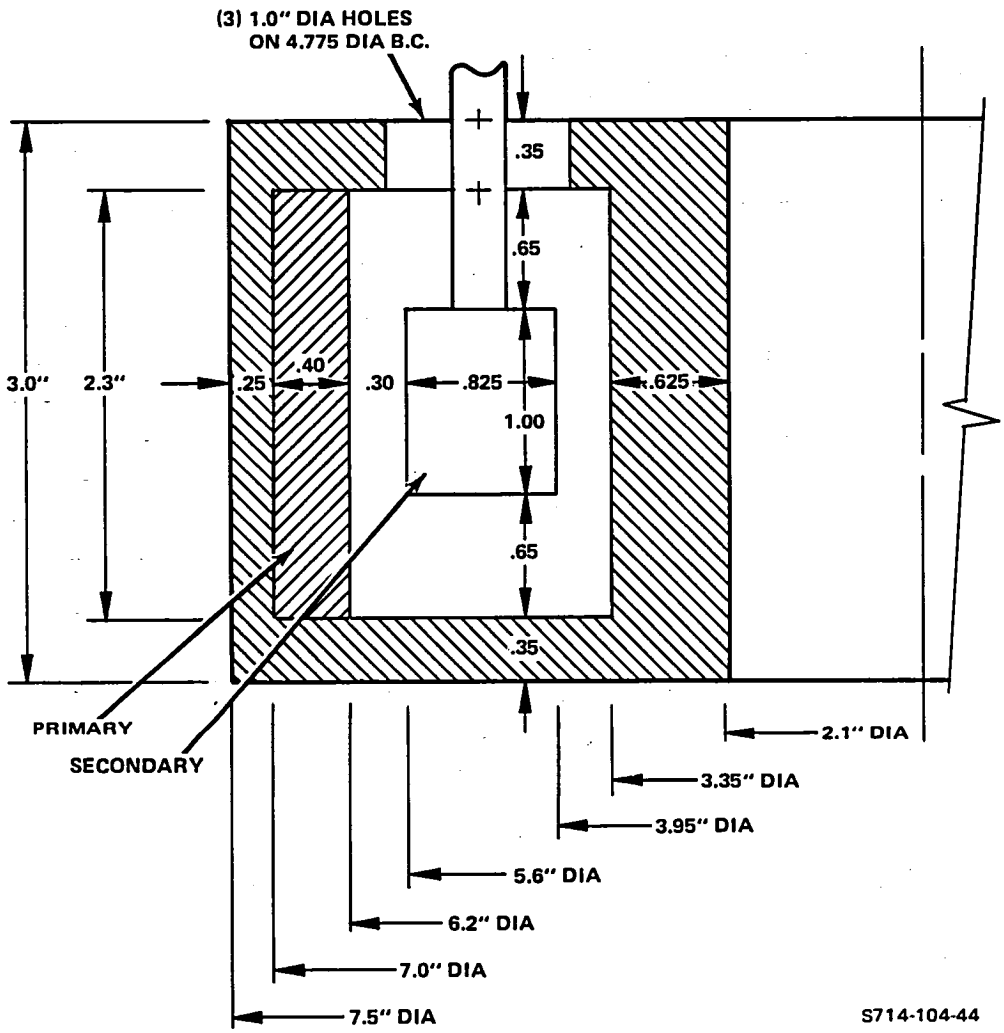

Figure A2-6
Baseline Transformer

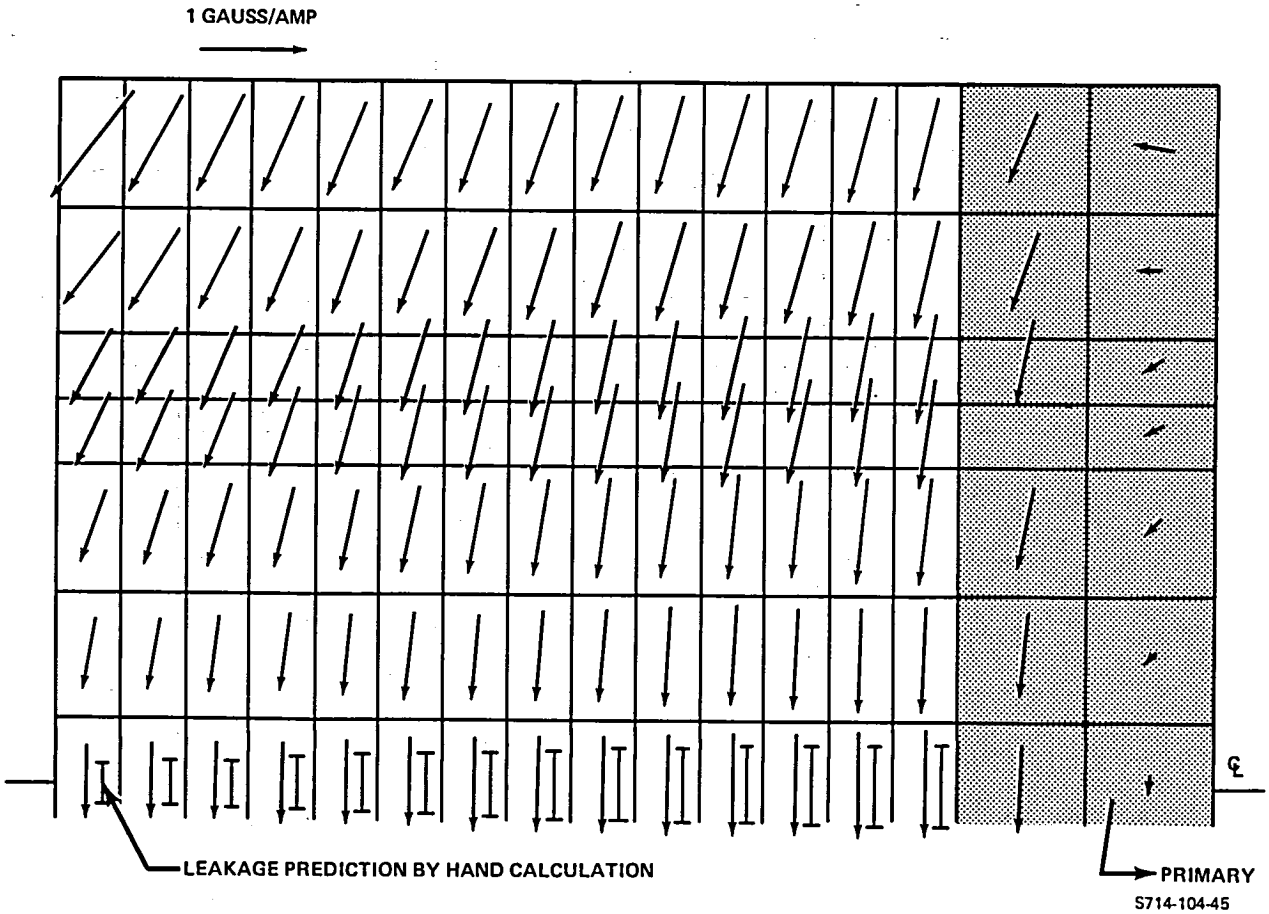

Figure A2-7
Flux Leakage Due to Unit Current in Primary

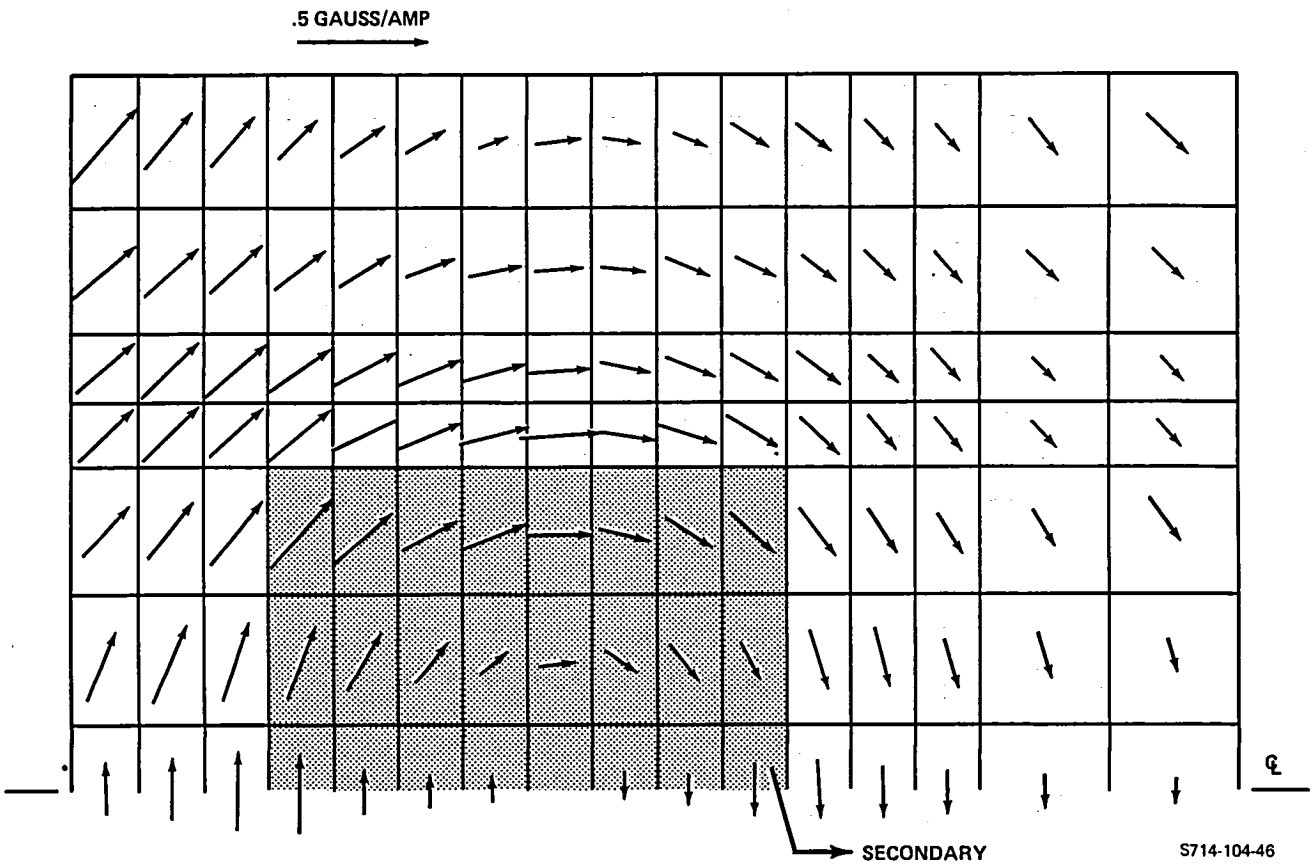

Figure A2-8
Flux Leakage Due to Unit Current in Secondary

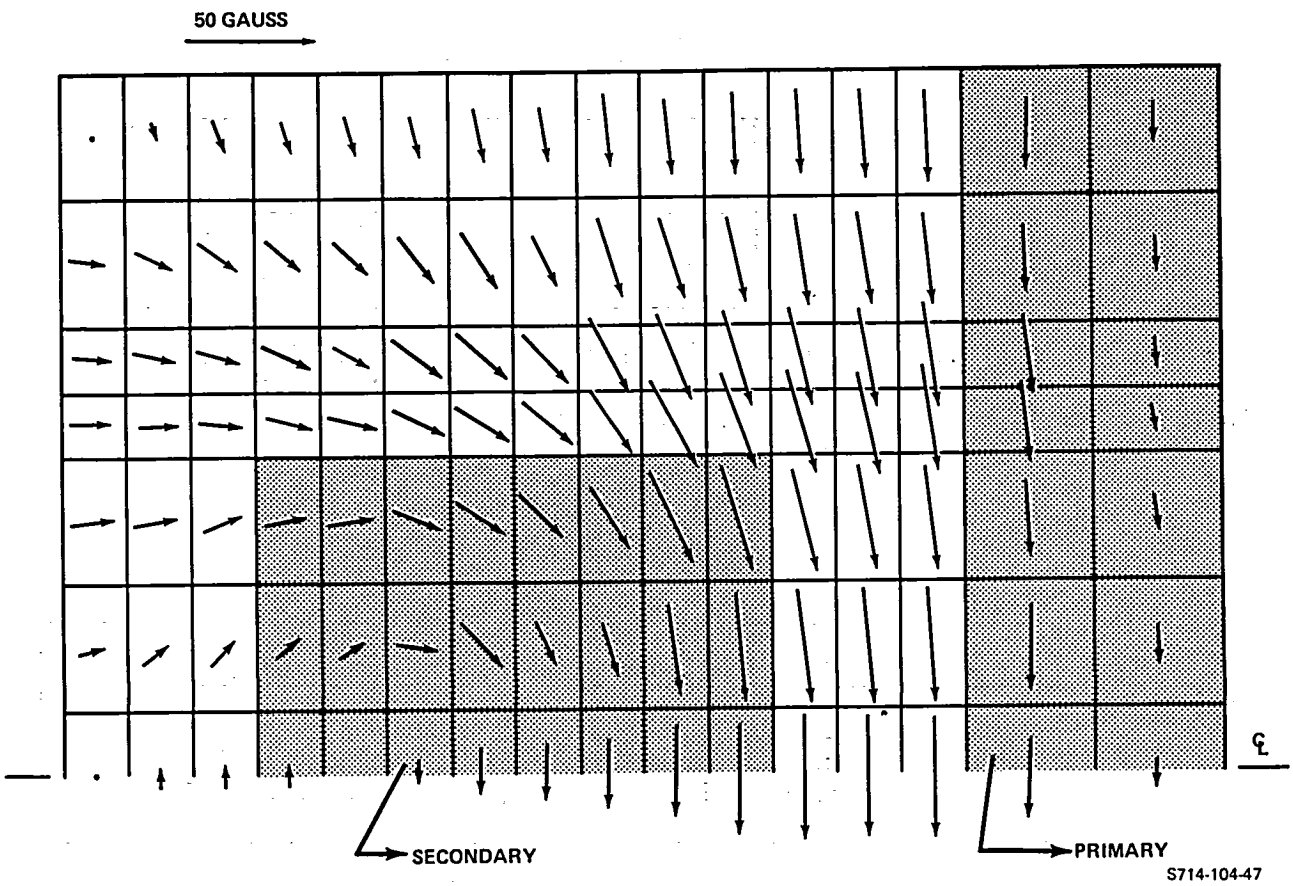

Figure A2-9
Flux Leakage at Full Load

TABLE A2-III - Inductance Summary

Inductance	Notation	Value (mh)
Primary - Self	L_{11}	1.329
Secondary - Self	L_{22}	.3802
Mutual	L_{12}	4.665

TABLE A2-IV - Power Coupling Summary

V_{IN}	I_{IN}	V_{OUT}	I_{OUT}
$100V_{rms}$	25.6A	28.1V	89.2A

Coupling factor: K = 1.329/(.3802 x 4.655)0.5 = .9990
operating at 10KHz and for the full load conditions

TABLE A2-V - Peak Force Summary

Secondary Coil Motion	Force/Torque, Direction
$\pm$ .22 inch, Axial $\pm$ .20 inch, Radial $\pm$ .75 degrees, Tilt	+ .00244 pounds, Axial + .00124 pounds, Radial + .00053 inch-pounds, Tilt

The direction of the forces generated are always in a direction to oppose the relative motion between elements.

Appendix 3

Baseline Transformer Fabrication Drawings

Part Number	Part
1551-10381	Core Segment (End)
1551-10382	Core Segment (Outer)
1551-10383	Core Segment (Inner)
1551-10384	Support Posts (Coil)
1551-10385	Coil, Primary
1551-10386	Coil, Secondary, with Support Posts

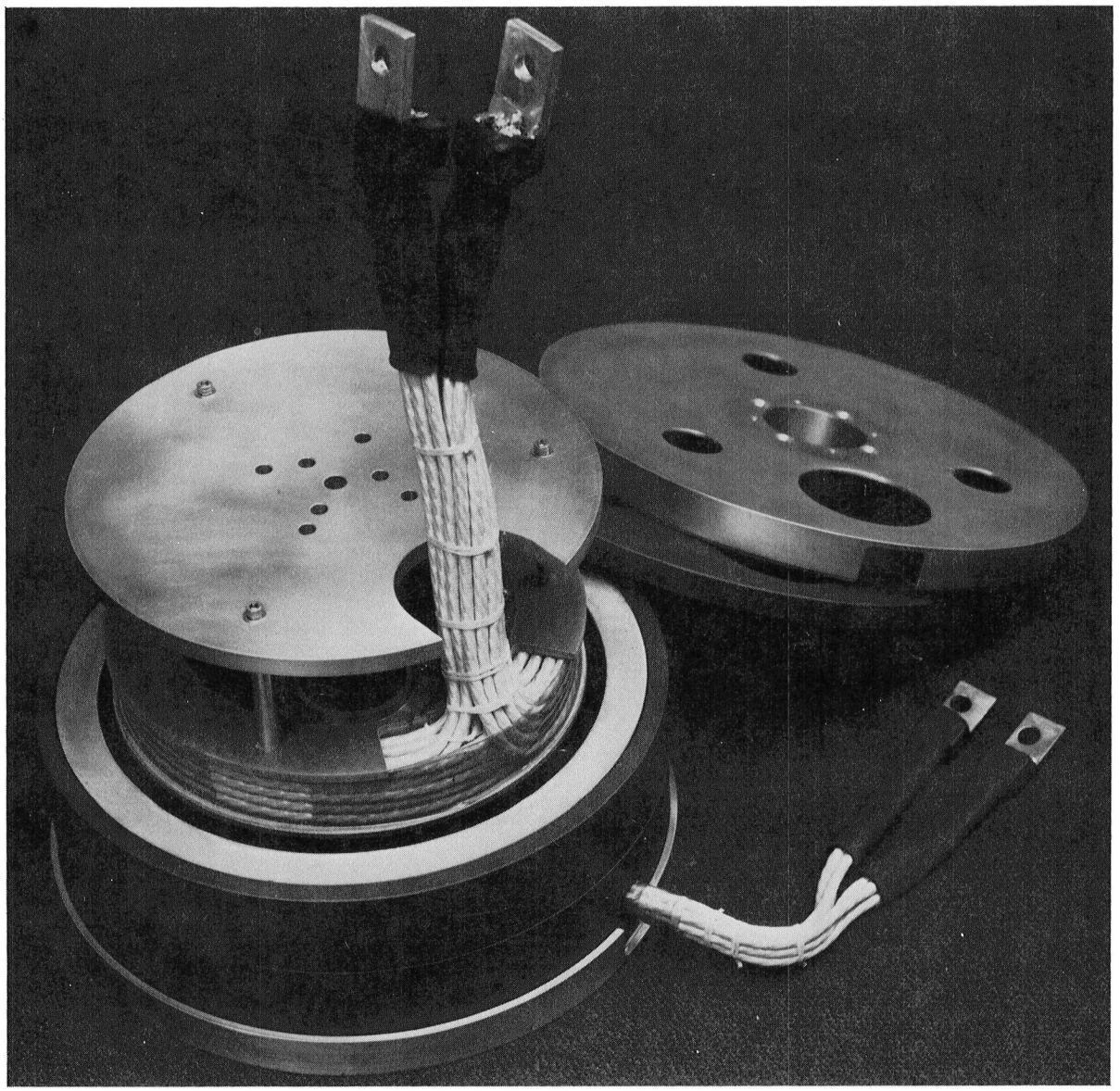

13-16366-3

Figure A3-1
Baseline Transformer

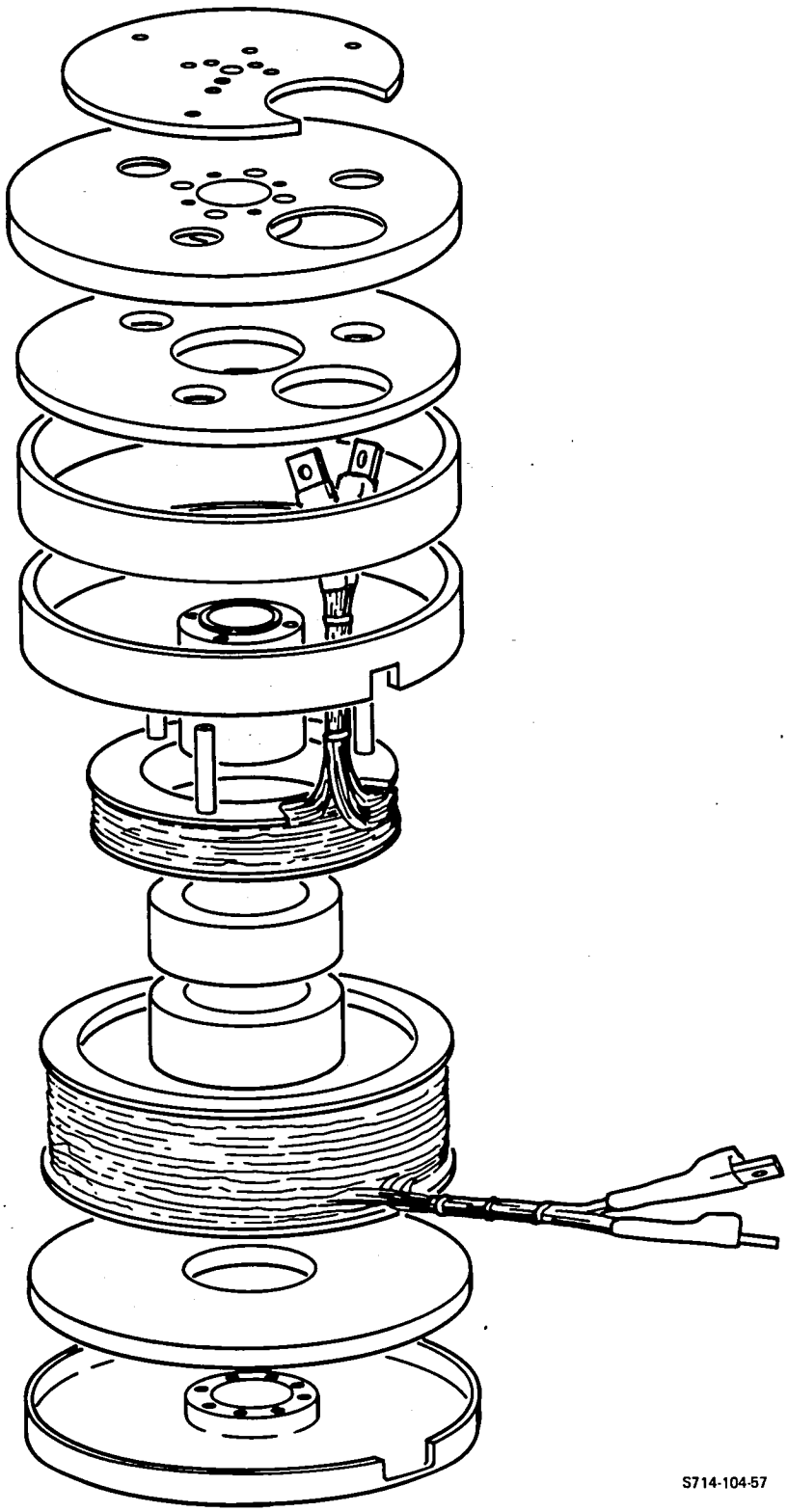

Figure A3-2
Baseline Transformer Explosion

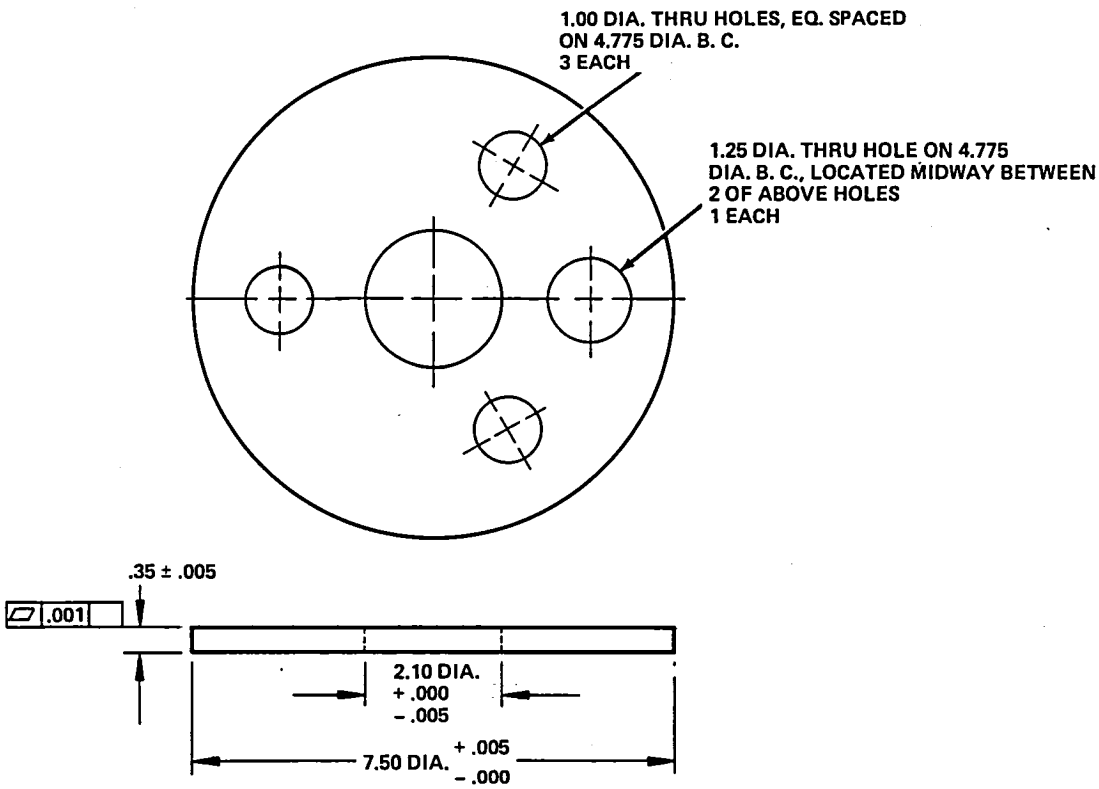

NOTE: MATERIAL – CERAMIC
MAGNETICS MN60 FERRITE

PART NO.	FEATURE
1551-10381-1	HOLES INCLUDED, TOLERANCE + .005 HOLE DIA. AND BC
1551-10381-2	HOLES OMITTED

1 EACH REQUIRED

CORE SEGMENT (END)

S714-104-48

Figure A3-3
Core Segment (End)

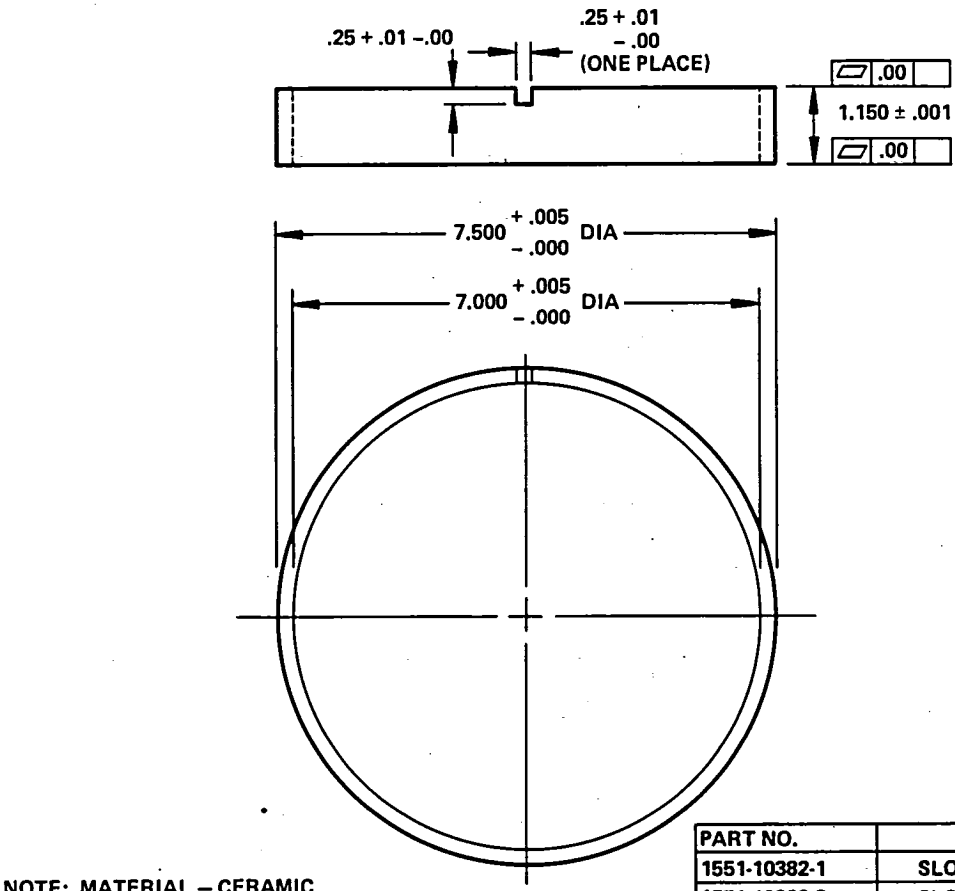

PART NO.	FEATURE
1551-10382-1	SLOT INCLUDED
1551-10382-2	SLOT OMITTED

1 EACH REQUIRED

NOTE: MATERIAL – CERAMIC
MAGNETICS MN60 FERRITE

S714-104-49

Figure A3-4
Core Segment (Outer)

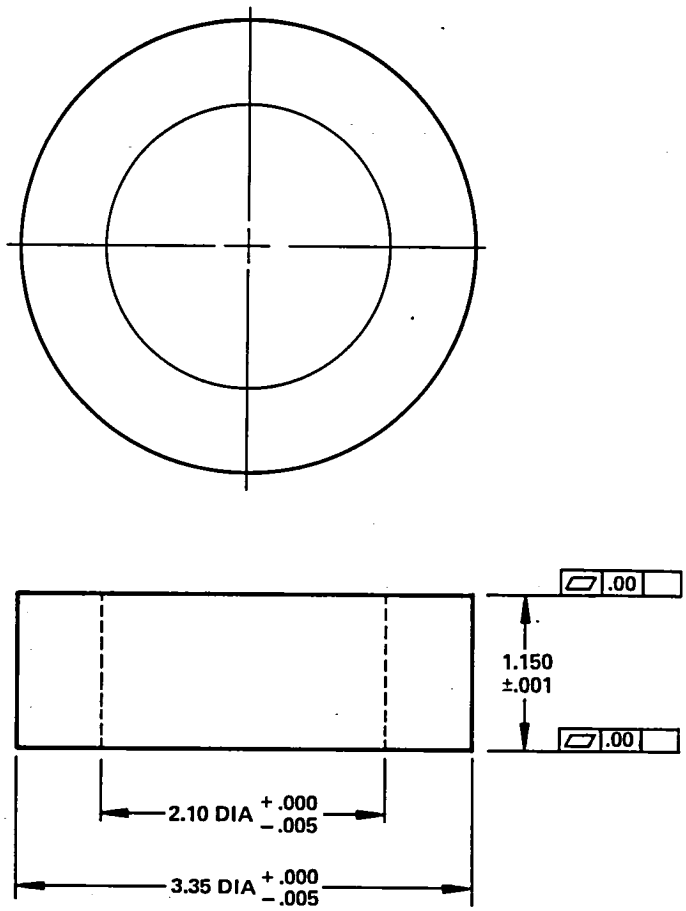

NOTE: 2 REQUIRED
MATERIAL-CERAMIC
MAGNETICS MN60 FERRITE

CORE SEGMENT (INNER)

S714-104-50

Figure A3-5
Core Segment (Inner)

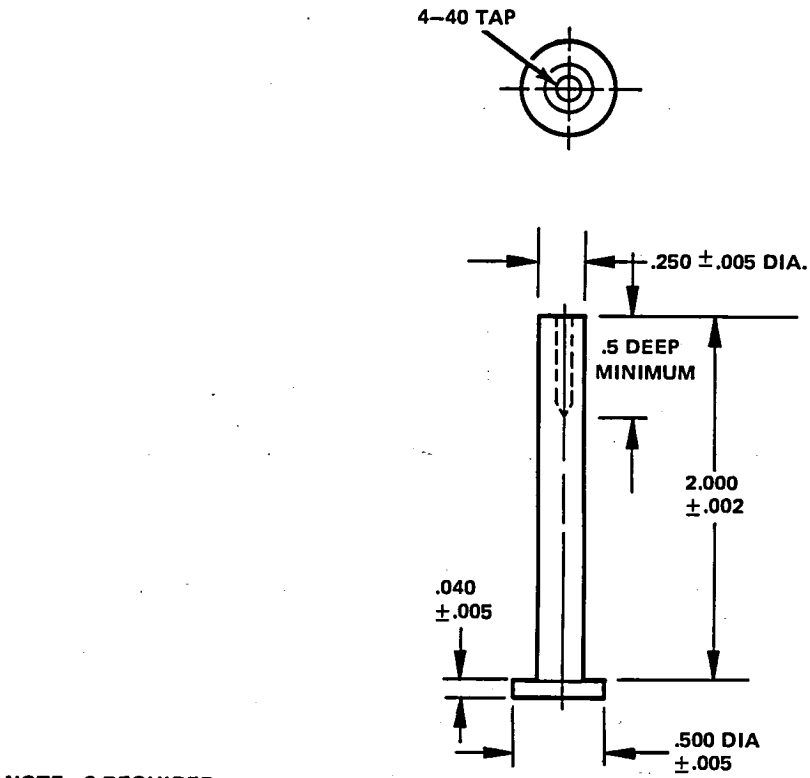

NOTE: 3 REQUIRED
MATERIAL ALUMINUM 6061

SUPPORT POSTS (COIL) S714-104-51

Figure A3-6
Support Posts (Coil)

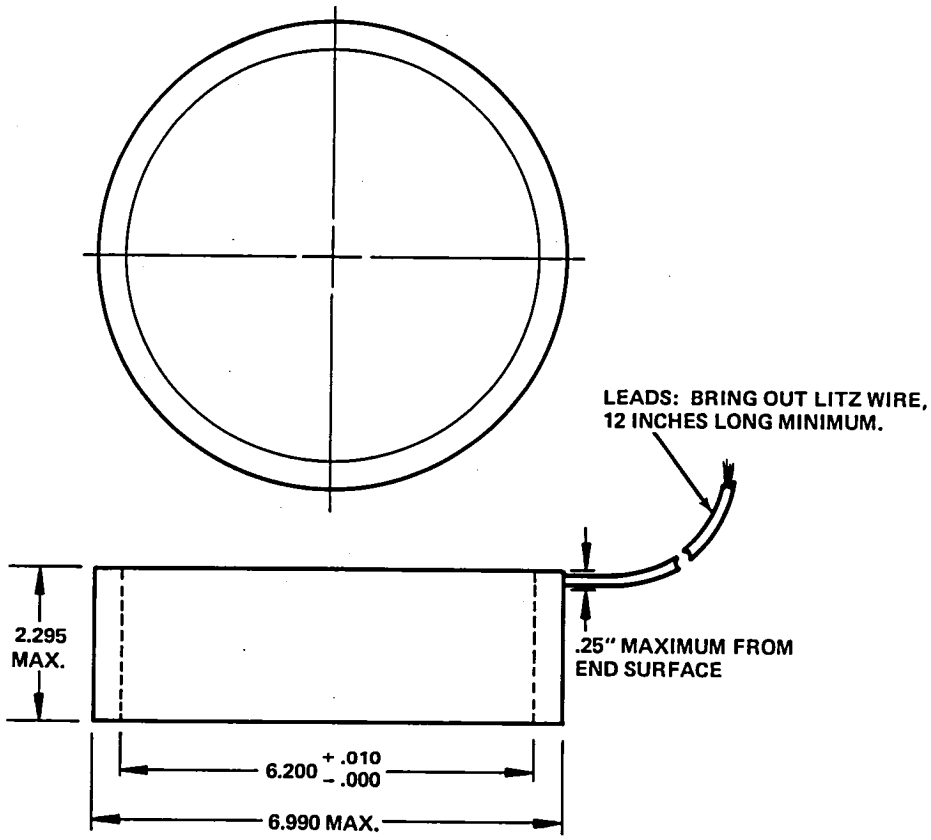

NOTE: WINDING: 7 TURNS,
630 STRANDS – NO. 33 AWG LITZ
WIRE WITH DOUBLE NYLON
WRAP, MAY BE MULTIPLE
BUNDLES TO OBTAIN THE
630 STRANDS, eg.,
6 BUNDLES, 105 STRANDS EA.

COIL, PRIMARY

S714-104-52

Figure A3-7
Coil, Primary

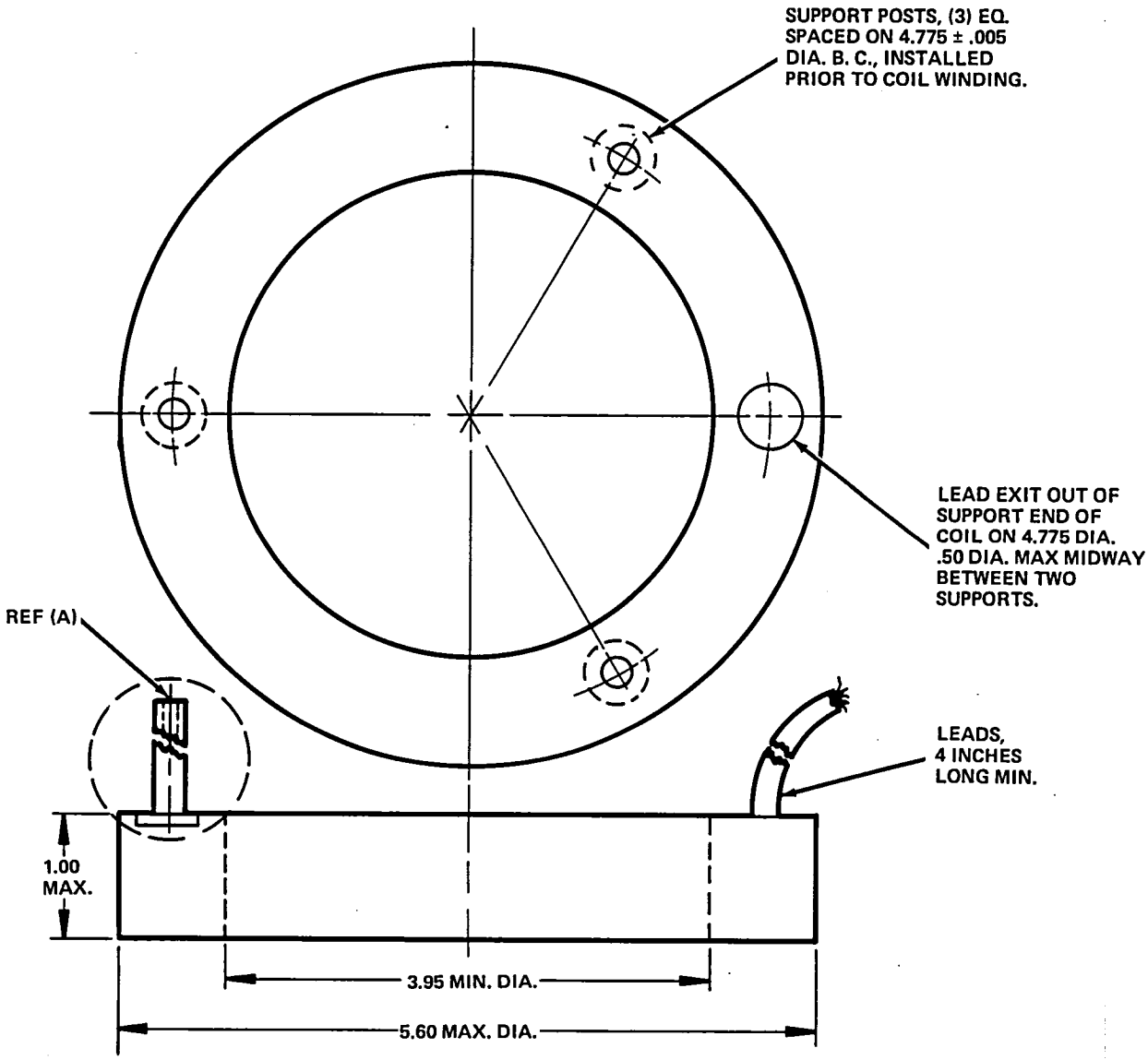

NOTE:
WINDING: 2 TURNS, 1995 STRANDS – NO. 33 AWG LITZ WIRE WITH SINGLE OR DOUBLE NYLON WRAP, MAY BE MULTIPLE BUNDLES TO OBTAIN THE 1995 STRANDS, eg., 19 BUNDLES, 105 STRANDS EACH.

LEADS: LITZ WIRE, 945 STRANDS MINIMUM – NO. 33 AWG WITH DOUBLE NYLON WRAP, 4 INCHES LONG MINIMUM.

REF (A): SUPPORT POSTS TO BE SUPPLIED BY SFS. SECTION SHOWS POST INSTALLED IN BOBBIN 3 PLACES. P/N 1551-10384.

S714-104-53

Figure A3-8
Coil, Secondary, with Support Posts

Appendix 4
AVS Converter Parts List

AVS Converter Parts List

Resistors

Qty	Description	Symbol	Part No.
8	1K, 1/8W	R1,R9,R15,R16, R31,R32,R41,R48	RN-60D
1	18.2K, 1/8W	R2	RN-60D
1	200, 1/8W	R3	RN-60D
1	6.49K, 1/8W	R4	RN-60D
1	1.02K, 1/8W	R5	RN-60D
7	10K, 1/8W	R6,R10,R13,R19, R28,R45,R46	RN-60D
1	60.4K, 1/8W	R7	RN-60D
1	8.66K, 1/8W	R8	RN-60D
1	187, 1/8W	R11	RN-60D
2	24.9K, 1/8W	R12, R14	RN-60D
2	43.2, 1/8W	R17, R18	RN-60D
2	649, 1/8W	R20, R21	RN-60D
6	100, 1/8W	R22,R23,R24,R25 R27,R49	RN-60D
1	274, 1/8W	R29	RN-60D
1	30.9K, 1/8W	R30	RN-60D
2	49.9K, 1/8W	R35, R36	RN-60D
2	100K, 1/8W	R37, R38	RN-60D
2	13.3K, 1/8W	R39, R40	RN-60D
3	4.99K, 1/8W	R42, R43, R47	RN-60D
1	20K, 1.8W	R44	RN-60D
1	4, 50W	R26	RH-50
1	.51, 1W	R33	RS-F1A
1	2, 3W	R34	RS-28
2	100, 1W	R50, R51	RS-F1A

Capacitors

Qty	Description	Symbol	Part Number
1	.01uF, 100v	C1	CK05BX103K, Centralab
1	.22uF, 200v	C2	CK05BX221K, Centralab
1	100uF, 150v	C3	39D107F150FP4, Sprague
2	.1uF, 200v	C4, C7	CK05BX101K, Centralab
1	1400uF, 756	C5	142G075AA2A, Sprague
1	10uF	C6	TF1407, Sprague
4	150pF, 200v	C8,C12,C13,C14	CKR05BX151KR, Centralab
2	.005uF, 100v	C9, C124	56A-D50, Sprague
1	100pF, 200v	C10	CKR05BX101KR, Centralab
1	.001uF, 200v	C11	CKR05BX102KR, Centralab
108	30uF, 100v	C16 thru C123	735P306X9100YVL, Sprague
1	2800uF, 75v	C125	282G075AB2A, Sprague

Diodes

Qty	Description	Symbol	Part Number
6	.4A, 400v	CR1 thru CR6	1N647
2	6.8v (zener)	VR1, VR2	1N4099
1	28.5v (transorb)	VR3	1N5556
1	10v (zener)	VR4	1N4104
3	220A	CR7,CR8,CR9	735P306X9100YVL Westinghouse

ICS

Qty	Description	Symbol	Part Number
5	Operational Amplifier	U1,U2,U4,U6,U7	LM101AH
4	Comparator	U3,U5,U8,U9	LM111H

Inductors

Qty	Description	Symbol	Part Number
2	.53 uH	L1, L2	(Fabricate per
2	155 uH	L3, L4	design spec)

Transformers

Qty	Description	Symbol	Part Number
1	1:3.5	T1	(Fabricate per
3	72:9:1	T2, T3, T4	design spec)
6	200:1	T5 thru T10	

Appendix 5

Schematic Diagram

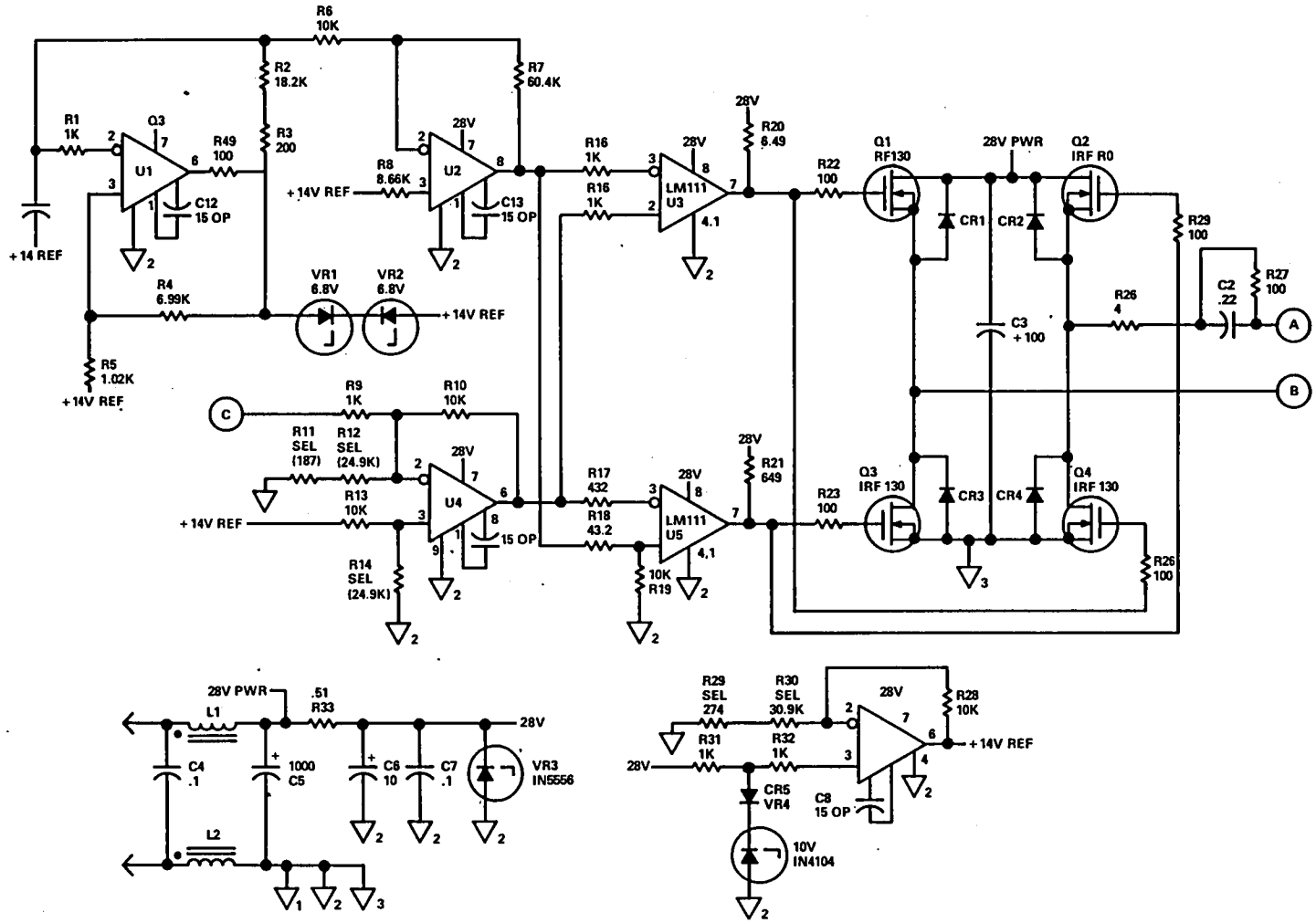

NOTES:

1. SELECT R29 AND R30 FOR +14 VDC AT U6, PIN 6.
2. SELECT R11, R12, R14, FOR 60% DUTY CYCLE AT T1 SECONDARY.

S714-104-64

Figure A5-1
Baseline Transformer Schematic Diagram

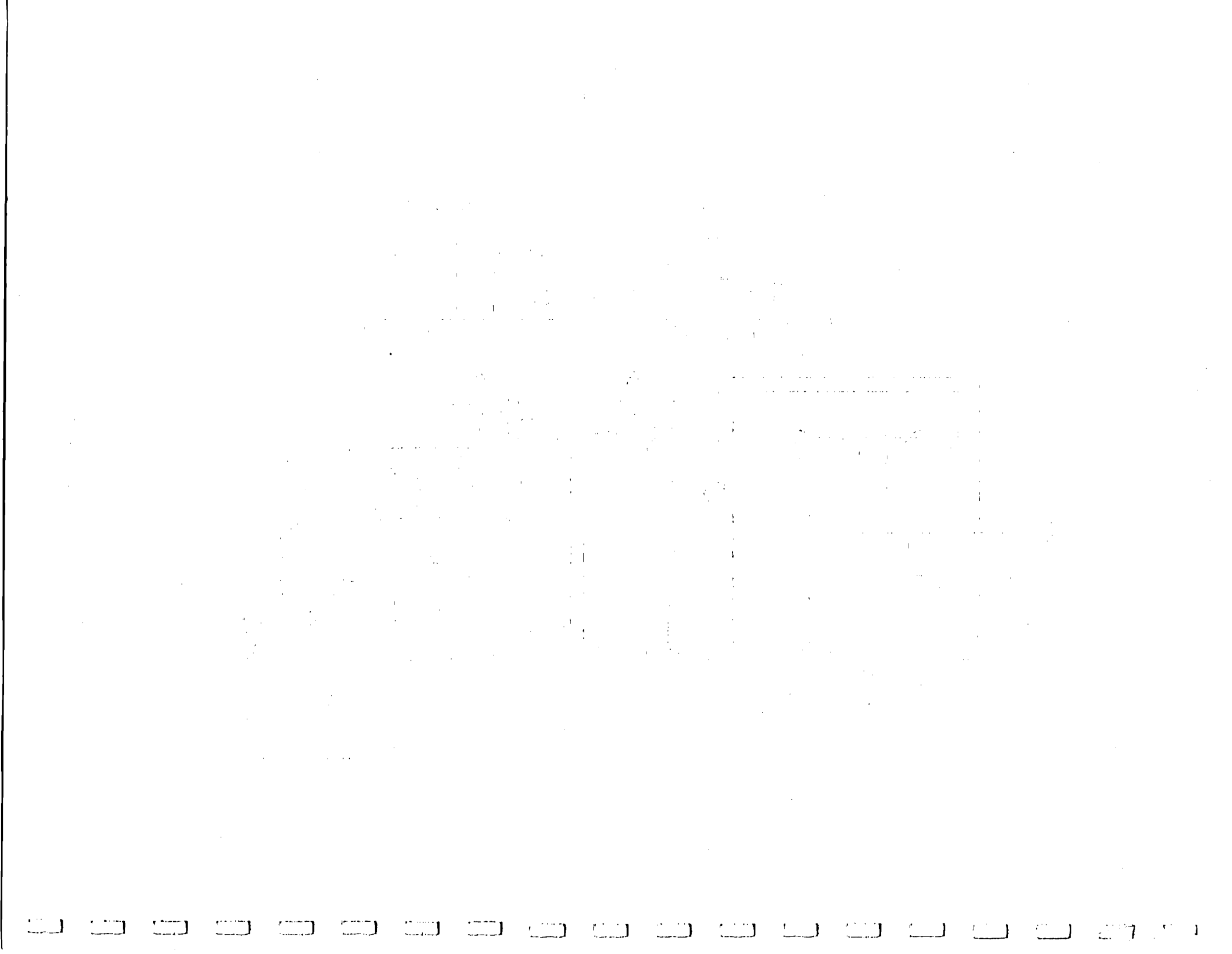

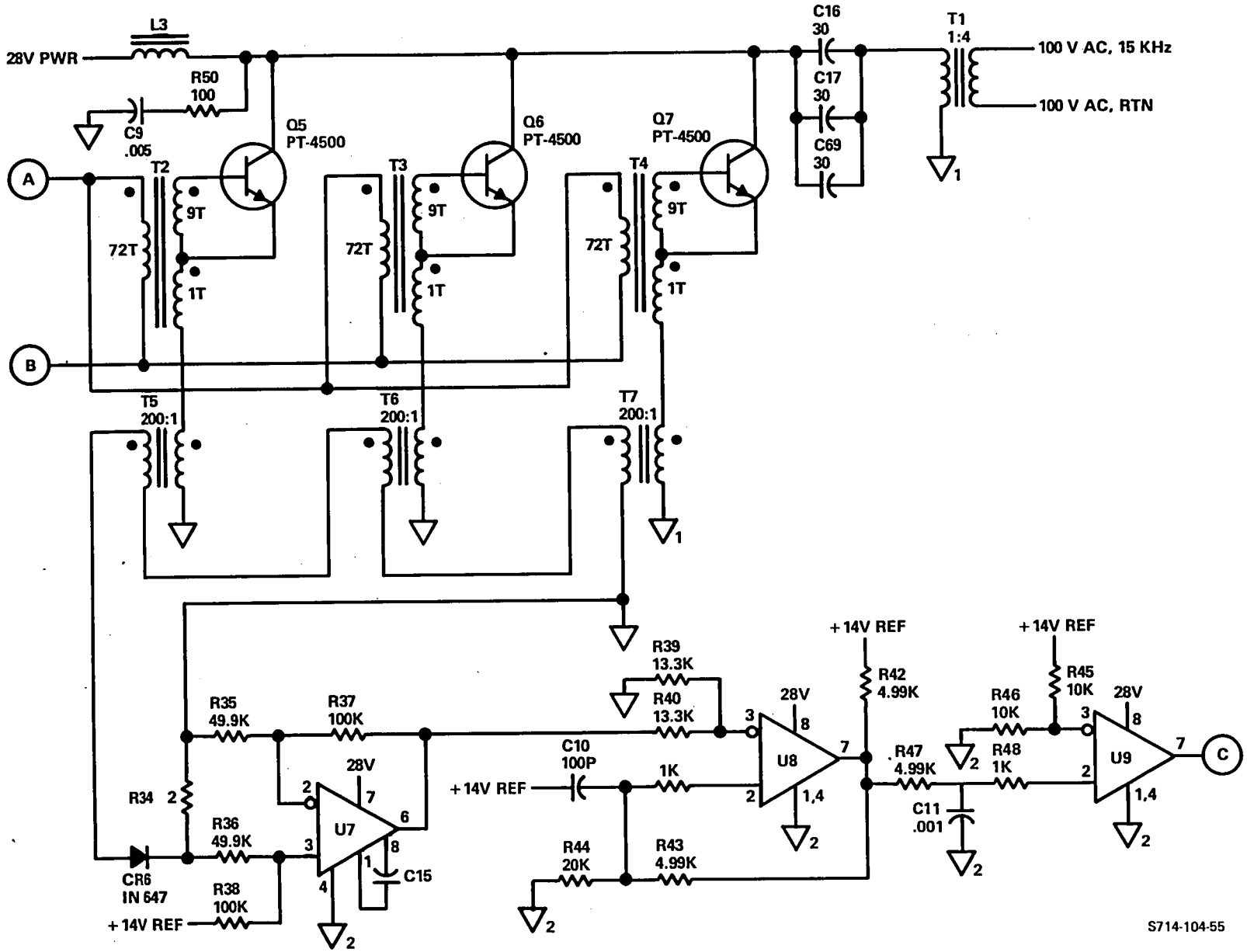

Figure A5-1
Baseline Transformer Schematic Diagram

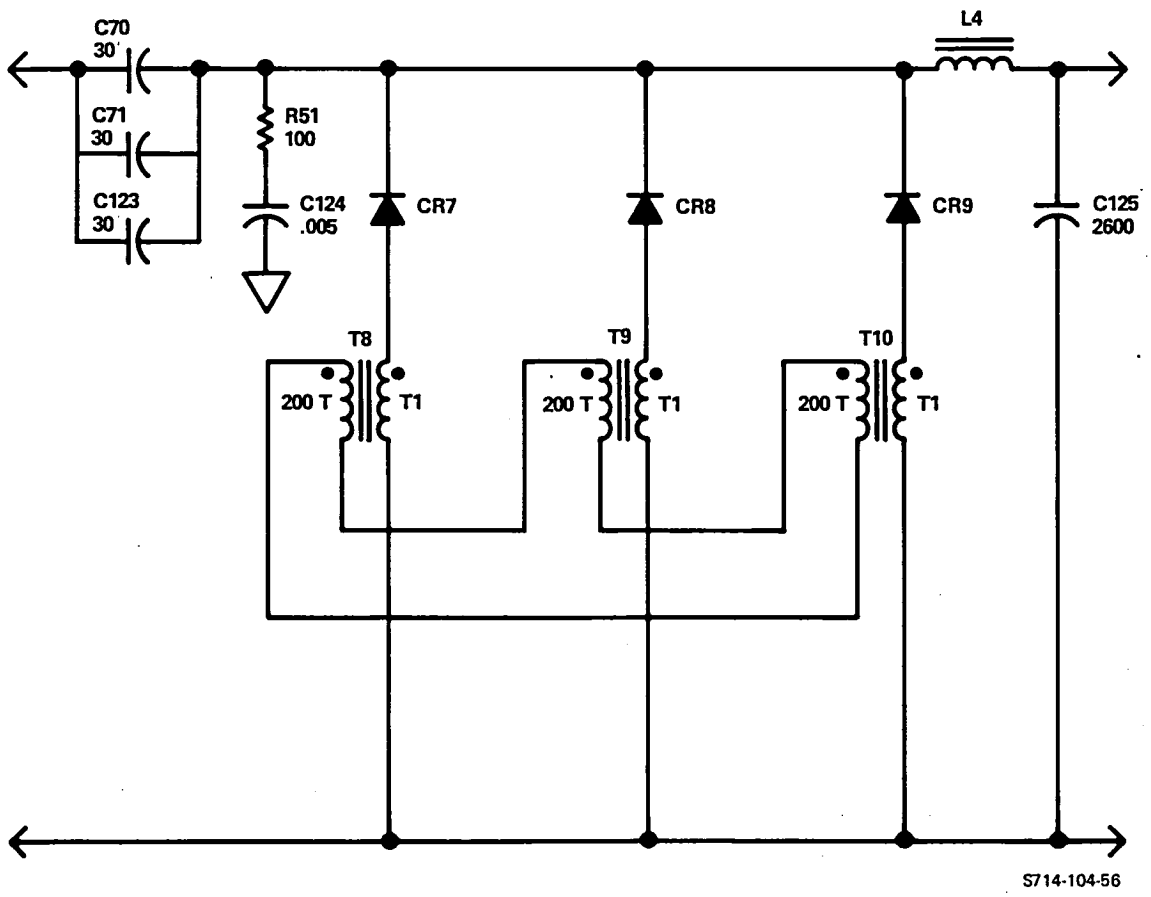

Figure A5-1
Baseline Transformer Schematic Diagram

NASA Contractor Report 172238
Distribution List
NAS1-16909

	No. Copies
NASA Langley Research Center Hampton, VA 23665	
Attn: Research Information Office, Mail Stop 151A	2
W. W. Anderson, Mail Stop 152	1
A Fontana, Mail Stop 161	1
J. C. Gowdey, Mail Stop 433	1
N. J. Groom, Mail Stop 494	1
C. R. Keckler, Mail Stop 161	21
NASA Ames Research Center Moffett Field, CA 94035	
Attn: Library, Mail Stop 202-3	1
Dryden Flight Research Facility P.O. Box 273 Edwards, CA 93523	
Attn: Library	1
NASA Goddard Space Flight Center Greenbelt, MD 20771	
Attn: Library	1
Philip Studer, Mail Stop 716.2	1
G. E. Rodriguez, Mail Stop 711.2	1
F. E. Ford, Mail Stop 711.0	1
L. W. Slifer, Mail Stop 711.0	1
NASA Lyndon B. Johnson Space Center 2101 Webster Seabrook Road Houston, TX 77058	
Attn: JM6/Library	1
EP5/R. R. Rice	1
EH3/F. M. Elam	1
NASA Marshall Space Flight Center Marshall Space Flight Center, AL 35812	
Attn: Library, Mail Stop AS24L	1
Rein Ise, Mail Stop JA51	1
John Owens, Mail Stop JA53	1
Dwight Johnston, Mail Stop JA52	1
Paul Golley, Mail Stop EB22	1
Harry Buchanan, Mail Stop ED15	1
Harvey Shelton, Mail Stop EE91	1
Douglas Nixon, Mail Stop EL54	1
Robert Smith, Mail Stop EL54	1
Frank Nola, Mail Stop EB24	1

	No. Copies
Jet Propulsion Laboratory 4800 Oak Grove Drive Pasadena, CA 91103	
Attn: 111-113/Library	1
198-112A/David Lehman	1
264-235/William Purdy	1
264-235/Ken Russ	1
T-1201/Edward Mettler	1
NASA Lewis Research Center 21000 Brookpark Road Cleveland, OH 44135	
Attn: Library, Mail Stop 60-3	1
NASA John F. Kennedy Space Center Kennedy Space Center, FL 32899	
Attn: Library, NWSI-D	1
National Aeronautics and Space Administration Washington, DC 20546	
Attn: RTH-6/Duncan McIver	1
RTH-6/John Dahlgren	1
RSE-5/Jerome Mullin	1
RSE-5/David Byers	1
United States Air Force Space Division P. O. Box 92960 Worldway Postal Center Los Angeles, CA 90009	
Attn: SD/YNSS/Maj. J. Baily	1
SD/YNSS/Lt. W. Possell	1
NASA Scientific and Technical Information Facility 6571 Elkridge Landing Road Linthicum Heights, MD 21090	25 plus original

1. Report No.	2. Government Accession No.	3. Recipient's Catalog No.
NASA CR-172238		

4. Title and Subtitle	5. Report Date
Final Report· Conceptual Design of a Noncontacting Power Transfer Device for the ASPS Vernier System	April 1984 ·
	6. Performing Organization Code 07187

7. Author(s)	8. Performing Organization Report No.
J. Kroeger, J. Drilling, and T. Gunderson	
	10. Work Unit No.

9. Performing Organization Name and Address	11. Contract or Grant No.
Sperry Flight Systems Space Systems Division Phoenix, AZ 85036	NAS1-16909, Task Number 3
	13. Type of Report and Period Covered Contractor Report
12. Sponsoring Agency Name and Address National Aeronautics and Space Administration Washington, D.C. 20546	14. Sponsoring Agency Code

15. Supplementary Notes

16. Abstract

A study was conducted to design a device to transfer power between noncontacting stationary and levitating platforms of the vernier subsystem of the Annular Suspension and Pointing System (ASPS). The power transfer mechanism was to: (1) require no physical contact between the two platforms, and (2) achieve high efficiency, high reliability, low weight, and low EMI susceptibility. Electromagnetic design considerations led to selection of an Ironless, Translatable Secondary Transformer. Electronics design considerations led to selection of a modified Cuk converter operating at a 10KHz frequency. The design transfers approximately 2500 watts output power with 99.2% efficiency.

17. Key Words (Suggested by Author(s))	18. Distribution Statement
Power Transfer Device. Noncontacting Transformer. Ironless. Translatable Secondary Transformer Design Cuk Converter	Unclassified - Unlimited

19. Security Classif. (of this report)	20. Security Classif. (of this page)	21. No. of Pages	22. Price
Unclassified	Unclassified		